PUZZLING STROMULE: THE ENIGMATIC PATHWAYS OF PLANT CELLULAR TRANSPORT

Zur Erlangung des akademischen Grades einer

DOKTORIN DER NATURWISSENSCHAFTEN

(Dr. rer. nat.)

von der KIT-Fakultät für Chemie und Biowissenschaften

des Karlsruher Instituts für Technologie (KIT)

genehmigte

DISSERTATION

von

M. Sc. Toranj Rahpeyma

1. Referent: Prof. Dr. Peter Nick

2. Referent: Prof. Dr. Tilman Lamparter

Tag der mündlichen Prüfung: 13. Februar 2025

Die vorliegende Arbeit wurde am Joseph Gottlieb Kölreuter Institut für Pflanzenwissenschaften (JKIP) des Karlsruher Instituts für Technologie (KIT), Lehrstuhl I für molekulare Zellbiologie, im Zeitraum von September 2020 bis September 2024 angefertigt.

Statement

Hiermit erkläre ich, Toranj Rahpeyma, dass ich die vorliegende Dissertation, abgesehen von der Benutzung der angegebenen Hilfsmittel, selbstständig verfasst habe.

Alle Stellen, die gemäß Wortlaut oder Inhalt aus anderen Arbeiten entnommen sind, wurden durch Angabe der Quelle als Entlehnungen kenntlich gemacht.

Diese Dissertation liegt in gleicher oder ähnlicher Form keiner anderen Prüfungsbehörde vor.

Zudem erkläre ich, dass ich mich beim Anfertigen dieser Arbeit an die Regeln zur Sicherung guter wissenschaftlicher Praxis des KIT gehalten habe, einschließlich der Abgabe und Archivierung der Primärdaten, und dass die elektronische Version mit der schriftlichen übereinstimmt.

Spielberg, December 2024
Toranj Rahpeyma

Acknowledgments

First and foremost, my deepest thanks go to Prof. Dr. Peter Nick. He introduced me to the captivating world of cell biology, transforming it from an interest into a passion. His stimulating discussions, invaluable advice, and lessons in resilience have been instrumental in my academic journey. Beyond being an exceptional scientific supervisor, he has been a mentor with a heart of gold, offering guidance that extended well beyond the confines of academia. His unwavering support has been invaluable, and for that, I am profoundly grateful.

A heartfelt mention goes to Dr. Manish Raorane, whose encouragement from day one has been a guiding light. His kindness and support have been pivotal.

I extend my sincere thanks to Prof. Dr. Tilman Lamparter for serving as the second reviewer and for his insightful contributions to the committee.

To my incredible colleagues, thank you for making each day in the lab a pleasure. Your camaraderie and support have been a wellspring of strength and joy. Together, we shared countless laughs, learned new techniques, and engaged in thought-provoking discussions. Through this journey, colleagues became friends. Special thanks to Emman, Kia, Chris, Nitin, Xuan, Nathalie, Nasim, and Islam.

I am also deeply grateful to Sabine Purpur, Dr. Michael Riemann, Dr. Gabriele Jürges Dr. Jathish Ponnu, and Dr. Sascha Wetters for their steadfast administrative and technical support, as well as for their warm daily interactions.

To the students I had the privilege of supervising, your enthusiasm and curiosity have been truly inspiring. You taught me as much as I hope I taught you. Thank you, Fabio, Leah, Javier, and Melina, for your active support and for keeping the spirit of inquiry alive.

Lastly, my deepest gratitude goes to my husband. His constant support and encouragement have been my anchor throughout this journey. Words cannot fully capture my appreciation for him.

December 2024

Toranj Rahpeyma

Abstract

Plastids are plant-specific organelles capable of forming stromules, highly dynamic projections extending from the plastid surface. These dynamic structures are believed to promote inter-organelle communication and trafficking of metabolites like proteins, lipids, and metabolic intermediates. These are triggered under various stress conditions, including exposure to hormones, reactive oxygen species, and pathogen-effector proteins. Despite early observations dating back over a century, their biological significance remained elusive until recent advancements in live-cell imaging techniques and fluorescent protein markers. Although, the formation and function of stromules are still unknown. Multiple factors, including plastid size, identity, and state of differentiation, can influence the formation of stromules. Recent studies have shown that overexpression of outer envelope chloroplast membrane proteins can significantly alter chloroplast morphology and induce stromule. The cytoskeleton, particularly actin filaments, and microtubules, plays a crucial role in stromule movement and anchoring.
This study aimed to elucidate the significance of stromules in various biological processes, focusing on their induction by MeJA. Key research questions addressed include the conditions promoting stromule production, factors influencing their formation and elongation, and the relationship between stromules and organelles in the JA biosynthesis pathway.

Results and Discussion

- **Induction of Stromule Formation:** Treatment with 100 μM MeJA or salicylic acid (SA) significantly increased stromule frequency and length in BY-2 cells expressing FP-tagged plastid outer membrane proteins. The lipoxygenase inhibitor phenidone blocked SA-induced stromule formation, suggesting crosstalk between SA and JA pathways in stromule regulation.
- **Role of Cytoskeleton:** The formation of stromules was shown to be age-dependent, increasing with cell age but suppressed in actively dividing cells, indicating a crucial role for microtubules. Significantly, the disruption of microtubules using oryzalin, a microtubule-depolymerizing agent, effectively blocked MeJA-induced stromule elongation, highlighting the critical role of microtubules in stromule formation.
- **Gene Expression Analysis:** The analysis focused on the differential expression of JA biosynthesis and signaling genes (AOC, OPR, JAZ1) in various treatments, with complex interactions between MeJA, SA, and cytoskeletal disruption. JAZ1 showed a marked induction

in response to MeJA, indicating its high sensitivity to jasmonate signaling. MeJA treatment significantly upregulated AOC and OPR, indicating a strong enhancement of the JA biosynthesis pathway. In contrast, pretreatment with Oryzalin, caused differential expression patterns, enhancing AOC expression while reducing OPR levels. This suggests that the inhibition of stromule formation by oryzalin altered gene expression, indicating that stromules are essential for maintaining the spatial dynamics necessary for efficient JA biosynthesis.

- **Organelle Communication:** Fluorescence microscopy provided further insights into the spatial dynamics of JA biosynthesis, showing that the JA biosynthesis protein JASSY co-localizes with stromules, suggesting that stromules facilitate the transport of OPDA during jasmonate biosynthesis and enhance biosynthesis efficiency. Additionally, peroxisomes tend to cluster around stromules, which could enhance the efficiency of jasmonate production by minimizing the distance that OPDA needs to travel between organelles. The rapid induction of stromules in response to MeJA and their association with JASSY and peroxisomes suggest a significant role in retrograde signaling from plastids to the nucleus.

Conclusion

These observations support a model where stromules facilitate inter-organelle metabolite exchange during JA biosynthesis and signaling. This study provides new insights into regulating stromules by stress-related phytohormones and their potential roles in retrograde signaling and organelle communication. The findings highlight stromules as dynamic platforms for coordinating cellular stress responses and hormone biosynthesis.

Zusammenfassung

Plastiden sind pflanzenspezifische Organellen, die in der Lage sind, Stromule zu bilden, hochdynamische Ausstülpungen, die sich von der Oberfläche der Plastiden erstrecken. Diese dynamischen Strukturen sollen die Kommunikation zwischen Organellen und den Transport von Molekülen wie Proteinen, Lipiden und Stoffwechselzwischenprodukten erleichtern. Sie werden unter verschiedenen Stressbedingungen induziert, einschließlich der Exposition gegenüber Hormonen, reaktiven Sauerstoffspezies und Pathogeneffektorproteinen. Trotz früher Beobachtungen, die über ein Jahrhundert zurückreichen, blieb ihre biologische Bedeutung bis zu den jüngsten Fortschritten in der Live-Cell-Imaging-Technik und fluoreszierenden Proteinmarkern unklar. Obwohl die Bildung und Funktion von Stromule noch unbekannt sind, kann die Bildung von Stromule durch mehrere Faktoren beeinflusst werden, einschließlich der Größe, Identität und Differenzierungszustand der Plastiden. Jüngste Studien haben gezeigt, dass die Überexpression von äußeren Hüllmembranproteinen der Chloroplasten die Morphologie der Chloroplasten erheblich verändern und Stromule induzieren kann. Das Zytoskelett, insbesondere Aktinfilamente und Mikrotubuli, spielt eine entscheidende Rolle bei der Bewegung und Verankerung von Stromule.

Diese Studie zielte darauf ab, die Bedeutung von Stromule in verschiedenen biologischen Prozessen zu klären, mit besonderem Fokus auf ihre Induktion durch MeJA. Wichtige Forschungsfragen umfassen die Bedingungen, die die Produktion von Stromule fördern, die Faktoren, die ihre Bildung und Verlängerung beeinflussen, und die Beziehung zwischen Stromule und Organellen im JA-Biosyntheseweg.

Ergebnisse und Diskussion

- **Induktion der Stromulibildung:** Die Behandlung mit 100 µM MeJA oder Salicylsäure (SA) erhöhte signifikant die Häufigkeit und Länge der Stromule in BY-2-Zellen, die FP-markierte Plastiden-Außenmembranproteine exprimieren. Der Lipoxygenase-Inhibitor Phenidon blockierte die SA-induzierte Stromulibildung, was auf eine Wechselwirkung zwischen den SA- und JA-Wegen bei der Regulierung der Stromule hinweist.
- **Rolle des Zytoskeletts:** Die Stromulenbildung war altersabhängig und nahm mit dem Zellalter zu, während sie in aktiv teilenden Zellen unterdrückt war – was auf eine wichtige Rolle der Mikrotubuli hinweist. Die Disruption der Mikrotubuli durch Oryzalin, einem Mikrotubuli-depolarisierenden Wirkstoff, blockierte die MeJA-induzierte Verlängerung von Stromulen

effektiv und unterstreicht die kritische Rolle der Mikrotubuli bei diesem Prozess.

- **Genexpressionsanalyse:** Die Analyse konzentrierte sich auf die differentielle Expression von JA-Biosynthese- und Signalisierungsgenen (AOC, OPR, JAZ1/2/3) in verschiedenen Behandlungen, mit komplexen Wechselwirkungen zwischen MeJA, SA und Zytoskelettstörung. JAZ1 zeigte eine deutliche Induktion als Reaktion auf MeJA, was auf seine hohe Empfindlichkeit gegenüber Jasmonat-Signalisierung hinweist. MeJA-Behandlung regulierte AOC und OPR signifikant hoch, was auf eine robuste Verstärkung des JA-Biosynthesewegs hinweist, während die Vorbehandlung mit Oryzalin differenzielle Expressionsmuster verursachte, die die AOC-Expression verstärkten, während die OPR-Spiegel reduziert wurden. Dies deutet darauf hin, dass die Hemmung der Stromulibildung durch Oryzalin die Genexpression veränderte, was darauf hindeutet, dass Stromule für die Aufrechterhaltung der räumlichen Dynamik, die für eine effiziente JA-Biosynthese erforderlich ist, wesentlich sind.
- **Organelle-Kommunikation:** Fluoreszenzmikroskopie lieferte weitere Einblicke in die räumliche Dynamik der JA-Biosynthese und zeigte, dass das JA-Biosyntheseprotein JASSY mit Stromule co-lokalisiert, was darauf hindeutet, dass Stromule den Transport von OPDA während der Jasmonat-Biosynthese erleichtern und die Biosyntheseeffizienz erhöhen. Darüber hinaus neigen Peroxisomen dazu, sich um Stromule zu gruppieren, was die Effizienz der Jasmonatproduktion erhöhen könnte, indem die Entfernung, die OPDA zwischen den Organellen zurücklegen muss, minimiert wird. Die schnelle Induktion von Stromule als Reaktion auf MeJA und ihre Assoziation mit JASSY und Peroxisomen deuten auf eine bedeutende Rolle bei der retrograden Signalisierung von Plastiden zum Zellkern hin.

Fazit

Diese Beobachtungen unterstützen ein Modell, bei dem Stromule den Austausch von Metaboliten zwischen Organellen während der JA-Biosynthese und -Signalisierung erleichtern. Diese Studie liefert neue Einblicke in die Regulierung von Stromule durch stressbezogene Phytohormone und ihre potenziellen Rollen in der retrograden Signalisierung und Organellenkommunikation. Die Ergebnisse heben Stromule als dynamische Plattformen zur Koordination zellulärer Stressreaktionen und Hormonbiosynthese hervor.

Contents

Abbreviations

MeJA = Methyl Jasmonate

SA = Salicylic acid

BY-2 cell = *Nicotiana tabacum* cell

NaCl = Sodium chlorid

MTs = Microtubules

AFs = ACTIN FILAMENTS

OPDA = 12-Oslo Phytodienoic acid

JAZ = Jasmonate ZIM-domain

AOC = Allene Oxide Cyclase

OPR = OPDA Reductase

Kan 50 = Kanamycin 50 mg/ml

Hyg 30 = Hygromycin 30 mg/ml

Spec 100 = Spectinomycin 100 mg/ml

Gen 50 = Gentamicin 50 mg/ml

GPP = Geranyl diphosphate

FPP = Farnesyl pyrophosphate

NBD-GPP = a fluorescent analog of geranyl pyrophosphate (GPP)

NBD-FPP = a fluorescent analog of farnesyl pyrophosphate (FPP)

1. Introduction

1.1. Stromules: an overview

Plastids, the plant-specific double-membrane organelles, are not just unique in their ability to form stromules, but also in the variability of stromule induction. Stromules, these stroma-filled tubules, are not just microscopic but also highly dynamic projections that extend from the inner or outer surface of all types of plastids in plant cells. This induction process is complex and diverse, varying across tissues and dependent on plant developmental stages (Natesan et al. 2005). They form in response to a variety of biotic and abiotic stress conditions, adding to the complexity of plant biology. These stromules, usually 0.35–0.85 μm in diameter, can reach lengths from 15 μm in tobacco to up to 200 μm in the mesocarp of tomato fruit (Gray et al. 2001; Kwok and Hanson 2004). They reportedly carry molecules up to 560 kDa (Köhler and Hanson 2000).

Research indicates that stromules, these dynamic projections, play a crucial role in plant biology by facilitating inter-organellar communication and trafficking of molecules such as proteins, lipids, and metabolic intermediates. However, their significance is truly highlighted under stress conditions. When plants are exposed to stress factors like sugar, hormones, reactive oxygen species, and pathogen effector proteins, stromules are induced to form and transfer molecules between interconnected plastids. This process is a key part of the plant's stress response and adaptation, underscoring the relevance and importance of our research in understanding these mechanisms (Hanson and Sattarzadeh 2011).

The stromule discovery dates back over a century, with the first observations of interconnections between plastids made by Gottlieb Haberlandt in 1888 and Gustav Senn in 1908 (Haberlandt 1888; Senn 1908). Despite these initial findings, the precise biological role of stromules remained unclear for many years. Recent advancements in live-cell imaging and the use of fluorescent protein markers have significantly improved our understanding of stromules. These technologies now allow researchers to visualize stromule dynamics in real-time, providing insights into their formation, function, and regulation (Schattat et al. 2011; Erickson et al. 2014).

Further research into stromules could clarify their role in plant physiology, particularly in stress responses and inter-organelle communication. Understanding the mechanisms that regulate stromule formation and function may have significant implications for plant biology and agricultural practices, especially in improving plant resilience to environmental stressors.

1.2. Stromules Formation and Breakage

The formation of stromules is a complex and dynamic process influenced by various factors, including the size, identity, state of differentiation, and density of plastids. One leading hypothesis is that stromules arise due to internal or external forces acting on the main plastid body, potentially anchored to the cytoskeleton. Another hypothesis posits that specific membrane proteins alter membrane lipid-protein interactions, inducing stromule formation. Additionally, local changes in protein concentration within or on the outer surface of the envelope membrane could generate these tubular projections (Domanov and Kinnunen 2006; Hanson and Hines 2018; Pucadyil and Schmid 2008; Stachowiak et al. 2010).

Recent studies have shown that high expression levels of outer envelope chloroplast membrane proteins such as AtLACS9, OEP7, and TM-CHUP1 in Arabidopsis thaliana and Nicotiana benthamiana can significantly alter chloroplast membrane morphology, resulting in a variety of stromule-like extensions (Breuers et al. 2012; Machettira et al. 2012). These stromules did not form when only inner membrane proteins were overexpressed. Breuers et al. (2012) demonstrated that protrusions induced by AtLACS9 in N. benthamiana involved both the inner and outer envelope chloroplast membranes.

In vitro studies further revealed that stromules could be formed from isolated plastids of N. benthamiana (Brunkard et al. 2016; Brunkard et al. 2015). These findings suggest that plant dynamin-related proteins on the outer envelope membrane might play a role not only in the formation but also in the breakage of stromules (Hanson and Sattarzadeh 2013; Ho and Theg 2016). It is speculated that strong membrane interactions with other proteins or organelles persist after plastid isolation, indicating that additional cytoplasmic proteins may influence stromule formation. The generation of stromules in preparations by Ho and Theg (2016) depended on the size and concentration of carrier proteins along the membrane. They found that stromules were stimulated only by proteins or protein complexes of 100 kDa or larger.

Contrary to early assumptions, DNA and ribosomes typically do not traverse through stromules

from the main plastid body, unlike mitochondrial genomes (Newell et al. 2012). Interestingly, studies have shown that stroma-containing bodies resulting from stromule breakage are directed into vacuoles for degradation during nutrient stress, a process dependent on the autophagy system (Hanson and Sattarzadeh 2013; Ishida et al. 2008). Despite these advancements, the exact mechanisms of stromule formation and the ultimate fate of broken stromules remain largely undetermined, inviting further research into this intriguing aspect of plant cell biology.

1.3. Interconnected Plastids and Stromule Communication

Köhler et al. (1997) introduced the first definition of interconnected plastids, exploring whether plastids frequently communicated with other plastid bodies (Kohler et al. 1997). Using photobleaching techniques, Köhler and Hanson (2000) observed that only a few plastids were connected at any time in cultured cells, and many stromules were present. This observation indicated that, unlike the endoplasmic reticulum, plastids are not usually part of an extensive network (Köhler and Hanson 2000). Schattat et al. (2012) reconfirmed the absence of a plastid network using a photoconvertible GFP technique (Schattat et al. 2012). When low laser power for photoconversion is used, the experiment can visualize the transfer of photoconverted protein through a stromule between plastids that are significantly distant from each other (Hanson and Sattarzadeh 2013).

This finding suggests that plastid bodies functionally connected by a stromule are daughter plastids, even if considerable distances separate them (Schattat et al. 2015). However, evidence for or against this hypothesis remains inconclusive. Researchers have reported that overexpression of AtLACS9 as an outer envelope membrane protein in N. benthamiana induces the formation of stromules that contact multiple chloroplasts, which are clearly not daughter plastids (Breuers et al. 2012).

Determining how stromules connect multiple separated plastids is a technical challenge, as interconnected plastids are rarely observed in wild-type plants not exposed to various stresses. Despite this, stromule-plastid interaction in cells under unusual conditions is a biological fact. Stromules can rapidly increase due to pathogen inoculation, protein overexpression, chemical treatments, or photosynthetic stress (Breuers et al. 2012; Brunkard et al. 2015; Caplan et al. 2015; Gray et al. 2012). This raises the question of whether stromules could be remnants of ancient communication systems involved in plant defense.

1.4. Stromules and Actin Cytoskeleton

Given that chloroplasts and other plastid bodies originated through the engulfment of cyanobacteria in a primary endosymbiosis event (Gould et al. 2008), stromules may represent just one example of tubular connecting structures in cells. For instance, mammalian immune cells exhibit specialized intercellular communications via cytonemes, a type of filopodium. Filopodia, as actin-rich tubular structures, extend through actin polymerization from cell to cell to gather spatial information and are involved in processes such as cell migration and pathogen infection (Atkinson 2017; Roy et al. 2011).

Microtubules (MTs), the most significant type of eukaryotic cytoskeletal elements, and actin filaments (AFs), the most minor, form dynamic networks that provide mechanical support to cells. Actin is a highly conserved globular protein essential for cell division, gene expression, and immunity in eukaryotic cells (Zhao et al. 2011). Studies have shown that inhibitors of actin microfilaments and microtubules affect stromule frequency, length, and movement regulation. For example, treatment of non-green tissue of *Nicotiana tabacum* with actin filament inhibitors Cytochalasin D and Latrunculin B, as well as co-treatment with AF and MT inhibitors, resulted in reduced stromule length, frequency, and looping back onto the main plastid body. These findings indicate that stromule movement is actin-dependent (Kwok and Hanson 2004; Kwok and Hanson 2003).

Additionally, Myosin XI family motor proteins have been implicated in stromule movement, length, and anchoring to the cytoskeleton. Treatment of Nicotiana with the myosin ATPase inhibitor 2,3-butanedione 2-monoxime (BDM) has demonstrated that myosin motors are likely involved in stromule dynamics, potentially moving stromules along actin filaments (Kumar et al. 2018; Natesan et al. 2009; Sattarzadeh et al. 2009). Kumar et al. (2018) further showed that dynamic stromules extend along microtubules, with actin filaments stabilizing the stromules. Early studies reported that stromules can direct chloroplast movement, and actin filament anchoring of stromules may guide chloroplast-to-nucleus connections during the innate immune response. Their results support a model in which microtubule-mediated stromule extension and actin filament-mediated stromule anchoring are complementary activities during stromule formation and movement (Kumar et al. 2018).

1.5. Stromules induction by stress treatments

1.5.1. Biotic Stress

Although the function of stromules is mainly unknown, they may serve as signal transmission channels from plastids to the nucleus or even to other cells. In terms of plant immunity, stromules are involved in effector-triggered immunity (Leontovyčová et al. 2019) and programmed cell death (PCD) (Caplan et al. 2015; Hanson and Sattarzadeh 2011).

In both plants and animals, nucleotide-binding domain and leucine-rich repeat (NLR) proteins are employed to respond to pathogen effectors. Plant NLR proteins recognize pathogen effectors and initiate ETI, often accompanied by hypersensitive response PCD (HR-PCD) (Caplan et al. 2015; Mur et al. 2006). The HR-PCD is preceded by the production of pro-PCD signals such as salicylic acid (SA), nitric oxide (NO), and reactive oxygen species (ROS, including H2O2 and O2-) induced during defense responses. Chloroplasts are a major source of these pro-defense signaling molecules in plants. Caplan et al. (2015) observed that stromules were induced in Nicotiana benthamiana plants infiltrated with H2O2, the SA analog INA, and during an N-mediated viral defense. Application of INA and H2O2 also induced stromules in Arabidopsis cTP-GFP plants. By forming complex associations and clustering around nuclei, stromules may help reach a threshold level of H2O2, SA, and other signaling molecules to induce HR-PCD in the cytosol and nucleus. This suggests that pro-defense molecules might be responsible for cell-to-cell signaling that induces stromules along the borders of HR-PCD.

Caplan et al. (2015) further demonstrated that the chloroplast protein N receptor-interacting protein 1 (NRIP1), which localizes to chloroplasts in unchallenged plants, relocates to the nucleus upon infection with tobacco mosaic virus (TMV). NRIP1 in N. benthamiana recognizes the TMV effector p50 by the NLR receptor N during ETI. Caplan et al. observed strong stromule induction in response to bacterial effectors in another experiment. The expression of Pseudomonas syringae bacterial effectors AvrB and AvrRpt2, and the co-expression of Xanthomonas campestris effector AvrBS2 and its receptor BS2, induced HR-PCD in N. benthamiana and extensive stromule proliferation. Thus, stromule induction is a general response during plants' viral and bacterial immune responses (Caplan et al. 2015).

1.5.2. Abiotic Stress

In addition to biotic stress from pathogens, various abiotic stress treatments can induce stromule

formation. Gray et al. (2012) demonstrated that Abscisic acid (ABA) is an effective inducer of stromule formation. ABA is primarily involved in the signaling pathways for drought and salt stress and modulates jasmonate (JA) and salicylate (SA) regulation. ABA down-regulates the expression of some nuclear genes that encode photosynthetic components required for functional chloroplast formation, whereas light treatment can upregulate these genes. Gray et al. (2012) observed stromule abundance in dark-grown wheat and tobacco seedlings and found that stromule frequency decreased upon illumination of dark-grown seedlings with red and far-red light treatments (Gray et al. 2012). However, Brunkard et al. (2015) demonstrated that stromule formation from Arabidopsis mesophyll chloroplasts can increase during the day compared to the night (Brunkard et al. 2015).

The inhibitory effect of chloroplast formation on stromule formation has also been suggested in tomato fruit and tobacco seedlings (Ahmad et al. 2016; Kwok and Hanson 2003; Waters et al. 2004). The light dependence of stromule induction is controversial, likely due to differences in plant growth and the types of plastids examined in each experiment. Although ABA induces many cold stress-responsive genes, the positive effect of cold temperature on stromule formation has not been detected. Instead, stromule abundance is inhibited by lower temperatures (Gray et al. 2012). Holzinger et al. (2007a) observed that long stromules and chloroplast protrusions formed at 20°C and 35°C in mesophyll cells of Arabidopsis thaliana (Holzinger et al. 2007).

Stromules have also been observed in response to changes in cellular sugar levels. Vacuum infiltration with either sucrose or glucose significantly increases stromule formation, whereas fructose or mannitol does not induce stromule formation (Schattat and Klösgen 2011). In conclusion, many intrinsic and extrinsic factors may control stromule induction and formation, acting synergistically or antagonistically. Understanding these interactions will be crucial for elucidating the role of stromules in plant physiology and stress responses.

1.6. Jasmonates and Jasmonic Acid Pathway

Research on plants' jasmonic acid (JA) biosynthesis has significantly progressed over the past few decades. The primary biosynthetic routes, the octadecane pathway starting from α-linolenic acid and the hexadecane pathway from hexadecatrienoic acid, are well-documented and extensively studied (Wasternack and Hause 2013). In *Nicotiana tabacum* BY-2 cells, JA

biosynthesis initiates in the protoplast, where these precursor acids are transformed into cis-12-oxo- phytodienoic acid (cis-OPDA) and dinor-12-oxo-phytodienoic acid (dn-OPDA) by the sequential action of 13-lipoxygenase, 13-allene oxide synthase, and allene oxide cyclase (Dave and Graham 2012). The COMATOSE ATP-binding cassette transporter facilitates subsequent transport of cis-OPDA and dn-OPDA to the peroxisome (Footitt et al. 2007). OPDA is transported into peroxisomes by a protein residing in the chloroplast outer membrane termed JASSY (Jasmonate Activated Secreted Protein) (Guan et al. 2019).

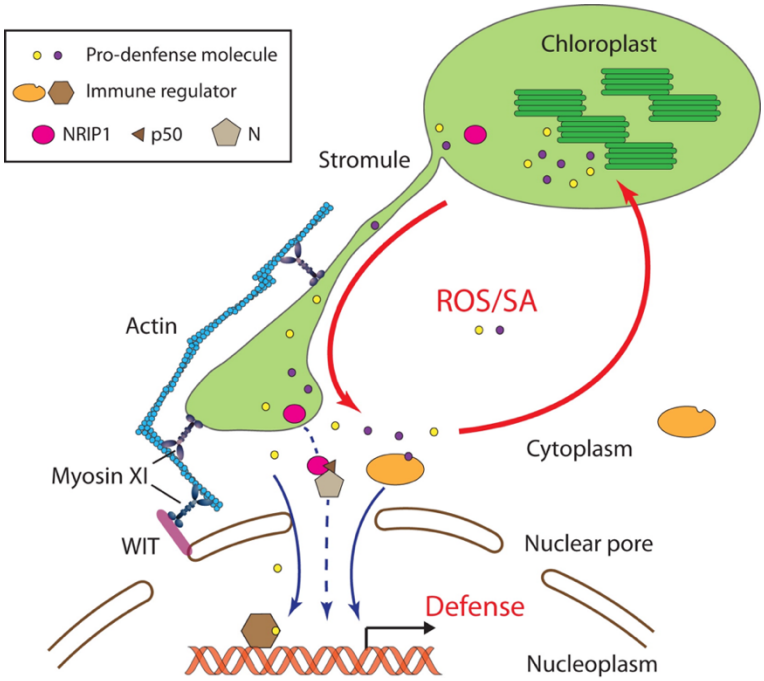

Figure A: Role of Stromules in Immune Signal Transmission to the Nucleus

During the initial phase of effector-triggered immunity, defense signals such as salicylic acid (SA) and reactive oxygen species produced in chloroplasts induce the formation of stromules. These stromules are shaped by the actin cytoskeleton, myosin XI, and myosin-interacting proteins like WIT, which extend their membranes and position their tips close to the nucleus without membrane fusion. Immune signals, including NRIP1, ROS, and SA, are released from stromules into the cytoplasm surrounding the nucleus, effectively reducing signal diffusion distances and increasing local concentrations to activate immune regulators within the nucleus. This process creates a feedback loop that amplifies stromule formation and the transmission of defense signals, thereby enhancing the plant's immune response. Figure inspired by Gu, Y. and Dong, X., (2015) (Gu and Dong 2015).

Within the peroxisome, these intermediates are reduced by OPDA reductase to 8-(3-oxo-2-(pent-2-enyl) cyclopenthyl) octanoic acid (OPC-8) and 6-(3-oxo-2-(pent-2-enyl) cyclopenthyl) octanoic acid (OPC-6). The conversion to JA proceeds through two and three cycles of β-oxidation, respectively (Ruan et al. 2019). The final JA product is transported into the cytoplasm via the JA transfer protein, where it can be further modified into various derivatives. One notable derivative, methyl jasmonate (MeJA), is synthesized by JA carboxyl methyltransferase, while the enzyme jasmonate resistant-1 forms jasmonoyl-L-isoleucine (JA-Ile). This synthesis pathway ensures a rapid and efficient production of defense signals in response to environmental stimuli (Figure B).

The JA-Ile pathway plays a key role in transcriptional control, activating JA-responsive genes. When JA-Ile accumulates, it is transported to the nucleus of the plant cell by jasmonic acid transfer protein 1 (JAT1), where it binds to SCFCOI1, triggering the degradation of jasmonate-ZIM domain (JAZ) proteins through the 26S proteasome. This degradation releases the corepressor TOPLESS (TPL), previously bound to JAZ via NINJA, thereby allowing the transcription factors to activate JA-responsive genes. This positive feedback loop includes the production of enzymes like AOS and AOC, which are integral to JA synthesis. Conversely, some genes promoted by this pathway induce the production of JAZ proteins, which inhibit gene expression in conjunction with NINJA and TPL, establishing a negative feedback mechanism. These intricate gene interactions provide adaptability to environmental changes (Ruan et al. 2019; Thines et al. 2007). Removing JAZ repressors is a crucial step in activating genes involved in defense responses and secondary metabolism (Figure C).

Research has demonstrated that when large plants are injured, jasmonates accumulate throughout the entire plant rather than solely at the site of the wound. This phenomenon has been observed in various higher plants, using methyl jasmonate (MeJA) to facilitate communication between damaged and undamaged plant parts through airborne transmission. Unlike Jasmonic Acid (JA), which requires carrier proteins to penetrate cell membranes, MeJA is a volatile phytohormone that can be easily transmitted through the air. Furthermore, this transmission mode is not limited to the same plant, as evidenced by studies such as Park et al. (2007). This inter-plant communication through volatile compounds highlights the sophisticated defense mechanisms evolved by plants to respond to herbivory and other stressors (Park et al. 2007). Jasmonates are crucial for mediating responses to various biotic and abiotic stresses. They play a significant role in the defense against herbivores and pathogens by

regulating the expression of defense-related genes. For instance, jasmonates can trigger the production of proteinase inhibitors and other anti-herbivore compounds that reduce the palatability of the plant to herbivores. Additionally, JA signaling can enhance the production of volatile organic compounds that attract natural predators of the herbivores, providing an indirect defense mechanism (Browse 2009; Kessler and Baldwin 2002).

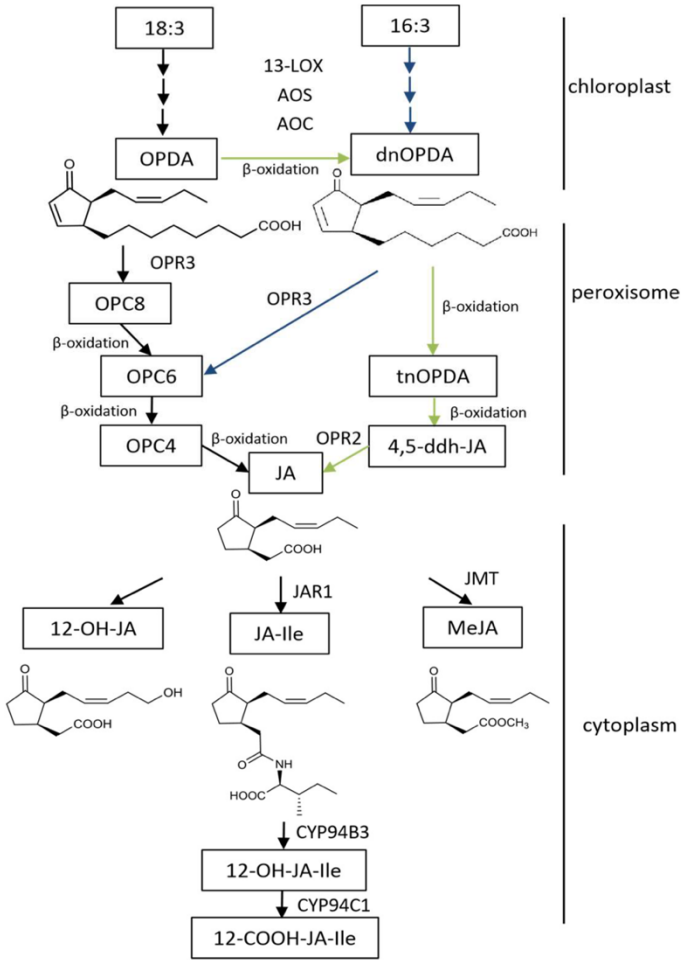

Figure B: Biosynthesis of Jasmonates

Enzymes and intermediates: α-LA (α-linolenic acid), HA (hexadecatrienoic acid), 13-LOX (13-lipoxygenase), 13-AOS (13-allene oxide synthase), AOC (allene oxide cyclase), cis-OPDA (12-oxo-phytodienoic acid), dn-OPDA (dinor-12-oxo-phytodienoic acid), CTS (COMATOSE), OPR3 (OPDA reductase), OPC-8 (8-(3-oxo-2-(pent-2-enyl)cyclopenthyl) octanoic acid), OPC-6 (6-(3-oxo-2-(pent-2-enyl)cyclopenthyl) octanoic acid), β-OX (β-oxidation), JA ((+)-7-iso-jasmonic acid), JAT1 (jasmonic acid transfer protein 1), JMT (jasmonic acid carboxyl methyltransferase), **MeJA** ((+)-methyl jasmonate), JAR1 (jasmonate resistant 1), JA-Ile (jasmonoyl-L-isoleucine). Figure inspired by Ruan et al. (2019) (Ruan et al. 2019).

The role of jasmonates extends beyond defense mechanisms. They participate in plant growth and development aspects, such as root growth, seed germination, and reproductive processes. Jasmonic acid (JA) signaling regulates the expression of genes involved in these activities, underscoring its important role in plant biology (Browse 2009). The dual role of jasmonates in growth and defense underlines the importance of tight regulation of JA signaling pathways to optimize plant fitness.

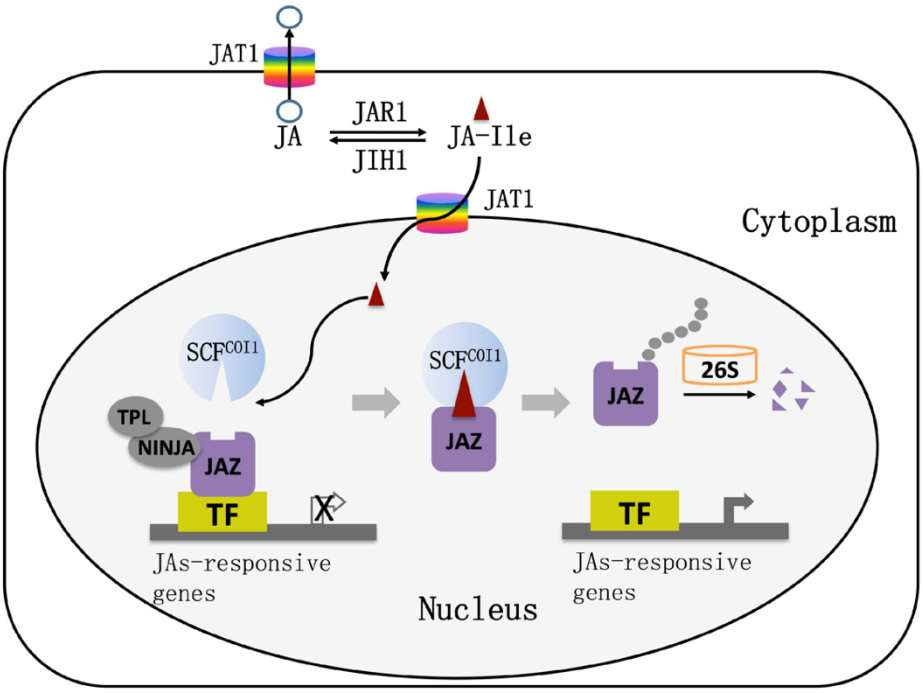

Figure C: Jasmonic Acid Signal Pathway

Components: JA-Ile (jasmonoyl-L-isoleucine), JAT1 (jasmonic acid transfer protein 1), SCF (Skp1, Cullin, and F-box proteins), COI1 (coronatine insensitive 1), JAZ (jasmonate ZIM-domain protein), TF (transcription factor), NINJA (NOVEL INTERACTOR OF JAZ), TPL (TOPLESS protein), 26S (26S proteasome). Figure inspired by Ruan et al. (2019) (Ruan et al. 2019).

Recent research has clarified the complex interactions between jasmonic acid (JA) signaling and other phytohormonal pathways, highlighting the intricate regulatory mechanisms that control plant defense responses. Notably, the relationship between JA and salicylic acid (SA) signaling pathways can produce either synergistic or antagonistic effects. This interplay fine-tunes the plant's immune response based on the specific type of stress it faces (Caarls et al. 2015). Additionally, ethylene and abscisic acid (ABA) pathways have been shown to converge with JA signaling, orchestrating a delicate balance between growth and defense strategies in

plants. This intricate hormonal crosstalk enables plants to respond appropriately to many environmental challenges (Wasternack and Hause 2013). Deciphering these complex interactions is pivotal for advancing our ability to engineer crops with enhanced stress tolerance, improving agricultural productivity and sustainability.

1.7. BY-2 Model Organism for Plant Cell Research

The *Nicotiana tabacum* cultivar Bright Yellow 2 (BY-2) cell line, initially isolated in 1972 in Osaka, Japan, from a callus induced on a seedling, has emerged as a pivotal model organism in plant cell biology. BY-2 cells, cultivated in a modified Linsmaier and Skoog (LS) medium supplemented with 0.2 mg/L 2,4-dichlorophenoxyacetic acid (2,4-D) at pH 5.8, are maintained in darkness at 27°C with continuous rotary shaking at 130 rpm to promote rapid proliferation and high cellular homogeneity (Nagata et al. 1992). These conditions, either in solid or liquid media supplemented with sucrose and an auxin-like hormone, facilitate optimal growth, with the cultivation cycle spanning a 7-day period during which cells undergo phases of division, expansion, and disintegration, yet do not reach a complete unicellular stage.

One of the distinguishing features of BY-2 cells is their rapid cell division, with a doubling time of approximately 14-18 hours, which is highly advantageous for experimental studies. This rapid growth enables the production of substantial cells in a relatively short period, while their homogeneity ensures consistent and reproducible experimental outcomes (Nagata and Kumagai 1999; Nagata et al. 2006; Nagata et al. 1992). The suspension culture system, where BY-2 cells exist as single cells or small clusters in a liquid medium, offers a balance between mimicking in vivo conditions and the simplicity and control of an in vitro environment, which is beneficial for studying cellular processes in a controlled setting (Nagata et al. 1992).

BY-2 cells have significantly contributed to our understanding of plant cell biology, serving as a model system to study various cellular processes such as cell cycle regulation, cytoskeleton dynamics, plant hormone signaling, intracellular trafficking, and organelle differentiation. For instance, research involving BY-2 cells has elucidated mechanisms of cell division and the roles of cytoskeletal components in plant cells (Nagata et al. 2006; Bhat 2004).

The uniform behavior of BY-2 cells in suspension culture facilitates the isolation and analysis of specific biochemical phenomena without the complexities associated with multicellular organism interactions. This makes BY-2 cells an ideal model for dissecting molecular and

cellular mechanisms underlying plant growth and development. In the realm of genetic engineering, BY-2 cells are invaluable. Techniques such as stable transformation using *Agrobacterium tumefaciens* have optimized these cells for various genetic studies. Recently, the CRISPR-Cas9 system has been employed to achieve precise gene inactivation in BY-2 cells, demonstrating the potential for detailed genetic modifications and enhancing our understanding of gene functions (Mercx et al. 2017)

Beyond fundamental research, BY-2 cells are extensively used in biotechnology to produce recombinant proteins. They offer an alternative host system for producing pharmacological proteins, including antibodies. The ability of BY-2 cells to secrete these proteins into the extracellular medium simplifies purification processes, reducing downstream processing costs compared to whole-plant systems. This capability positions BY-2 cells as a promising tool in molecular farming and biologics production (Frontiers in Plant Science, 2016). Furthermore, BY-2 cells have been used to produce therapeutic proteins with human-like glycosylation patterns, which are crucial for the efficacy and safety of these medicines. The containment and control offered by cell suspension cultures, and advanced genetic engineering tools available for BY-2 cells make them a robust system for producing high-value biologics (Mercx et al. 2017).

1.8. Scope of this study

The principal objective of this study is to elucidate the significance of stromules in various biological processes. To this end, we have implemented both physiological and molecular experiments to investigate the impact of methyl jasmonate (MeJA) on stromule formation.
Key research questions to be addressed include:

- **What conditions promote the production of stromules, and which factors influence their formation and elongation?**

  Developing a reliable observation method for stromules is essential. This involves employing plant cells with fluorescent markers tagging plastids and stromules. These tagged cells will be exposed to different stimuli, and stromule dynamics will be carefully observed using advanced microscopy. Since stromules are known to extend from plastids in response to stress, examining the antagonistic and synergistic effects of different stress triggers, along with their interactions, on stromule formation is crucial.

- **How is the biosynthesis pathway of MeJA regulated during stromule formation, and what is the relationship between stromules and organelles in this process?**
  This research will investigate the key genes involved in the jasmonic acid (JA) biosynthesis pathway, which controls the production of JA intermediates in chloroplasts and peroxisomes. We will analyze the expression patterns of these genes under different stromule-producing conditions to understand the regulatory mechanisms of MeJA biosynthesis and the interaction between organelles and stromules.

By exploring these questions, this study aims to provide a detailed understanding of the conditions and regulatory factors that influence stromule formation, as well as the complex role of MeJA in these processes.

2. Materials

2.1 List of Microscopes

Table 2.1-2.4 enumerate all instruments and materials utilized in this research.

Table 2.1: Microscopy and Imaging Instruments

These devices were employed for live-cell imaging of BY-2 cells and the macroscopic examination of callus structures.

Spinning Disk Confocal Microscope		
Equipment		**Manufacturer**
Microscope	Axio Observer.Z1 (inverted Microscope)	Carl Zeiss Microscopy GmbH, Jena, Germany
Objective	Plan-Apochromat 63x/1.40 Oil DIC M27 (oil objective)	
Reflector	Analy.DIC Trans.L (Bruinsma et al.)	
Camera (Adapter)	AxioCam MRm	
Effective NA	1.4	
Light/Laser source	TL LED (9.44 Volt) / HXP-120 laser dual spinning disc scan head	Leistungselektronik JENA GmbH, Jena Germany (Laser)
AOTF1.Laserline connected to spinning disk confocal scan head. (Excitation: 488 nm and 590 nm). Yokogawa CSU-X1 Spinning Disk Unit	Yokogawa Electric Corporation, Tokyo, Japan (Confocal Scanner Unit)	AOTF1.Laserline connected to spinning disk confocal scan head. (Excitation: 488 nm and 590 nm). Yokogawa CSU-X1 Spinning Disk Unit
Fluorescence Stereo Zoom Microscope		
Equipment		**Manufacturer**
Microscope	Axio Zoom.V16	Carl Zeiss Microscopy GmbH, Jena, Germany
Objective	PlanNeoFluar Z 1.0x (Zoom 0.7)	
Filters	450 – 490, 500 – 550 (GFP) / 538 – 562, 570 – 640 (RFP)	
Reflector	38 HE eGFP (EGFP) / 43 HE DsRed (mCherry)	

Beam Splitter	495 (GFP) / 570 (RFP)	
Camara (Adapter)	Axiocam 705 mono (0.63x Adapter)	
Effective NA	0.25	
Light/Laser source	DL450 Lamp HXP-120	Leistungselektronik JENA GmbH, Jena, Germany
ApoTome Fluorescence Microscope		
Equipment		**Manufacturer**
Microscope	Axio Imager.Z1	Carl Zeiss Microscopy GmbH, Jena, Germany
Objective	Plan-Apochromat 63x/1.40 DIC M27 (oil objective)	
Filters	488 - 512, 520 - 550	
Reflector	Transmission (Bruinsma et al.) / 46 HE Yellow Fluoresc. Prot (phiYFP)	
Beam Splitter	515	
Camera (Adapter)	Axiocam 503 (1x Adapter)	
Effective NA	1.4	
Light/Laser source	TK Halogen Lamp (4.25 V) / HXP-120 (excitation 488 nm)	Leistungselektronik JENA GmbH, Jena Germany

2.2. List of Kits

Table 2.2: Inventory of Kits Utilized in This Study

Purpose	kit	Provider
PCR purification	MSB Spin PCRapace	Stratec molecular, Birkenfeld
Plasmid extraction	Roti-Prep Plasmid Mini	Carl Roth GmbH + Co. KG, Karlsruhe
RNA extraction	Roboklon, Universal RNA Kit	Sigma-Aldrich, Darmstadt
Gateway cloning	Gateway™ BP Clonase™ II	Thermo Fisher Scientific Inc., Waltham, M USA
Gateway cloning	Gateway™ LR Clonase™ II	Thermo Fisher Scientific Inc., Waltham, M USA

2.3. List of Plasmids

Table 2.3: Plasmids Used in Cell Transformation and Gateway Cloning Procedures

Plasmid	Bacterial selection	Plant selection	Description	Provider
PDONR Vector	Zeocin	_	Gateway cloning	Thermo Fisher Scientific
pK7FWG.2 (GWV12)	Spec 100	Kan 50	Plant expression vector C-terminal fusion to GFP-Gateway cloning	VIB-UGent Center for Plant Systems Biology
pK7WGF.2 (GWV13)	Spec 100	Kan 50	Plant expression vector N-Terminal fusion to GFP-Gateway cloning	VIB-UGent Center for Plant Systems Biology
pK7RWG.2	Spec 100	Kan 50	Plant expression vector C-terminal fusion to RFP-Gateway cloning	VIB-UGent Center for Plant Systems Biology
pCAMBIA1300 tpFNR-mEOS	Kan 50	Hyg 30	Plant expression vector N-terminal fusion to mEOS Stroma marker	kindly provided by Professor Dr. Jaideep Mathur
pCAMBIA1300 At.SFR2-RFP	Kan 50	Hyg 30	Plant expression vector N-terminal fusion to RFP-Outer plastid membrane marker	kindly provided by Professor Dr. Jaideep Mathur
tpFNR.GFP-PTS1.RFP	Gen 50/Kan 50	Hyg 30	Plant expression vector N-terminal fusion to mCherry-Peroxisome marker combined with N-terminal fusion to mEGFP-Stroma marker via Golden Gate cloning	kindly provided by Dr. Martin Hartmut Schattat

2.4. List of Primers

Table 2.4: Primers Employed for Gene Expression Analysis and Gateway Cloning

Primer name	Purpose	Sequence 5' - 3'	Annealing temp.	mRNA Accession No.
JAZ1 FW	Gene Expression Analysis	CCAATTGCGAGACGAAATTCACTTAC	60 °C	AB433896
JAZ1 RV		CCAAGCCATGCCTTATTTTCCTCATTC		
JAZ2 FW		GCAGCACCTGCTCAACTGACC	60 °C	AB433897
JAZ2 FW		GCACCACATTAGGAGGAACGCAACC		
JAZ3 FW		GGATTCCGGTCGATTCGCCG	60 °C	AB433898
JAZ3 FW		CCAAGGCTGAGATCTCCAAAGGAAC		
OPR3 FW		GGTAGGGTTGGAAGTGAAGAGG	60 °C	XM_016592560
OPR3 RV		ATGACACAAGATCAGCATCACC		
AOC4 FW		AGAGAATTGGAATAACAGCAGG	60 °C	XM_016586618
AOC4 RV		AAGTGTCCTCGTAAGTCAAGT		
L25 FW		GTTGCCAAGGCTGTCAAGTCAGG	60 °C	L18908
L25 RV		GCACTAATACGAGGGTACTTGGGG		
JASSY FW	Gateway Cloning	ATGAGAACGGAGGGTCAGAG	64 °C	XM_016595169
JASSY RV		CGATGACTTGGCAATCAAAGAC		

3. Methods

1.1. Plant material / cell culture

In this investigation, *Nicotiana tabacum* cv. "Bright Yellow 2" (voucher KIT 8579) was employed as an effective model system to explore stromule formation. Specifically, the *Nicotiana tabacum* L. cv. Bright Yellow 2 (BY-2 cells) (Nagata et al. 1992) was cultivated in a liquid medium comprising 4.3 g/L Murashige and Skoog basal salts, 30 g/L sucrose, 200 mg/L KH2PO4, 100 mg/L inositol, 1 mg/L thiamine, and 0.2 mg/L (0.9 µM) 2,4-D, with the pH adjusted to 5.8. The cells underwent weekly subculturing by transferring 1.5 ml of stationary-phase cells into 30 ml of fresh medium contained within 100 ml Erlenmeyer flasks. Cultures were maintained at 26 °C under constant agitation at 150 rpm using an IKA Labortechnik KS260 basic orbital shaker (IKA, Germany). Stock calli were routinely sub-cultured on solid media containing 0.8% (w/v) Danish agar (Roth, Germany) every four weeks. For the transgenic strains, both suspension cultures and calli were maintained in the same medium as the non-transformed wild-type (BY-2 WT), supplemented with plant selective antibiotic to ensure selective pressure.

1.2. PCR Protocol

The target gene was amplified in a 25 µl reaction mixture containing the following components: 16 µl of nuclease-free H2O (Lonza, Biozym), 5X Q5 Reaction Buffer (New England Biolabs), 200 µM dNTPs (New England Biolabs), 0.5 µM of each forward and reverse primer, 100-150 ng of cDNA template, and 0.75 units of Q5 High-Fidelity DNA Polymerase (New England Biolabs).

The thermal cycling conditions were as follows:

- Initial denaturation at 98°C for 30 seconds

35 cycles of:

- Denaturation at 98°C for 10 seconds
- Annealing at 55–65°C for 30 seconds
- Extension at 72°C for 20–30 seconds per kilobase
- Final extension at 72°C for 2 minutes

Agarose gel electrophoresis was performed using NEEO ultra-quality agarose (Carl Roth, Karlsruhe, Germany) to evaluate the PCR products. DNA visualization was facilitated by

SYBRsafe (Invitrogen, Thermo Fisher Scientific, Germany) or Midori Green Xtra (Nippon Genetics Europe GmbH) dyes, along with blue light excitation. Fragment sizes were determined using 100 bp or 1 kb size standards (New England Biolabs).

1.3. RNA extraction and cDNA synthesis

Thirty milliliters of four-day-old BY-2 cells underwent various treatments while being positioned on an orbital shaker (150 rpm) at 26°C in darkness. Following treatment, cells were harvested at specific intervals, as outlined in Section 3.2. To extract RNA, the liquid medium was filtered off using a Büchner funnel, and the cells were transferred into 2 ml reaction tubes, with 100 mg of cells per tube. The refilled tubes containing cells were immediately frozen in liquid nitrogen and subsequently ground using a Tissuelyser (Qiagen) equipped with a 5 mm steel bead.

Total RNA was extracted employing an enhanced RNA extraction technique using the Universal RNA Purification Kit, following the manufacturer's instructions (Roboklon). The integrity and purity of the RNA preparation were verified by electrophoresis on a 1% (w/v) agarose gel. RNA concentration was measured using a Nanodrop spectrophotometer (peqlab Biotechnologie GmbH, ND-1000 Spectrophotometer, Erlangen, Germany).

For cDNA synthesis, 100 ng of template RNA was converted into cDNA using SuperScript® II Reverse Transcriptase (Thermo Fisher Scientific). Reverse transcription was performed on 1 µg of RNA to synthesize cDNA using the M-MuLV reverse transcriptase. To achieve the desired final RNA concentration of 1 µg, a primary mastermix containing 0.4 µl of 10 mM dNTPs and 1 µl of oligo dT (100 µM) was prepared and mixed with the corresponding amount of RNA. The reaction volume was adjusted to 16 µl with RNase-free water based on the RNA concentration.

After incubation of the primary mastermix at 65°C for 5 minutes, a secondary mastermix consisting of 2 µl of reverse transcriptase buffer, 0.25 µl of M-MuLV reverse transcriptase, 0.50 µl of RNase inhibitor, and 1.25 µl of RNase-free water was added. The reaction was then continued at 42°C for 60 minutes, followed by 90°C for 10 minutes, and finally at 12°C for the final storage phase. The quality of the cDNA was verified by PCR using primers specific for the L25 gene, serving as a reference gene (Table 2.4).

1.4. Gateway-cloning and transformation

To investigate the expression, and subcellular localization of the candidate gene (JASSY), fluorescent labeling was conducted using Gateway recombination cloning technology (Gateway® Technology with Clonase® II by Invitrogen™ Life Technologies) according to the supplier's user guide. Constructs for expression in tobacco BY-2 cells were generated in two steps using the Gateway cloning method: the BP reaction to create the entry clone and the LR reaction to create the expression clone.

- **Primer Design and PCR Amplification**

For the initial amplification of genes, PCR was performed using attB1 and attB2 primer pairs. These primers were modified by appending specific sequences, listed in Table 2.4, to their ends:

- **attB1 sequence:** 5' GGGGACAAGTTTGTACAAAAAAGCAGGCTTC 3' + Forward primers
- **attB2 sequence:** 5' GGGGACCACTTTGTACAAGAAAGCTGGGTC 3' + Reverse primers (without stop codon)

The PCR conditions included an annealing temperature of 64°C, as specified in previous protocols.

- **Cloning Steps**

1. BP Reaction: This step involves the creation of the entry clone using the amplified gene fragments flanked by attB sequences.
2. LR Reaction: This step involves the recombination of the entry clone with a destination vector to create the expression clone.

By following these steps, we successfully generated constructs for studying the JASSY gene in tobacco BY-2 cells, enabling detailed analysis of its subcellular localization and regulatory mechanisms.

1.4.1. BP reaction

The PCR products were incorporated into the pDONR/Zeo vector (Invitrogen) using the BP reaction. This reaction was set up with 1 µl of PCR product (50-150 ng), 1 µl of pDONR/Zeo (150 ng/µl), 1 µl of BP Clonase II enzyme, and TE buffer to achieve a final volume of 5 µl.

The reaction mixture was incubated at 25°C for 18 hours. To terminate the reaction, 1 µl of

proteinase K was added, followed by an additional incubation at 37°C for 10 minutes. The resultant mixture was then transformed into E. coli DH5α competent cells via heat shock. Specifically, the BP reaction product was mixed with 100 µl of chemically competent DH5α cells and placed on ice for 30 minutes. The mixture was then heat-shocked in a 42°C dry bath for 60 seconds and promptly returned to ice for 2 minutes. Afterward, 950 µl of LB medium was added, and the cells were incubated at 37°C with continuous shaking at 180 rpm for 2 hours.

Following incubation, the cells were centrifuged at 3000 rpm for 2 minutes, and the supernatant was discarded, leaving approximately 100 µl of medium. The cell pellet was resuspended in this remaining medium and plated on LB-agar plates containing 0.1% ampicillin, 0.2% IPTG, and 0.8% X-gal. The plates were incubated overnight at 37°C and subsequently stored at 4°C until screening.

Colonies, indicating successful transformation, were picked and transferred to 1 ml of liquid LB medium containing 0.1% ampicillin in sterile eppendorf tubes. These cultures were incubated at 37°C with shaking at 180 rpm. After 2 hours, 1 µl of the culture was taken for colony PCR to confirm the presence of the transformed vector.

- **Colony PCR**

The colony PCR was set up with a 20 µl reaction volume consisting of:

- 10.9 µl of nuclease-free H2O (Lonza, Biozym)
- µl of 10X ThermoPol Buffer (New England Biolabs)
- 200 µM dNTPs (New England Biolabs)
- 0.2 µM of each forward and reverse primer (refer to Table 2.4 for primer details)
- 100-150 ng of DNA template (colony PCR culture)
- 0.1 µl of Taq polymerase (New England Biolabs)

The thermal cycler conditions were as follows:

- Initial denaturation at 94°C for 1 minute

30 cycles of:

- Denaturation at 94°C for 30 seconds
- Annealing at 55-65°C for 30 seconds
- Extension at 68°C for 1 minute per kilobase
- Final extension at 68°C for 5 minutes

This process confirmed the successful amplification of the target gene, verifying the presence of the desired construct in the transformed E. coli cells.

Post-transformation, the cells were spread on LB agar plates containing 50 µg/ml zeocin and incubated overnight at 37°C. The next day, a single colony was picked and cultured in 5 ml of liquid LB medium with 50 µg/ml zeocin at 37°C, with continuous shaking at 180 rpm. The plasmids were extracted the following day using the Roth®-Prep Plasmid MINI kit (Roth, Germany), and successful insertion was confirmed through sequencing (GATC Biotech, Cologne, Germany). These entry clones were then used in the subsequent LR reaction.

1.4.2. LR reaction

The LR reaction was utilized to clone expression vectors fused with GFP. The reaction setup included the following components:

- 1 µl of entry clone (50-150 ng)
- 1 µl of pK7FWG.2 (150 ng/µl)
- 1 µl of LR Clonase II enzyme
- TE buffer, added to reach a total volume of 5 µl

The LR reaction was incubated at 25°C for 18 hours. To stop the reaction, 1 µl of proteinase K was added and incubated at 37°C for 10 minutes. The procedure for the LR reaction mirrored the steps used in the BP reaction, including E. coli DH5α transformation and colony PCR, except for using 100 µg/ml Spectinomycin as the selection antibiotic. Following sequencing confirmation of the constructs, the expression vectors were introduced into *Agrobacterium tumefaciens* for further applications.

1.4.3. Transformation of *Agrobacterium tumefaciens* with FP-labelled expression plasmids

To introduce FP-labeled expression plasmids into *Agrobacterium tumefaciens* (strain LBA4404; Invitrogen Corporation, Paisley, UK), 100 µl of chemo-competent cells were initially thawed on ice. Then, 500 ng of the expression vector containing the target genes was added to the cells. The freeze-thaw transformation method, as described by Weigel and Glazebrook (2006), was employed (Weigel and Glazebrook 2006). The mixture of cells and plasmid was rapidly frozen in liquid nitrogen for 5 minutes and then warmed to 37°C in a dry bath for 10 minutes. Following this, 900 µl of antibiotic-free LB medium was added under sterile conditions, and the cells were

incubated with shaking at 180 rpm for 3 to 5 hours. After incubation, the transformed cells were plated on LB agar containing 100 µg/ml rifampicin, 300 µg/ml streptomycin, and 100 µg/ml spectinomycin. The plates were kept in the dark at 28°C for 2-3 days.

Post incubation, several single colonies were picked and inoculated into 1 ml of LB liquid medium containing the same selective antibiotics. These cultures were grown overnight at 28°C with vigorous shaking. To verify the presence of the desired gene, colony PCR was conducted on the overnight cultures using specific primers, as detailed in the BP reaction section.

One colony that was confirmed to be positive through PCR was chosen for further application. This confirmed colony was then used to establish stable transgenic tobacco BY-2 cell lines, facilitating subsequent experiments in plant cell research. This methodology ensures the effective transformation of *Agrobacterium tumefaciens* with the FP-labeled expression plasmid, enabling further detailed studies.

1.5. Generation and Stabilization of Transgenic Tobacco BY-2 Cell Lines

Following the method described by Buschmann et al. (2011), with modifications for enhanced performance, stable transgenic cell lines overexpressing the JASSY gene were established (Buschmann et al. 2011). This involved two main preparations: BY-2 WT cells and *Agrobacterium tumefaciens* cells.

- **Preparing BY-2 WT Cells**

Initially, 1.5 ml of 7-day-old BY-2 WT cells were sub-cultured and maintained for four days under standard conditions: 26°C with continuous shaking at 150 rpm. Subsequently, two flasks, each containing 30 ml of suspension culture, were pooled and washed twice with 700 ml of Paul's medium (containing 4.3 g/l Murashige and Skoog salts, 10 g/l sucrose, pH 5.8). The washing was performed using a Nalgene reusable bottle top filter and a nylon mesh with 70 µm pores.

- **Preparing *Agrobacterium tumefaciens* Cells**

A 150 µl overnight culture of a colony, which had been verified by colony PCR, was added to 5 ml of LB liquid medium containing selective antibiotics and shaken vigorously overnight at 28°C. The following day, 1.5 ml of this culture was transferred to 5 ml of fresh LB medium

without antibiotics and incubated for 4-6 hours at 150 rpm until an OD600 of 0.8 – 1 was achieved. The Agrobacterium cells were then centrifuged at 8000 g for 8 minutes at 4°C. After discarding the LB supernatant, the pellet was resuspended in 180 µl of Paul's medium, ensuring a homogenous suspension by pipetting.

- **Co-cultivation and Selection**

Six milliliters of prepared BY-2 WT cells were combined with 180 µl of the Agrobacterium suspension and shaken on an orbital shaker at 100 rpm and a 30° angle for five minutes. This mixture was then spread onto petri plates covered with a single layer of sterile filter paper and solidified Paul medium with 0.5% (w/v) Phytagel™ (Sigma-Aldrich), without antibiotics. The plates were sealed with parafilm and incubated in the dark at 22°C for four days.

Following this incubation, the filter paper and cell plaques were transferred to MS agar plates containing 300 mg/ml cefotaxime and selective antibiotics (100 mg/ml kanamycin and 100 mg/ml hygromycin). These plates were incubated at 26°C in the dark. After approximately four weeks, the developing calli were moved to new MS agar plates with the same antibiotics to promote further growth.

To verify the expression of JASSY in the transgenic cell lines, RNA was extracted, and cDNA was synthesized as previously described. Quantitative PCR (qPCR) was then performed to assess gene expression levels.

1.6. Analysis of Gene Expression via Quantitative PCR (qPCR)

To explore potential post-transcriptional regulation in tobacco, the transcript levels of five key genes (JAZ1, KAZ2, JAZ3, AOC4, and OPR3) were quantified using quantitative real-time PCR (qPCR). This experiment utilized the CFX96 Touch™ Real-Time PCR Detection System from Bio-Rad Laboratories GmbH (Munich) and employed the specific qPCR primers listed in Table 2.4.

Each qPCR reaction was prepared in a 20 µl volume, comprising 200 nM of each primer and dNTP, 1x GoTaq Buffer, 2.5 mM MgCl2, 0.5 units of GoTaq polymerase, 1x SYBR Green, and 1 µl of cDNA diluted 1:20. The precise component volumes were 4 µl of 5x GoTaq Buffer, 0.4 µl of 5 mM dNTP mix, 0.4 µl of 10 µM forward primer, 0.4 µl of 10 µM reverse primer, 0.1 µl of GoTaq Polymerase (Promega), 0.95 µl of SYBR Green, 1 µl of cDNA template (diluted 1:10),

1 µl of 50 mM MgCl2, and 11.75 µl of ddH2O.

The thermal cycler conditions were established as follows: an initial denaturation at 95°C for 3 minutes, followed by 40 cycles of 94°C for 10 seconds and 60°C for 20 seconds. During the extension phase, 72°C was maintained for 15 seconds, with a plate read step after each cycle. Ribosomal Protein L25, identified as the most stable housekeeping gene, was used as an internal control. Each biological replicate was tested in three technical replicates. The real-time data obtained were analyzed using the $2^{-\Delta Ct}$ method as described by Livak and Schmittgen (2001) (Livak and Schmittgen 2001).

The Ct values (cycle threshold; the cycle number at which the fluorescence signal exceeds the threshold) were recorded for individual samples. Relative gene expression was determined by calculating the difference in Ct values between the target genes and the housekeeping gene ($\Delta Ct = Ct_{\text{target}} - Ct_{\text{endogenous control}}$). The $2^{-\Delta Ct}$ method was applied to quantify relative expression levels, illustrating gene expression under various treatment conditions controlled by the 35S promoter. To evaluate statistical significance in gene expression differences across treatments, Analysis of Variance (ANOVA) was conducted using IBM SPSS Statistics 29.0 (IBM, Armonk, USA), followed by Tukey's Honestly Significant Difference (HSD) multiple range test, with the significance threshold set at $P \leq 0.01$. The data presented represent mean values derived from a minimum of three independent replicates.

1.7. Drug Treatment Approuch

Methyl jasmonate (MeJA), a stress-related plant hormone sourced from Sigma-Aldrich Chemie GmbH, was dissolved in 50% ethanol (EtOH) to achieve final concentrations of 30, 50, and 100 µM. Similarly, salicylic acid (SA), another stress-related hormone from Sigma-Aldrich, was prepared in 1% dimethyl sulfoxide (DMSO) at a concentration of 100 µM. Oryzalin, procured from Chem Service, Inc. (West Chester, USA), was used as a microtubule polymerization inhibitor at a concentration of 10 µM. Latrunculin B, obtained from Sigma-Aldrich (Germany), was employed to inhibit actin polymerization at 2 µM. Additionally, phenidone from Sigma-Aldrich (Germany) was used at a concentration of 2 mM to inhibit lipoxygenases and modulate jasmonic acid (JA) accumulation. Both latrunculin B and phenidone were dissolved in 1% DMSO.

Stock solutions were prepared as follows: 10 mM for oryzalin, 1 mM for latrunculin B, 1 M for

phenidone, 100 µM for SA, and 30, 50, and 100 µM for MeJA. In the experimental setup, 1 mL of 4our-day-old BY-2 cells was treated with 1 µL of oryzalin, 2 µL of phenidone, 2 µL of latrunculin B, 1 µL of SA, and 1 µL of MeJA. These treatments were administered to tobacco BY-2 cells four days post sub-culturing. For the MeJA, SA, oryzalin, and latrunculin B treatments, the cells were incubated with the respective agents for one hour, with DMSO and EtOH serving as controls. The phenidone treatment involved a 30-minute incubation prior to analysis. Depending on the experimental design, drug treatments were applied either individually or in combination. Following treatment, the cells were prepared for subsequent microscopy, gene expression analysis (quantitative PCR (qPCR) analysis).

1.8. Fluorescent Tracker Days

Actin filament visualization was achieved following a protocol adapted from Maisch and Nick (2007), entailing a meticulous series of steps to ensure optimal staining fidelity (Maisch and Nick 2007). Initially, 0.5 mL of BY-2 cell suspension underwent fixation for 10 minutes in a freshly prepared solution comprising 1.8% w/v paraformaldehyde in 0.1 M PIPES buffer supplemented with 5 mM MgCl2 and 10 mM EGTA, maintaining a neutral pH of 7. Subsequent permeabilization of cells occurred through exposure to a 1% glycerol solution in the same buffer for an additional 10-minute interval. Following permeabilization, cells underwent dual 10-minute washes in the buffer to remove excess fixative and permeabilization agent. Subsequently, cells were incubated in darkness with 0.66 µM TexasRed-Phalloidin (Sigma-Aldrich Chemie GmbH, München) for 35 minutes to selectively label actin filaments. Unbound dye was thoroughly removed through a sequence of three 10-minute washes in phosphate-buffered saline (PBS) featuring a pH of 7.2, comprising 0.15 M NaCl, 2.7 mM KCl, 1.2 mM KH2PO4, and 6.5 mM Na2HPO4. Following staining, cells were mounted for examination under a spinning disc microscope, facilitating high-resolution visualization.

To elucidate the spatial relationship between actin filaments and stromules, an experimental paradigm incorporating BY-2 cells expressing tpFNR fused with mEOS as a stroma marker was employed. Prior to fixation and actin filament staining, these cells were subjected to a pre-incubation period of one hour with 100 µM MeJA. This pre-treatment aimed to modulate cellular responses and enable the examination of potential correlations between actin dynamics and stromule morphology.

1.9. Enhanced Cellular Visualization: Uniting Confocal Imaging with AI Analysis

To achieve enhanced spatial resolution visualization of individual BY-2 cells, we employed spinning disk confocal microscopy. Images were acquired using an AxioObserver Z1 inverted microscope (Zeiss, Jena, Germany) equipped with a Yokogawa CSU-X1 Spinning Disc Unit (Yokogawa Electric Corporation, Tokyo, Japan). A high-resolution Plan-Apochromat 63x/1.40 Oil DIC M27 oil immersion objective was utilized for optimal magnification and numerical aperture. Fluorescent proteins were excited using laser lines at 488 nm for GFP (EGFP) and 590 nm for RFP (mCherry or mRF12). Z-stack images were acquired to capture the three-dimensional structure of BY-2 cells. This approach allowed for the systematic division of each cell into multiple optical sections, enabling comprehensive examination of cellular structures throughout the entire volume. Images were captured using the Z-Stack program, which facilitated the acquisition of a series of images at precisely defined focal planes. To ensure data integrity and facilitate subsequent analysis, image files were saved in both proprietary CZI and universal TIFF formats.

Following acquisition, post-processing was carried out, which included cropping and adjustments to brightness/contrast. This was achieved using the image processing features within Zen desk 3.6, as well as Adobe Photoshop.

The quantitative assessment of stromules was significantly enhanced through the integration of advanced artificial intelligence (AI) techniques. Utilizing the APEER Viewer platform, developed through a collaboration between ZEISS and ZEISS arivis Cloud, we implemented a sophisticated AI model specifically tailored for deep image analysis of plant cell structures. This model employed pixel-based semantic segmentation, trained on a comprehensive dataset of 100 BY-2 cell images in CZI format, to accurately identify and delineate plastids and stromules.

For precise measurements and analysis, we employed Zeiss ZEN desk version 3.6 software. This powerful tool facilitated the extraction of quantitative data from the AI-processed images, including accurate measurements of stromule lengths and quantities. The software's advanced capabilities allowed for high-throughput analysis of cellular structures, significantly enhancing the efficiency and reliability of our data collection process.

Our experimental design involved the systematic treatment of BY-2 cells with various

phytohormones and inhibitors at different developmental stages, ranging from 0 to 5 days post-subcultivation. On average, 30 BY-2 cells were analyzed per experimental condition, ensuring a robust sample size for statistical analysis

For statistical evaluation, we implemented the Fligner-Killeen test using Python's SciPy library (scipy.stats.fligner). This non-parametric test, which uses the median as the measure of central tendency, was chosen for its robustness in assessing variance equality, particularly in datasets where outliers may be present, or normality assumptions are not met. The Fligner-Killeen test's resilience to departures from normality makes it particularly suitable for biological data, where natural variability and potential outliers are common (Fligner and Killeen 1976).

By combining cutting-edge AI-driven image analysis with rigorous statistical methods, we were able to achieve a comprehensive and nuanced understanding of stromule dynamics in response to various cellular stimuli and developmental stages.

4. Results

Our investigation into stromule formation and dynamics in tobacco BY-2 cells was driven by the need to develop a controlled system for inducing and studying these enigmatic plastid extensions. The main objective was to create a solid experimental framework for conducting time-course analyses, exploring the factors involved in stromule formation, and studying their interactions with other cellular structures, especially the cytoskeleton.

We systematically explored various conditions that could reliably trigger stromule formation. Our approach included a variety of treatments, such as different phytohormones and abiotic stresses. This study aimed to identify the most effective methods for inducing stromules, providing a foundation for further investigations into stromules formation, function, and regulatory.

4.1. Induction of Stromule Formation by Stress-Related Phytohormones in Tobacco BY-2 Cells

We first examined the effects of various stress-related phytohormones to develop a reliable method for inducing stromules in BY-2 cells. Previous research has provided convincing evidences that plant stress-response signal molecules, including hydrogen peroxide (H2O2), salicylic acid (SA), and abscisic acid (ABA), play crucial roles in the induction of stromules (Caplan et al. 2015). Building on this knowledge, we aimed to expand our understanding by investigating the effects of methyl jasmonate (MeJA) on stromule induction. Our choice to focus on MeJA was motivated by its well-established role in plant stress responses and its potential involvement in plastid-to-nucleus retrograde signaling. By comparing MeJA with SA, we aimed to demonstrate whether different stress-related phytohormones induce stromules through similar or separate mechanisms. To this end, we treated BY-2 cells with 100 µM MeJA or 100 µM SA for one hour, four days post-subcultivation. This concentration and duration were selected based on former studies indicating efficacy of phytohormones in triggering stress responses in plant cells. Our experimental design allowed us to directly compare the stromule-inducing capabilities of these two important stress-related phytohormones.

Our findings revealed that exogenous MeJA (100µM) induced stromule formation at levels

comparable to those induced by exogenous SA (100µM) (Figure 1). The induction of stromule formation by stress-related phytohormones in tobacco BY-2 cells was investigated using confocal microscopy and frequency distribution analysis. Panels A, B, and C of Figure 1 present geometric projections of confocal z-stacks for representative cells expressing Sensitive to Freezing 2 (SFR2) localized in the outer plastid membrane in fusion with mRFP. Untreated control cells (Figure 1A) exhibit a baseline level of stromule formation with varied lengths. In contrast, cells treated with 100 µM of Methyl Jasmonate (MeJA) for 1 hour (Figure 1B) and cells treated with 100 µM of Salicylic Acid (SA) for 1 hour (Figure 1C) show a noticeable increase in stromule formation with more pronounced and elongated structures.

The frequency distributions of stromule lengths are represented in Figure 1D through pie charts for untreated control cells, MeJA-treated cells, and SA-treated cells. The lengths are categorized into four groups: <10 µm, 10-20 µm, 20-30 µm, and >30 µm. In control cells (n=363), most stromules are less than 10 µm long, with fewer stromules in the longer categories.

However, both MeJA-treated (n=1036) and SA-treated cells (n=1051) show a shift towards longer stromule lengths compared to the control (n=363). Notably, there is an increase in the proportion of stromules in the 20-30 µm and >30 µm categories. Specifically, the proportion of stromules over 30 µm increased to around 10% in both MeJA and SA-treated cells, compared to less than 5% in control cells. Panel E uses a bar graph to illustrate the frequency shifts in stromule lengths for the three conditions. The frequencies are percentages for the length categories 20-30 µm and >30 µm. In control cells, the frequency of stromules in 20-30 µm and 30 µm categories is relatively low compared to the total number of stromule population across all three experimental conditions. Both MeJA and SA treatments significantly increase the frequency of stromules in these length categories. Statistical analysis indicates significant differences ($P<0.05$) between the control and treated groups, as denoted by different letters (Figure 4), based on the non-parametric Fligner-Killeen test.

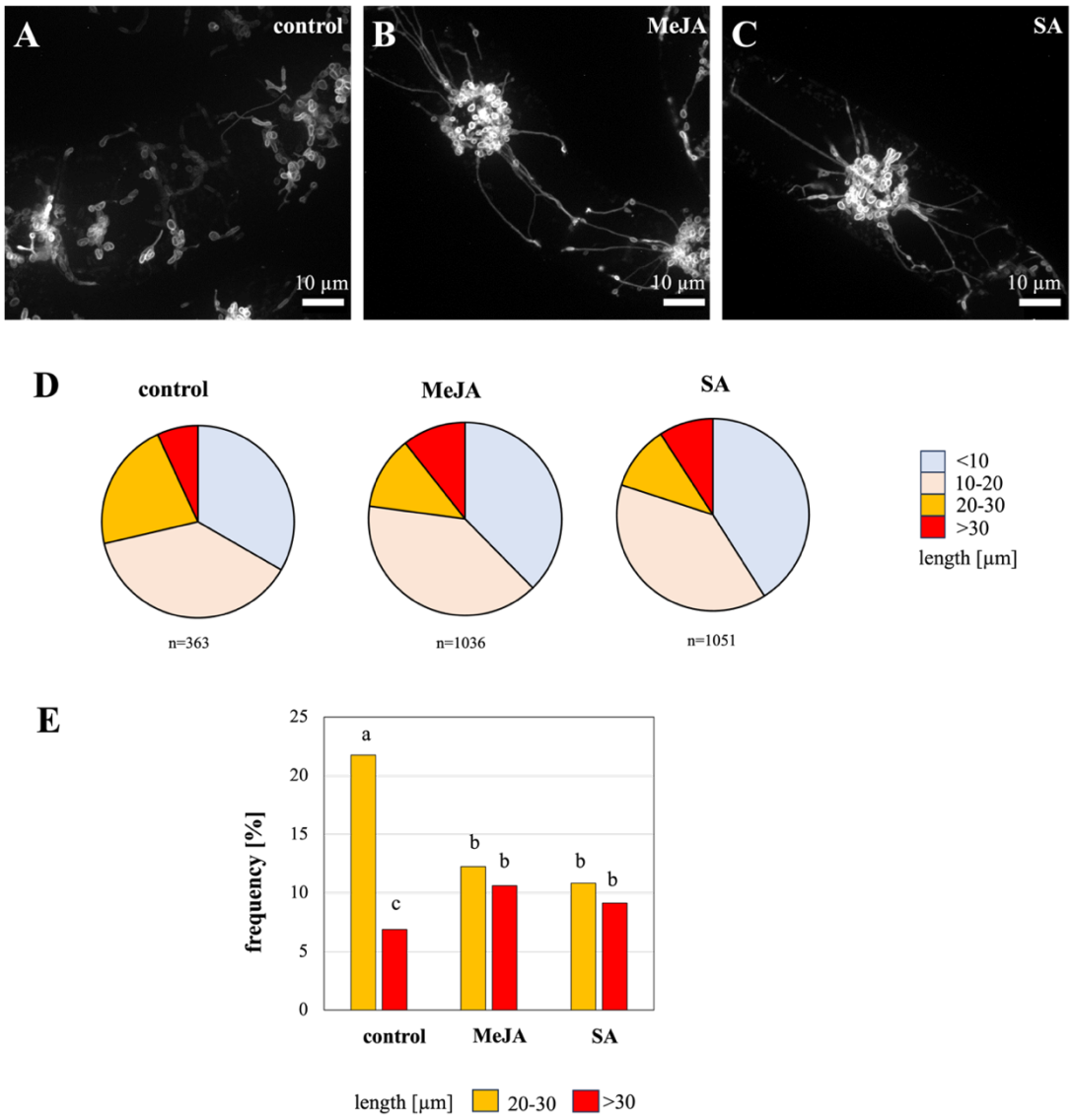

Figure 1. Induction of stromulation by stress-related phytohormones in tobacco BY-2 cells. A-C Geometric projections of confocal z-stacks for representative cells expressing Sensitive to Freezing 2 (SFR2) localised in the outer plastid membrane in fusion with mRFP. **A** Untreated control cell. **B** Cell after treatment with 100 µM of Methyl Jasmonate (MeJA) for 1 h. **C** Cell after treatment with 100 µM of Salicylic Acid (SA) for 1 h. **D** Frequency distributions of stromule length for the three conditions. **E** Shifts in frequency for stromules 20-30 µm and >30 µm in length. Different letters indicate differences significant at $P<0.05$ based on the non- parametrical Fligner-Killeen test.

The new data in Figures 4A and 4B further supports these findings. Figure 4A displays heatmaps illustrating the distribution of stromule lengths under various treatments. Specifically, the heatmap shows that the incidence of stromules in the >30 µm range is highest for MeJA and SA treatments, with values reaching over 35 for both treatments. The quantified incidence of stromules under three conditions demonstrates that methyl jasmonate (MeJA) and salicylic acid (SA) significantly increase longer stromules compared to the control group.

This statistical finding highlights the impact of MeJA and SA on stromule formation, suggesting that these phytohormones play a crucial role in regulating stromule dynamics.

4.2. SA-Induced Stromule Formation Blocked by Phenidone

To further elucidate the mechanisms controlling stromule formation, we investigated the potential role of jasmonic acid (JA) biosynthesis in SA-induced stromule formation. We used phenidone, a known inhibitor of lipoxygenase, which is critical in the octadecanoid pathway and is responsible for JA synthesis. We aimed to determine whether basal JA levels are necessary for SA-induced stromule formation, thereby uncovering potential crosstalk between these stress-signaling pathways. This experiment aimed to bridge the gap in understanding how different phytohormones cooperate or antagonize each other in regulating plastid dynamics.

Our study analyzed tobacco BY-2 cells expressing the Sensitive to Fr (SFR2) protein, localized in the outer plastid membrane in fusion with mRFP, using confocal z-stack projections. The untreated control group (Figure 2A) displayed stromules with varying lengths, predominantly less than 10 µm. In contrast, cells treated with 2 mM phenidone for 90 minutes (Figure 2B) showed a reduction in stromule formation, with the distribution of stromule lengths remaining similar to the control, primarily less than 10 µm.

Treatment with 100 µM SA for 60 minutes (Figure 2C) significantly increased stromule formation, resulting in a higher frequency of longer stromules, particularly those measuring 20-30 µm and longer than 30 µm. However, pre-treatment with 2 mM phenidone for 30 minutes followed by treatment with 100 µM SA for 60 minutes (Figure 2D) markedly reduced the SA-induced stromule formation. The frequency of longer stromules (20-30 µm and >30 µm) was significantly decreased compared to cells treated with SA alone. The frequency distributions of stromule lengths under the four conditions are summarized in Figure 2E. In the untreated control and phenidone-treated cells, stromules predominantly measured less than 10 µm in

length, with 363 and 321 stromules counted, respectively. SA treatment, with 1051 total stromules counted, showing a considerable increase in the frequency of stromules measuring 20-30 µm and longer than 30 µm. This effect was significantly reduced by pre-treatment with phenidone, with only 146 stromules counted.

Figure 2F presents the frequency of stromules in different length categories. The data indicate significant shifts in stromule length distribution, with SA treatment increasing the frequency of longer stromules. Different letters above the bars indicate statistically significant differences ($P<0.05$) based on the non-parametric Fligner-Killeen test.

The data from Figure 4 further elucidates the effects of phenidone and SA on stromule formation. Figure 4A shows that the control group has a baseline incidence of stromules. At the same time, SA treatment markedly increases stromule incidence, particularly in the 30-40 µm length range, indicating a strong stimulatory effect of SA on stromule formation. When cells are treated with SA in the presence of phenidone, the incidence of stromules is significantly reduced compared to SA treatment alone, indicating that phenidone effectively inhibits the increase in stromule formation induced by SA. Figure 4B shows that the combined treatment of SA and phenidone results in a significant reduction in stromule incidence compared to SA alone, reinforcing the inhibitory effect of phenidone.

The results demonstrate that phenidone effectively blocks the formation of stromules induced by SA, suggesting a potential role for phenidone in modulating plastid dynamics in response to SA signaling. These findings highlight the complex interplay between SA and JA pathways in regulating stromule formation.

4.3. Oryzalin Inhibits MeJA-Induced Stromule Elongation

Expanding upon our findings of MeJA-induced stromule formation, we aimed to investigate the role of the cytoskeleton in this process. Specifically, we focused on microtubules, given their known involvement in organelle movement and cellular architecture. To analyze the contribution of the microtubules to stromule initiation, elongation, and maintenance, we employed Oryzalin, a microtubule-depolymerizing agent. This experiment was designed to provide insights into the molecular mechanisms that control stromule dynamics and their interaction with cellular architecture.

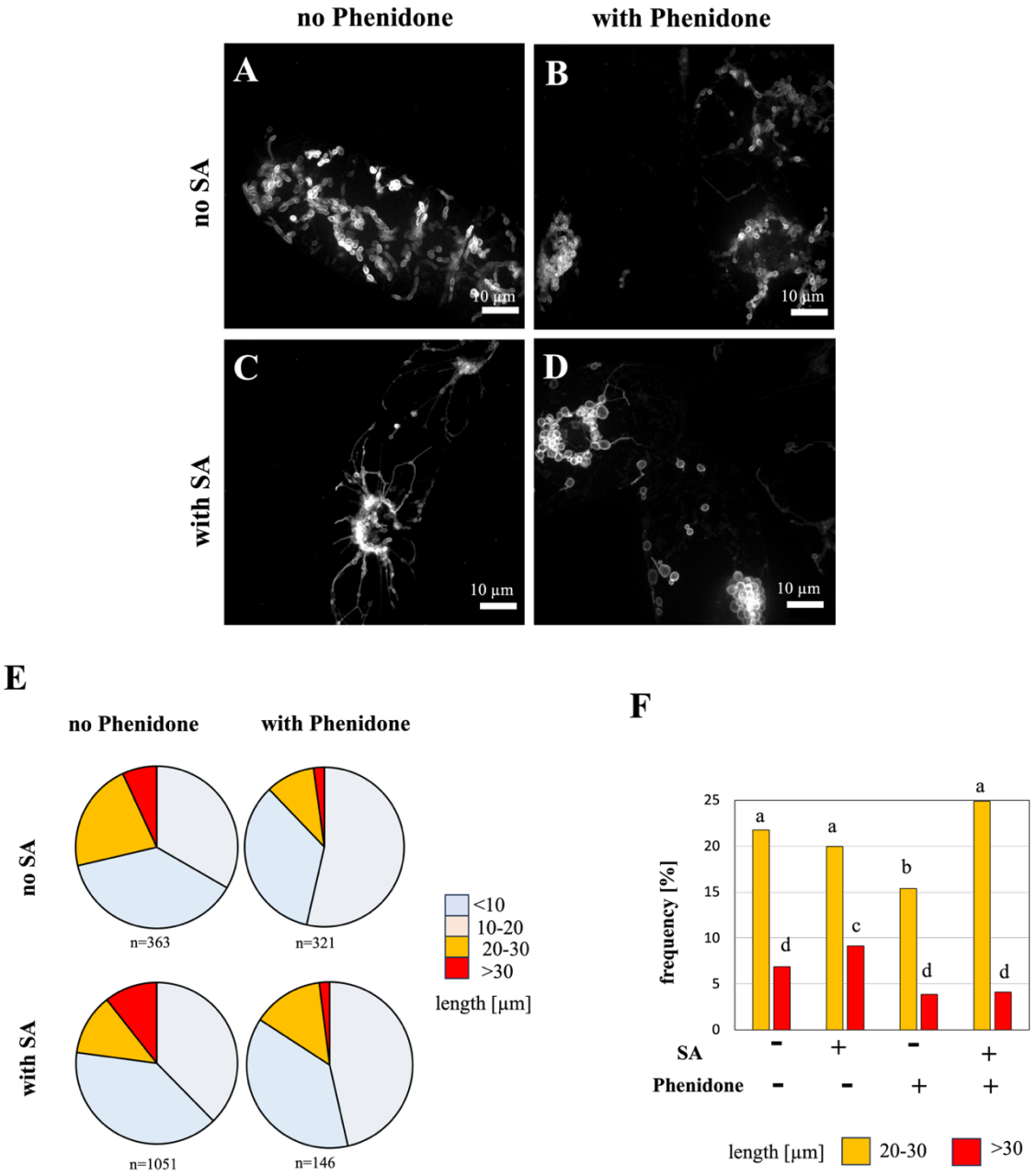

Figure 2. SA-induced stromulation can be blocked by phenidone, and lipoxygenase inhibitor. Representative tobacco BY-2 cells expressing Sensitive to Freezing 2 (SFR2) localised in the outer plastid membrane in fusion with mRFP are shown. Images are geometric projections of confocal z-stacks. **A** Untreated control. **B** Treatment with 2 mM of phenidone for 90 min. **C** Treatment with 100 µM of Salicylic Acid (SA) for 60 min. **D** Treatment with 100 µM of SA following a pre-treatment with 2 mM phenidone for 30 min. **E** Frequency distributions of stromule length for the four conditions. **F** Shifts in frequency for stromules 20-30 µm and >30 µm in length. Different letters indicate differences significant at $P<0.05$ based on the non- parametrical Fligner-Killeen test.

To elucidate the role of microtubules in MeJA-induced stromule formation, we treated tobacco BY-2 cells expressing Sensitive to Freezing 2 (SFR2) with MeJA and/or Oryzalin. The cells were visualized using confocal z-stacks to observe stromule formation under different treatment conditions. In the untreated control group (Figure 3A), cells exhibited a baseline level of stromule formation. When treated with 100 µM of Oryzalin for 120 minutes (Figure 3B), there was a noticeable reduction in stromule formation compared to the untreated control, suggesting that Oryzalin disrupts microtubule dynamics, thereby affecting stromule formation. Treatment with 100 µM of MeJA for 60 minutes (Figure 3C) significantly increased stromule formation, indicating that MeJA is a potent inducer of stromule formation. However, when cells were pre-treated with 10 µM of Oryzalin for 60 minutes followed by 100 µM of MeJA (Figure 3D), there was a marked reduction in stromule formation compared to cells treated with MeJA alone.

In Figure 3E, quantitative analysis of stromule lengths under different treatment conditions revealed that in the untreated control group (n=363) and Oryzalin-treated cells (n=321), most stromules were shorter than 10 µm. In contrast, MeJA-treated cells (n=1036) significantly increased the proportion of longer stromules, with notable frequencies in the 20-30 µm and >30 µm length categories. Cells treated with both Oryzalin and MeJA (n=297) exhibited a distribution similar to the control and Oryzalin-treated cells, underscoring the inhibitory effect of Oryzalin on MeJA-induced stromule elongation. Statistical analysis of the frequency distributions of stromule lengths, as shown in Figure 3F, validated these observations. The frequency of stromules in the 20-30 µm and >30 µm categories was significantly higher in MeJA-treated cells compared to other conditions. Different letters in the graph indicate significant differences at $P<0.05$ based on the non-parametric Fligner-Killeen test.

Figure 4 provides a more detailed view of the effects of oryzalin on MeJA-induced stromule formation. MeJA treatment alone markedly increased in stromule incidence across all length classes, with a particularly pronounced effect on stromules in over 30 µm range. In contrast, oryzalin treatment alone decreased in stromule incidence compared to the control, especially for longer stromules. When cells were pre-treated with oryzalin before MeJA application (Ory+MeJA), the MeJA-induced increase in stromule formation was largely prevented, with the distribution and total incidence of stromules resembling those of the oryzalin-only treatment. This finding collectively suggests that Oryzalin can effectively block the MeJA-induced stromule formation, supposedly by disrupting the microtubule network.

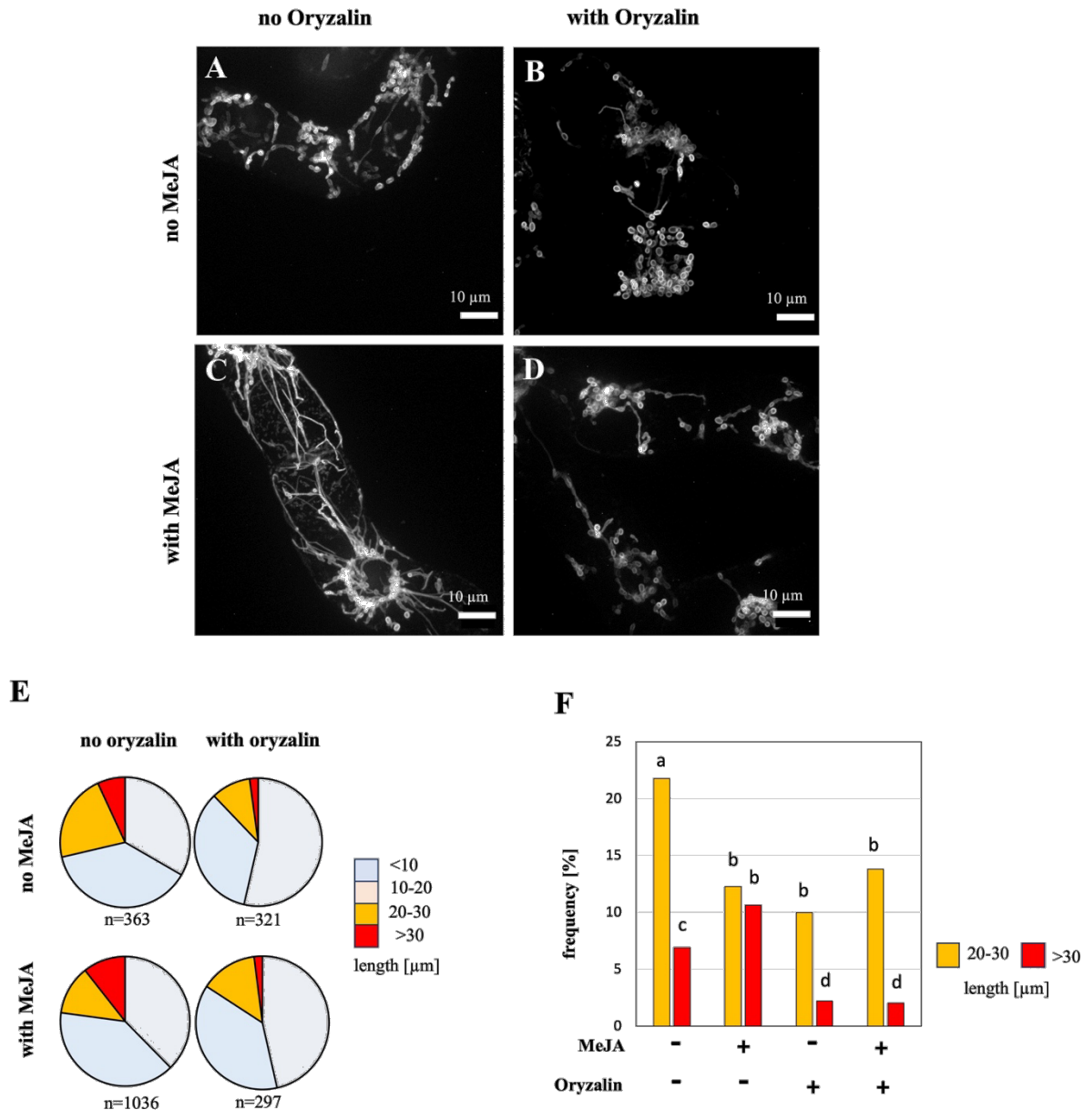

Figure 3. MeJA-induced stromulation can be blocked by Oryzalin, a microtubule-eliminating herbicide. Representative tobacco BY-2 cells expressing Sensitive to Freezing 2 (SFR2) localised in the outer plastid membrane in fusion with mRFP are shown. Images are geometric projections of confocal z-stacks. **A** Untreated control. **B** Treatment with 100 µM of Oryzalin for 120 min. **C** Treatment with 100 µM of MeJA for 60 min. **D** Treatment with 100 µM of MeJA following a pre-treatment with 10 µM of Oryzalin for 60 min. **E** Frequency distributions of stromule length for the four conditions. **F** Shifts in frequency for stromules 20-30 µm and >30 µm in length. Different letters indicate differences significant at $P<0.05$ based on the non- parametrical Fligner-Killeen test.

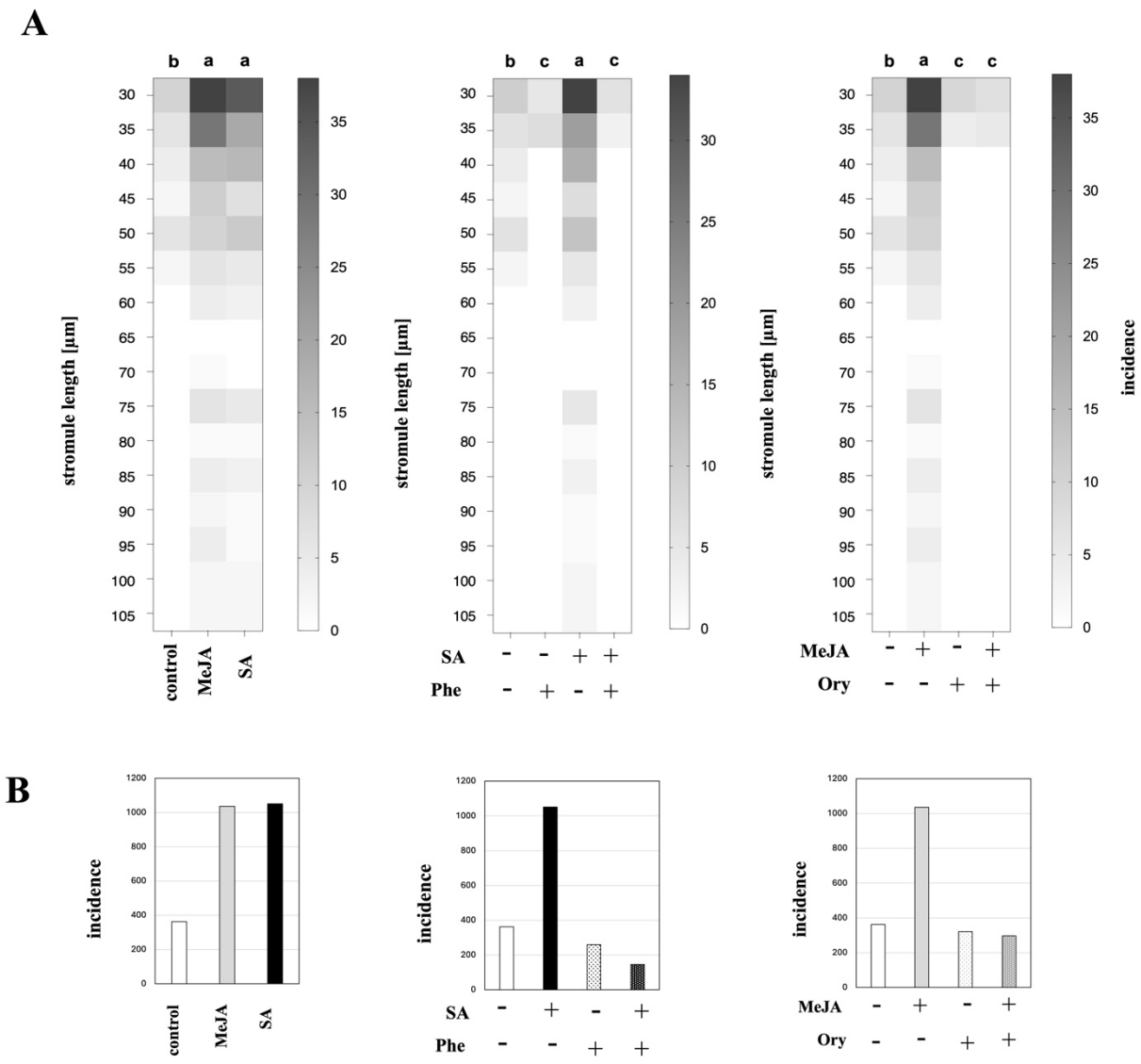

Figure 4. Incidence of stromules depending on their length depending on treatment. A Distribution over different length classes (numbers indicate the center of the respective class). **B** Total incidence of stromules. Incidence refers to the total number of stromules detected by the AI-driven image analysis algorithm in a population of 30 individual cells. Conditions are control untreated, MeJA 100 µM of Methyl Jasmonate for 60 min, SA 100 µM of Salicylic Acid for 60 min, Phe 2 mM of Phenidone for 90 min, Phe+SA 100 µM of SA following a pre-treatment with 2 mM phenidone for 30 min, Ory 100 µM of Oryzalin for 120 min, Ory+MeJA 100 µM of MeJA following a pre-treatment with 10 µM of Oryzalin for 60 min.

4.4. Response of Jasmonate Synthesis and Jasmonate Response Genes to Factors that Modulate Stromulation

To explore deeper into the molecular mechanisms of stromule regulation, we examined the expression profiles of key genes involved in jasmonate synthesis and signaling under various stromule-modulating conditions. Our investigation focused on determining a link between transcriptional alterations and observed phenotypic changes in stromule formation. By analyzing genes such as Allene Oxide Cyclase (AOC), OPDA Reductase (OPR), and JAZ family members, we aimed to reveal the complex regulatory network controling stromule dynamics and its relationship with plant stress responses.

Under various treatments, our analysis examined steady-state transcript levels for Allene Oxide Cyclase (AOC), OPDA Reductase (OPR), which positively control JA synthesis, and the jasmonate response gene JAZ1, JAZ2, and JAZ3, that in protein level act as negative regulators for JA signaling pathway. JAZ/TIFY repressor proteins have been identified as crucial regulators of jasmonic acid (JA) signaling and play a significant role in the crosstalk between JA and salicylic acid (SA) pathways. During normal growth conditions, when JA hormone levels are low, JAZ-proteins act as inhibitors of transcription factors that that regulate the expression of JA-responsive genes (Chini et al. 2007; Yang et al. 2019).

The intracellular compartmentalization of jasmonate biosynthesis is showed in Figure 5B. The pathway begins in the plastid with α-Linolenic Acid, converted by Lipoxygenase (LOX) to 12,13(S)-Allene Oxide via Allene Oxide Synthase. This intermediate is then processed to 12-Oxo-Phyto-Dienoic Acid (OPDA) by Allene Oxide Cyclase (AOC) in the plastid. Then, OPDA is processed by OPDA Reductase (OPR) in the peroxisomes to produce Jasmonic Acid (JA) (Schaller et al. 2004). JA is converted to JA-Ile in the cytoplasm, leading to the indirect activation of JA-responsive genes, including the JAZ genes themselves, in the nucleus. This compartmentalization highlights the complex cellular logistics required for jasmonate biosynthesis and signaling.

As described in Figure 5A, the results reveal differential expression patterns among the genes of interest. The jasmonate response gene JAZ2 demonstrated the most pronounced expression,

with transcript levels reaching approximately 0.190 relative units, followed by JAZ3 at around 0.025. In contrast, AOC, OPR, and JAZ1 show relatively low transcript levels, all below 0.025 relative units. Analysis of gene expression fold changes illustrated in Figure 5C demonstrated distinct responses to methyl jasmonate (MeJA) and salicylic acid (SA) treatments. AOC showed moderate induction in response to MeJA, with an approximately 20-fold increase in expression. The response to SA was less pronounced, with a minimal increase in AOC transcript levels. Interestingly, the highest induction for AOC was observed under the Ory-MeJA treatment, with approximately a 40-fold increase in expression (Figure 5D).

OPR3, encoding 12-oxophytodienoate reductase, exhibited the most pronounced response to MeJA treatments. The MeJA treatments resulted in the highest induction, with approximately 40-fold increases in expression (Figure 5C). Interestingly, the Ory.MeJA combinations did not enhance OPR3 expression to the same extent as MeJA alone, suggesting a possible inhibitory effect of oryzalin on OPR3 induction by MeJA (Figure 5D). In contrast, SA shows fold inductions generally lower than those observed for MeJA in OPR (Figure 5C).

JAZ1, a jasmonate response gene, exhibited the most dramatic changes in expression. MeJA treatment induced a significant induction of JAZ1, showing approximately 150-fold increase, which demonstrates its high sensitivity to jasmonate signaling. In contrast, SA treatment had a minimal effect on JAZ1 expression, showing only a slight increase in transcript levels. Interestingly, despite exogenous MeJA incubation, expression of JAZ1 was significantly induced in the treated cells that stromule formation was prevented by applying oryzalin as an inhibitor of microtubule polymerization (Figure 5D, Supplemental Figure S4).

The response of target genes to Phenidone, Oryzalin, and salicylic acid (SA) treatments appears minimal. AOC, OPR, and JAZs show minimal responses to phenidone alone and in combination with SA post-treatment. These observations align with the primary function of these genes in jasmonate biosynthesis pathway (Figure 5E, F). Phenidone, which inhibits lipoxygenase, has silenced JA-dependent signaling pathways (Bruinsma et al. 2010; Caarls et al. 2015). Leon-Reyes et al. reported that exogenous application of SA led to the downregulation of JA-responsive genes involved in JA biosynthesis, such as LOX, AOS, AOC, and OPR, despite their belief that SA-mediated suppression of the jasmonic acid signaling pathway functions independently of jasmonic acid biosynthesis (Leon-Reyes et al. 2010). Furthermore, a study found that applying agents like oryzalin and Latrunculin B, which disrupt

the cytoskeleton, led to the activation of salicylic acid-responsive genes without affecting the jasmonic acid signaling pathway (Matoušková et al. 2014). Therefore, the impact of oryzalin on the expression of AOC, OPR, and JAZs may be attributed to the antagonistic effect of SA or its negative influence on stromule formation. Our findings highlight the complex regulatory dynamics between SA and JA signaling pathways.

4.5. Rapid Induction and Temporal Stability of Stromule Lengths in MeJA-Treated BY-2 Cells

To gain a deep understanding of stromule formation dynamics, we conducted a time-course analysis of MeJA-induced stromulation. This experiment was designed to elucidate how quickly stromules are produced following MeJA treatment and whether their length distribution changes over time. Through monitoring the temporal dynamics of stromule formation, we aimed to highlight the potential role of stromules in rapid stress signaling.

The heatmap in Figure 6 illustrates the temporal distribution of stromule lengths and their incidence in MeJA- treated BY-2 cells, measured at 10-minute intervals over 60 minutes. Stromule lengths are categorized, ranging from 10 µm to 100 µm. The most prominent feature of the heatmap is the incidence of stromules in the 10-40 µm range across all time points (Figure 6). Statistical significance ($P<0.05$) was determined using the non-parametric Fligner-Killeen test, with the same letter "a" denoting no significant differences in stromule length distribution over time. This suggests that MeJA treatment predominantly induces stromules in BY-2 cells, and this induction occurs rapidly, which is evident from the earliest 10-minute time point.

Temporal analysis of the heatmap reveals a remarkably consistent distribution pattern of stromule lengths throughout the 60-minute observation period. The initial stromule length distribution induced by MeJA treatment is maintained over an hour. While shorter stromules (10-30 µm) are most predominate, longer stromules (40-100 µm) are also consistently present, although at lower frequencies.

The immediate establishment of a consistent stromule length profile that stay for at least one-hour post-induction suggests that MeJA triggers a quick cellular response, potentially related to defense signaling or plastid communication processes, which remains steady without significant alterations in stromule dynamics during the initial phase of treatment.

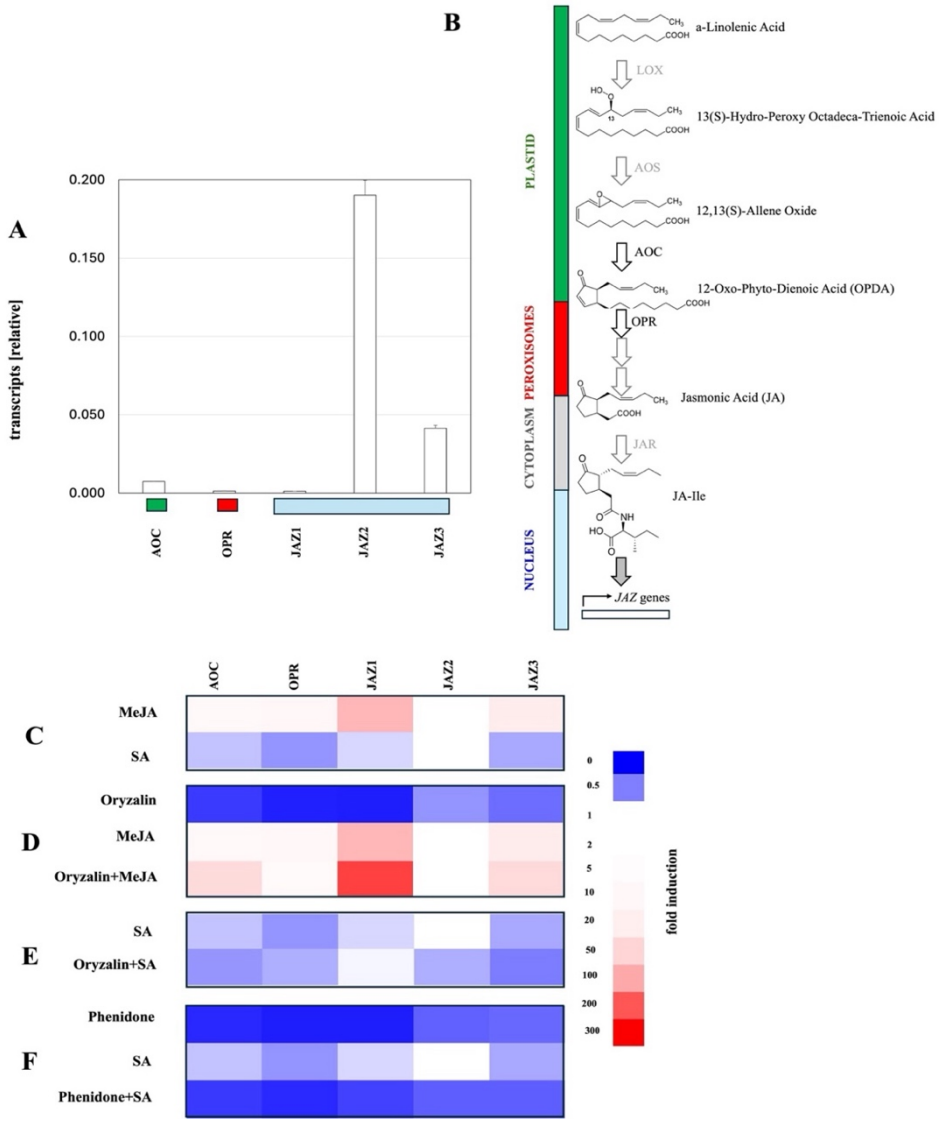

Figure 5. Response of jasmonate synthesis and jasmonate response genes to factors modulating stromulation. A Steady-state transcript levels for Allene Oxide Cyclase (AOC), OPDA Reductase (OPR), and jasmonate response genes JAZ1, JAZ2, JAZ3 in relative units. Incidence of stromules depending on their length depending on treatment. **B** Intracellular compartimentalisation of jasmonate biosynthesis and response to show the localisation of the gene products for the tested transcripts. **C** Response of gene expression to MeJA and SA. **D** Dependence of the MeJA response on Oryzalin, eliminating microtubules. **E** Dependence of the SA response on Oryzalin. **F** Dependence of the SA response on Phenidone. Conditions are: MeJA 100 µM of Methyl Jasmonate for 60 min, SA 100 µM of Salicylic Acid for 60 min, Oryzalin 10 µM of Oryzalin for 120 min, Oryzalin+MeJA 100 µM of MeJA for 60 min following a pre-treatment with 10 µM of Oryzalin for 60 min, Oryzalin+SA 100 µ of SA for 60 min following a pre-treatment with 10 µM of Oryzalin for 60 min. Data represent means of three independent experimental series, each in technical triplicates. C-F fold-induction over control values.

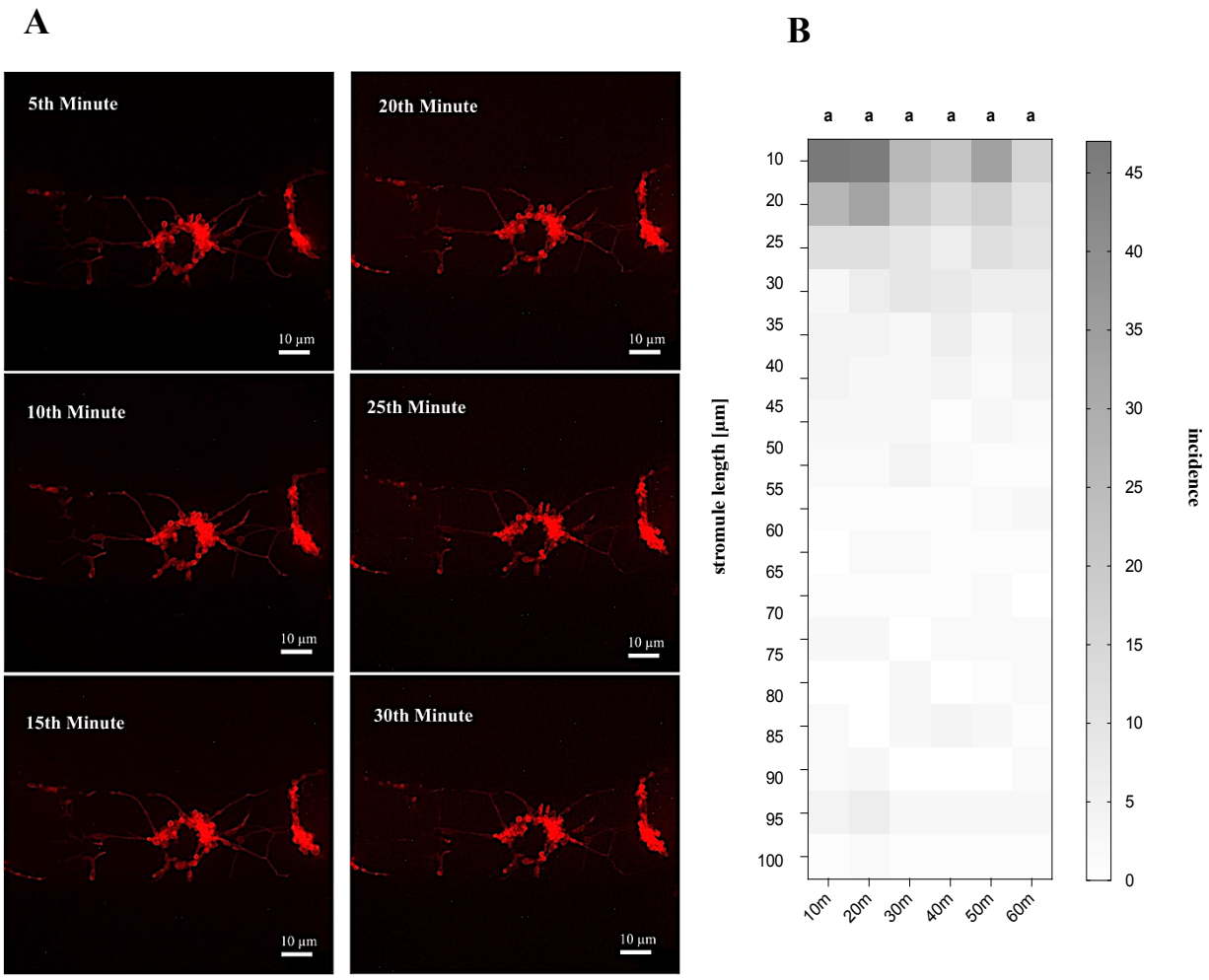

Figure 6. Distribution and Incidence of Stromule Lengths Over Time in MeJA-Treated BY-2 Cells. A Confocal Images present the monitoring of a BY-2 cell treated with MeJA, with observations recorded every five minutes over a thirty-minute period. **B** The heatmap depicts the incidence and distribution of stromule lengths in BY-2 cells treated with 100 µM Methyl jasmonate (MeJA) over a 60-minute period. Stromule lengths are categorized into 10 µm intervals (y-axis, 10-100 µm) and observed at 10-minute intervals (x-axis, 10-60 minutes). The incidence of stromules is represented by grayscale intensity, with darker shades indicating higher frequency. Statistical analysis using the Fligner-Killeen test revealed no significant differences in stromule length distribution over time ($P>0.05$), as denoted by the consistent letter "a" across time points.

4.6. Aging-Dependent Stromulation in BY-2 Cells Treated with Methyl Jasmonate

Considering that cellular responses can vary during developmental phases, we investigated the impact of cell age on MeJA-induced stromule formation. This experiment was desinged to explore whether the abality to form stromule changes as cells age. We examined stromule characteristics across different cell ages to uncover potential links between cellular senescence, stress responses, and plastid dynamics.

Stromulation patterns in BY-2 cells were observed to differ significantly with cell age and division status following treatment with methyl jasmonate (MeJA). The experiment examined cells grown in liquid MS medium over five days, with MeJA treatment applied for 1 hour at a concentration of 100 μM. This approach allowed for a comprehensive analysis of stromule formation dynamics across different stages of cellular development.

Figure 7A presents microscopic images demonstrating the differential incidence of stromules in BY-2 cells during their terminal division phase. Typically, BY-2 cells exhibit a notable proliferation rate, doubling every 13 hours. This process involves spending 2 hours in the G1 phase, 5 hours in the S phase, and 4 and 2 hours in the G2 and M phase, respectively. Cells in the G0 phase are rarely observed due to continuous cellular activity (Nagata et al. 1992). In the present study, the observed population of dividing cells appeared to be in the late stage of the M phase, either completing cytokinesis or entering a new interphase cycle. During this time, microtubules (MTs) were involved in forming the phragmoplast at the cell's midpoint or were active in the perinuclear region, forming the interphase cortical array (Granger and Cyr 2000). Essentially, during this phase, the interphase microtubule network stays largely disassembled.

The heat map in Figure 7B quantifies the frequency distributions of stromule lengths across seven experimental conditions, including cells from day 0 to day 5 and actively dividing cells. The data reveal a distinct correlation: both the length and frequency of stromules increase as cell age (Figure 7A, B). On zero-day, BY-2 cells were in the stationary phase, where growth had stopped, and cells reached their maximum size. Cells remain metabolically active, but their metabolic activity slows. Vacuoles expand in cells with the largest size, while connections become shorter in confined spaces.

Our observations reveal that stromules exhibit shorter lengths on day 0. While the incidence of stromules increases with aging, longer stromules become evident during days 4 and 5 of the experimental period. Actively dividing cells, represented in the "Dividing Cells" column, display minimal stromulation compared to non-dividing. Statistical analysis using the non-parametrical Fligner-Killeen test confirmed significant differences ($P<0.05$) in stromule length distributions among the conditions, as indicated by the different letters (a-e) above each column in the heat map (Figure 7 B).

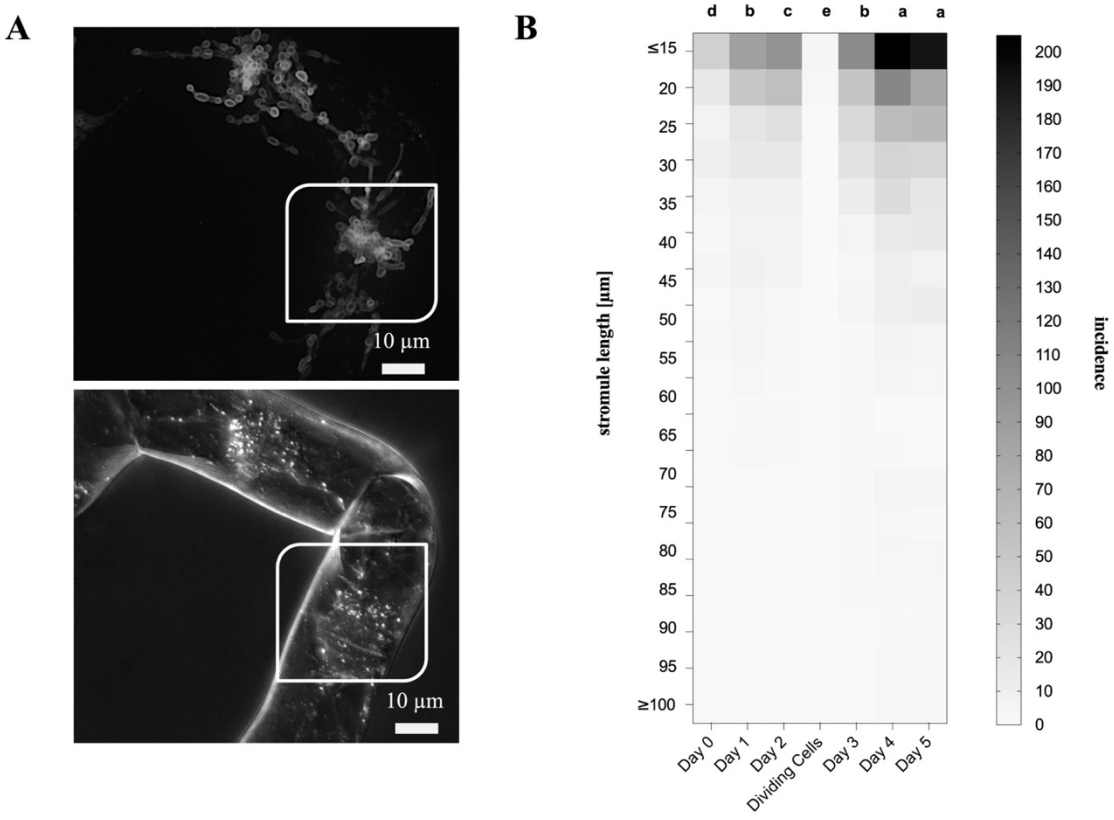

Figure 7. Stromulation patterns in aging BY-2 cells treated with methyl jasmonate. **A** Microscopic images of BY-2 cells at the end of division phase (white box). Scale bars: 10 µm. **B** Heat map representing frequency distributions of stromule lengths in BY-2 cells from day 0 to day 5 and in actively dividing cells. Cells were treated with 100 µM methyl jasmonate for 1 hour. Darker shades indicate higher frequencies. Y-axis shows stromule length (µm), X-axis shows cell age/condition. Different letters (a-e) indicate statistically significant differences ($P<0.05$) based on the non-parametrical Fligner-Killeen test.

An examination of the heat map reveals specific patterns across the age groups. On day 1, stromule length increases, followed by a significant decrease on the second day and then an increase again on the third day. Day 1 cells predominantly exhibit stromules in the 10-70 µm range, with the highest frequency around 10-20 µm. As cells age, there is a noticeable shift towards longer stromules.

According to the study conducted by M. SRBA et al. 2016, in samples of BY-2 cells cultured with an initial dilution of 7.5 X, the mitotic index peaks on the second day and gradually decreases until it approaches zero in the stationary phase (Srba et al. 2016). Therefore, in the sample taken from the day 2 BY-2 cells, a significant percentage of cells were in the division phase, followed by a notable decrease in stromule length. By Day 3, a variety of stromule lengths is again observed, ranging from 10 to 70 µm, with peak frequencies around 10-20 µm. Days 4 and 5 show the most dramatic shift, with stromule lengths frequently extending beyond 70 µm and reaching up to 100 µm. The column actively dividing cells shows minimal stromulation across all length categories.

This progressive increase in stromule length and frequency with cell age, along with the notable decrease in stromule formation during cell division, highlights the dynamic regulation of stromule in response to cellular age and division status in MeJA-treated BY-2 cells.

4.7. Localization of JASSY and Peroxisomes in Rilation to Stromules during Jasmonate Signaling in BY-2 Cells

To further clarify the functional significance of stromules in jasmonate signaling, we examined the spatial relationships between stromules, JASSY (Jasmonate-Activated Transformed Protein), and peroxisomes. This experiment was designed to test the hypothesis that stromules act as dynamic platforms for organizing multi-organelle metabolons that play a role in hormone biosynthesis and signaling. The jasmonate biosynthesis pathway involves multiple cellular compartments, with OPDA produced in plastids and subsequently transported to peroxisomes for conversion to jasmonic acid. JASSY, a chloroplast outer membrane protein, plays a crucial role in facilitating this inter-organelle transport of OPDA.

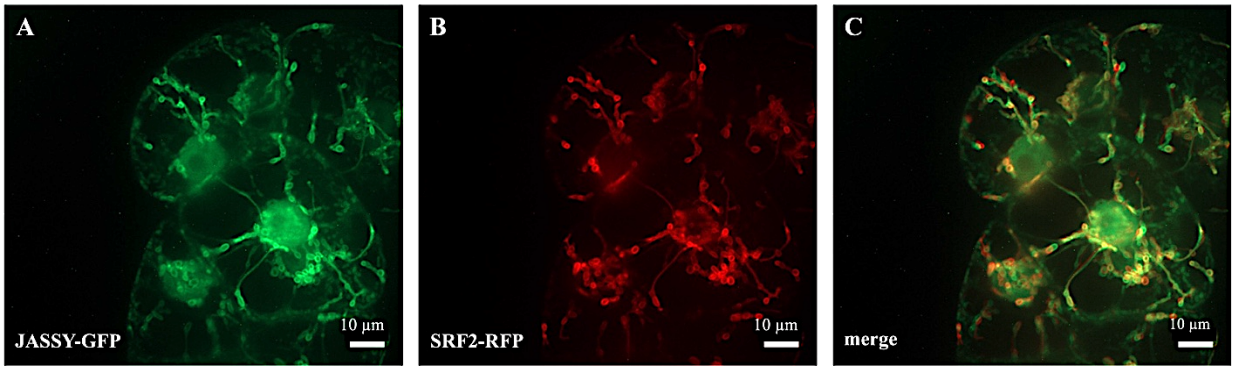

Figure 8: Fluorescence microscopy presents the dynamic interplay of chloroplast components in jasmonate signaling within double transgenic BY-2 cells treated with MeJA for one hour. A GFP-labeled JASSY-chloroplast outer membrane protein, exhibiting intricate chloroplast structures with extensive branching. **B** SFR2-RFP-labeled stromules, showcasing tubular extensions emanating from plastids. **C** Merged image demonstrating significant co-localization (yellow) of JASSY and stromules, suggesting their potential functional relationship in jasmonate biosynthesis and signaling pathways.

Fluorescence microscopy revealed that GFP-tagged JASSY protein, which localizes to the chloroplast outer membrane, exhibited extensive branching patterns within chloroplasts of MeJA-treated BY-2 cells (Figure 8A). Stromules labeled with SFR2-RFP showed significant co-localization with JASSY (Figure 8C), indicated by the yellow-orange coloration where green and red signals overlap. Our findings demonstrate JASSY protiens extend beyond the main body of chloroplasts and integrate into the stromule structure. This observation highlights the potential role of stromules in facilitating the transport of OPDA during jasmonate synthesis, as JASSY expands its cellular reach through these plastid extensions.

We also examined the spatial relationship between peroxisomes and stromules following MeJA treatment (Figure 9A). The main image shows an overview of the cells, with green stromules (labeled by tpFNR-mEGFP) and red fluorescent peroxisomes (marked by PTS1-mCherry). Peroxisomes appear as numerous small dots distributed throughout the cell. In Figure 9A, two inset images show close-ups of peroxisome clusters around stromules, clarifying their spatial relationship. Our observations indicate that while peroxisomes tend to cluster around stromules in certain areas, their overall distribution within the cell lacks a specific pattern.

The co-localization of JASSY with stromules and the clustering of peroxisomes around these structures provide visual evidence supporting the hypothesis that stromules play a significant role in jasmonate signaling, possibly by facilitating the efficient transport of OPDA from chloroplasts to peroxisomes.

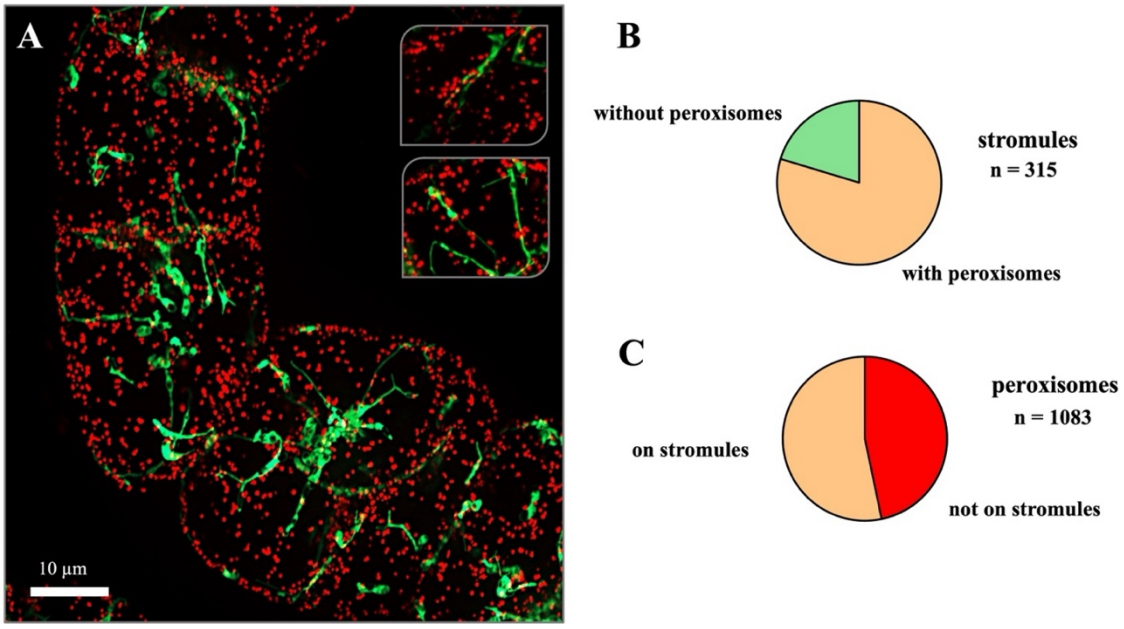

Figure 9: Fluorescence microscopy reveals the intricate relationship between stromules and peroxisomes as assessed by double visualisation of the stroma marker N-terminal fragment of ferredoxin NADPH oxidoreductase (tpFNR-mEOS, green) and the peroxisomal marker PTS1-mCherry (red). A Representative cell expressing both markers. A geometric projection of a confocal z-stack through the cells is shown to illustrate the total population of peroxisomes. **B, C** Mutual colocalisation scored from individual confocal sections of a stack (to exclude false positive values from overlay of different z-planes. **B** Frequency of stromules not adjacent to peroxisomes (green) as compared to stromules that are decorated by peroxisomes (orange). **C** Frequency of peroxisomes not adjacent to a stomule (red) as compared to peroxisomes that have contact to a stromule (orange). Insets provide magnified views of peroxisome clusters surrounding stromules, highlighting potential functional interactions between these organelles under MeJA-induced stress conditions.

5. Discussions

This study has significantly advanced our understanding of stromule dynamics and their potential roles in plant cellular signaling, particularly stress responses and inter-organelle communication. Our key findings reveal that stress-related phytohormones, specifically methyl jasmonate (MeJA) and salicylic acid (SA), induce stromule formation and elongation in tobacco BY-2 cells. Notably, inhibition of JA biosynthesis through phenidone application prevents SA-induced stromule formation. Furthermore, SA treatment leads to downregulation of JA-related genes (AOC, OPR, JAZ1). These results collectively suggest a complex interplay between SA and JA signaling pathways in stromule regulation.

We also have uncovered complex relationships between jasmonate signaling pathways and stromule formation. The presence of JASSY, a protein involved in jasmonate biosynthesis, within stromules and the clustering of peroxisomes around stromules provide convincing evidence for the role of stromules in facilitating inter-organelle communication and metabolite exchange.

Our gene expression analysis revealed a nuanced response to MeJA treatment in the presence of a microtubule-depolymerizing agent, oryzalin. Notably, AOC (Allene Oxide Cyclase) showed enhanced expression under MeJA-oryzalin treatment, suggesting a compensatory mechanism in response to disrupted stromule formation. In contrast, OPR (OPDA Reductase) expression was reduced under these conditions, indicating a potential bottleneck in JA biosynthesis when stromule formation is inhibited. The expression of JAZ1 showed significant induction in MeJA-oryzalin-treated cells, despite preventing stromule formation. This unexpected increase in JAZ1 expression may represent a feedback mechanism to regulate JA signaling pathway, when inter-organelle communication through stromules is disrupted.

Furthermore, we observed an age-dependent increase in stromule formation within BY-2 cells, revealing a novel aspect of plastid dynamics during cellular senescence. These findings introduce stromules as key components of a complex cellular network that can regulate jasmonate biosynthesis and signaling in response to both environmental stimuli and developmental phases. Given these findings, several intriguing questions raise that warrant further discussion:

5.1. How do stromules orchestrate the symphony of stress signaling in plant cells?

Our findings demonstrate that both MeJA and SA similarly induce stromule formation, suggesting that stromules may serve as integration points for distinct stress signaling pathways. This observation is interesting because MeJA and SA often act antagonistically in plant defense responses. The comparable effects of these hormones on stromule induction suggest that stromule formation might be a general stress response mechanism rather than a pathway-dependent process.

The shift towards longer stromules (20-30 µm and >30 µm) in both MeJA- and SA-treated cells (Figure 1D, E) indicates that these phytohormones not only increase stromule frequency but also promote stromule elongation. This phenomenon could serve multiple purposes: **Enhanced inter-organelle communication:** Longer stromules may facilitate more efficient signal transduction or metabolite exchange between plastids and other cellular compartments during stress responses. **Increased cellular Monitoring:** Extended stromules could act as "cellular antennae," allowing plastids to sample a larger volume of the cytoplasm for stress signals or metabolites. **Energy-efficient plastid repositioning:** The formation of longer stromules might allow plastids to extend their reach within the cell without the energetically demanding process of organelle movement (Hanson and Sattarzadeh 2011).

Our experimental results demonstrated that phenidone inhibits SA-mediated stromule formation, suggesting that a basal level of JA signaling may be necessary for SA-induced stromule formation. It points to a hierarchical or priming effect in stress signal integration, where JA prepares the cellular machinery for stromule formation, then SA can trigger or enhance. SA may enhance or alter an existing JA-dependent mechanism rather than function through an independent pathway. However, the complete inhibition of JA (via prednisone) removes this priming effect, preventing SA from inducing stromules. This reveals complex crosstalk beyond simple antagonism, wherein SA and JA pathways collaborate in certain cellular responses while still showing antagonism in gene expression.

Furthermore, the similar response to MeJA and SA implies that stromules may serve as cellular "stress barometers", with their length and frequency potentially indicating the overall cellular stress state. This provides an opportunity to investigate stromules in plant cells as general stress sensors.

5.2. Are stromules the cellular tightrope walkers, balancing on microtubules to shape plant stress responses?

Our results demonstrated that oryzalin, which depolymerizes microtubules, effectively inhibited MeJA-induced stromule elongation. This finding aligns with previous studies showing that the key role of the cytoskeleton in both the formation and maintenance of stromules (Kumar et al. 2018; Natesan et al. 2009). In our observation, oryzalin treatment significantly reduced the formation of stromules longer than 20 μm, indicating that microtubules may be crucial in stromule extension beyond a specific length threshold. This raises an intriguing question: Why are microtubules more critical for extending longer stromules? One possible explanation is that longer stromules need more structural support to maintain their extended shape against cellular forces. Microtubules likely provide this necessary support. Additionally, the association of stromules with microtubules could facilitate the transport of proteins and other molecules along these extended structures, enhancing their functional capacity in inter-organelle communication.

Additionally, it is essential to consider the role of actin filaments (AFs) in stromule dynamics. Both microtubules and actin filaments play crucial roles in organelle movement. Our observations demonstrated that despite the absence of AFs in the presence of latrunculin B, stromules still form, though with some differences compared to untreated cells (Supplemental Figure S2). Research by Matoušková et al. (2014) provides indirect support for this finding, as they demonstrated that exogenous salicylic acid reduced AFs in the leaf cells of Arabidopsis thaliana (Matoušková et al. 2014). While salicylic acid may decrease actin levels, our results indicated an induction of stromule formation in salicylic acid-treated BY-2 cells. This finding suggests that AFs are not essential for stromule formation but may play a modulatory role. The main point is that AFs do not drive stromule extension, which is dependent on microtubules. Instead, they provide the critical anchoring infrastructure that helps stromules to maintain specific positions and facilitate directed movement (Kumar et al. 2018).

The differential effects of cytoskeletal disruption on stromule formation versus maintenance, as evidenced by the time-course analysis (Figure 6), provide new insights into the dynamics of stromule. Erickson et al. (2018) demonstrated that not all stromules are associated with microtubules. They identified two types of stromule movement: microtubule-dependent and microtubule-independent. Microtubule-dependent stromules were found to move slower and be

more stable than microtubule-independent stromules, which were fast-moving and short-lived. Interestingly, they also observed that microtubule-independent stromules are most likely the result of interactions with actin (Erickson et al. 2018). Drawing upon this knowledge and our experimental observations, the stromules produced in MeJA-treated BY-2 cells are largely microtubule-dependent stromules, which move slowly and have a longer lifespan.

Within just 60 minutes of applying MeJA, we observed a marked increase in both the frequency and length of stromules, indicating a rapid response mechanism that likely relies on microtubules. This rapid induction is complemented by their remarkable stability in length throughout the observation period, as shown in the heatmap in Figure 6. Such stability implies that once formed, stromules can maintain their structure without continuous remodeling.

This observation reminds us to consider the following question: How do stromules maintain their structure and function over time? What mechanisms regulate the transition from stromule formation to maintenance? A model is hypothesized, in which the initial formation and elongation of stromules are fundamentally driven by microtubule tracks. Once formed, stromules may develop structural autonomy, possibly through the employment of membrane-stabilizing proteins or the establishment of interactions with AFs (Kumar et al. 2018) or/and endoplasmic reticulum (Schattat et al. 2011).

5.3. Do stromules serve as cellular highways for metabolic messengers in the plant stress response network?

The localization of JASSY, a protein involved in jasmonate biosynthesis, to stromules (Figure 8) and the clustering of peroxisomes around these structures (Figure 9) provide strong evidence for the role of stromules in facilitating inter-organelle communication and metabolite exchange. This spatial arrangement could optimize the efficiency of JA production by minimizing the distance OPDA must travel between organelles, clearly indicating a crucial role for stromules in coordinating JA biosynthesis. The distribution of peroxisomes within the cell may not follow a distinct pattern, but their tendency to cluster around stromules in specific areas is significant. While the high abundance of peroxisomes can complicate the identification of definitive patterns, this study clearly highlights the interaction between peroxisomes and stromules. It is also essential to emphasize that this investigation focused on BY-2 plastids rather than chloroplasts, may limit the significance of peroxisome clustering around plastid circles to

particular functions (Baillie et al. 2020; Mathur 2021; Oikawa et al. 2019). Nevertheless, our observations demonstrating a defined spatial relationship between stromules and peroxisomes prompt us to propose a model in which stromules serve as dynamic platforms that organize multi-organelle metabolons involved in stress signaling and hormone biosynthesis. According to this model, the formation of stromules in response to stress-related phytohormones facilitates transporting enzyme complexes, signaling molecules or metabolic intermediates between plastids and other cellular organelles (Hanson and Sattarzadeh 2011), thereby enhancing the efficiency and specificity of stress responses.

The differential expression patterns of jasmonate synthesis and response genes (AOC, OPR, JAZ1, JAZ2, JAZ3) under various treatments (Figure 5) further support this model. The pronounced induction of JAZ genes, particularly JAZ1, in response to MeJA treatment, is consistent with their established role as negative regulators of jasmonate (JA) signaling pathways (Chini et al. 2007). It is well established that the degradation of JAZ proteins in exogenous MeJA leads to the activation of JA-responsive gene expression. It is important to note that the regulation of JA-signaling primarily occurs post-translationally and one of the mechanisms involved is the degradation of JAZ-proteins, which act as inhibitors of JA-mediated responses (Caarls et al. 2015). Therefore, it is clear that the transcript responses of JAZs do not directly engage in JA signaling; instead, they play a crucial role in modulating the response to JA (Ismail et al. 2012).

There are several interesting points to discuss regarding the induction of JAZ expression in the presence of MeJA or/and oryzalin: **1.** The induction of JAZ expression genes, particularly JAZ1, in response to MeJA treatment aligns with their known role as negative regulators of JA signaling. This is likely a feedback mechanism that modulates the JA response. When JA levels rise due to exogenous MeJA, the plant effectively upregulates JAZ genes to control and prevent an excessive response to JA. **2.** The induction of JAZ expression genes when stromule formation is inhibited by oryzalin is particularly intriguing. Several hypotheses could explain this:

a) Disrupted JA signaling: If stromules play a role in JA signaling or transport of JA precursors, their inhibition might lead to a perceived decrease in JA signaling. The plant may respond by upregulating JAZ genes to suppress the already diminished JA response further.

b) Accumulation of OPDA: If oryzalin partially inhibits stromule function, it could be assumed that the synthesis of 12-oxo Phytodienoic acid (OPDA), an intermediary chemical in the production of JA, takes place within plastids but requires stromule-mediated transport to complete the JA synthesis. The accumulation of OPDA may lead to negative feedback loop, resulting in reduced levels of JA and subsequent induction of JAZ expression.

c) Stress response: The plant might perceive Oryzalin-induced microtubule depolymerization as a stress. This stress response could involve complex crosstalk between different hormone pathways, potentially leading to JAZ upregulation as part of a broader stress adaptation mechanism.

The differential effects observed on early (AOC) and late (OPR) jasmonic acid (JA) biosynthesis genes in the presence of both oryzalin and methyl jasmonate (MeJA) further support the proposed model. Specifically, the upregulation of AOC and the downregulation of OPR in the presence of MeJA—where oyrzalin disrupts stromule formation—suggests that stromules are essential in the full induction of OPR by possibly facilitating the transport of intermediates between cellular compartments. Moreover, the induction of AOC expression in response to MeJA clearly leads to the production of OPDA. Under these stress conditions, the cells demand active jasmonic acid production. In the absence of stromules (as observed in Ory-MeJA treated cells), OPDA becomes inaccessible and accumulates within the chloroplast. Consequently, to balance the pseudo-deficiency of OPDA, the cell strategically upregulates AOC expression (Figure 5, Supplemental Figure S4).

In conclusion, the arrangement of JASSY and peroxisomes near stromules along with gene expression data indicate that stromules are vital components of a cellular network that modulates jasmonate biosynthesis and signaling. Our results support the idea that stromules function as pathways for metabolic messengers in the plant stress response. This model helps explain how plants rapidly adjust their cellular architecture to environmental stresses.

5.4. How does cellular senescence influence stromule dynamics?

Cellular senescence and its impact on stromule dynamics are fascinating aspects of plant cell biology, as highlighted by the results presented in this study. The findings that stromule frequency and length increase with cell age in BY-2 cells (Figure 7) underscore a previously overlooked aspect of plastid dynamics during cellular senescence. This phenomenon provides

valuable insights into how plastids adapt during cellular development and senescence stages.

As cells age, they experience a range of metabolic changes. We observed that at the initial stage (day 0), cells exhibit a high percentage of senescence, characterized by reduced frequency and length of stromules. Subsequently, BY-2 cells in their middle age phase (specifically days 4 and 5) display enhanced stromule formation and elongation. Previous studies have clearly demonstrate that as plant cells age, autophagy activity increases, and in autophagy-deficient mutants, there is an observed increase in both the frequency and visibility of stromules (Ishida et al. 2008; Su et al. 2020; Yanagisawa and Chuong 2023). This is further evidence suggesting that stromules may be more numerous, elongated, or possibly both, in young active plant cells. Collectively, these adaptive responses could be vital for several reasons:

- **Metabolic Efficiency:** As cells age, their metabolic processes often become less efficient. Extended stromules could enhance the exchange of metabolites between plastids and other cellular compartments, helping to maintain essential metabolic pathways despite age-related decline.

- **Signaling:** The enhanced stromule formation may improve retrograde signaling from plastids to the nucleus. This enhancement allows for better communication about the organelle's status and needs as the cell ages. Such improved signaling could be vital for initiating the necessary gene expression changes to respond to the challenges of senescence.

- **Organelle Interactions:** The expanded stromule network in larger, older cells facilitates greater physical contact between plastids and other organelles, such as mitochondria and the endoplasmic reticulum. These interactions might be essential for maintaining cellular homeostasis during the senescence process.

The variations in stromule length across different days of culture correlate with changes in the mitotic index. The significant decrease in stromule length on day 2, coinciding with peak mitotic activity, followed by a gradual increase in subsequent days, suggests that stromule dynamics are tightly regulated in response to the cell's physiological state and developmental stage. The observed absence of stromule formation during active cell division, particularly in the M phase, contrasts the senescence-related increase (Figure 7). As noted, the interphase microtubule network stays largely disassembled during the M phase. The reduced stromule formation in actively dividing cells may be related to the reorganization of the cytoskeleton

during mitosis. During rapid division, cells may also prioritize energy and resources for replication processes, temporarily suppressing stromule formation. As cells age and division rates slow, the shift towards increased stromulation could represent a reallocation of cellular resources towards maintenance and stress response mechanisms.

In conclusion, these observations suggests that stromules may serve a compensatory function in maintaining plastid activity and facilitating inter-organelle communication as cells undergo metabolic changes during senescence.

5.5. How Can We Decode Stromules Language, from Plastid Whispers to Nuclear Roars?

Stromules, or stroma-filled tubules, serve as dynamic channels for plastid-to-nucleus signaling. They effectively decode the "language" of plastids and translate it into nuclear responses. These tubular extensions of plastids are essential for retrograde signaling, a process through which organelles convey their physiological status to the nucleus. This enables adaptive gene expression in response to environmental stimuli and stress conditions.

The rapid induction of stromules in response to methyl jasmonate (MeJA) treatment and their association with JASSY and peroxisomes strongly provide evidence for their role in retrograde signaling. Recent studies have indicated the role of stromules in transmitting reactive oxygen species (Vitha et al. 2001) and calcium signals from chloroplasts to nuclei during pathogen responses and abiotic stress (Caplan et al. 2015). ROS can modulate the expression of nuclear genes involved in stress responses, photosynthesis, and other processes (Tripathy and Oelmüller 2012). A key player in the retrograde signaling pathway is 12-oxo-phytodienoic acid (OPDA), a crucial molecule synthesized in chloroplasts and transported to the cytosol and peroxisomes. OPDA acts independently of jasmonates (JAs) to trigger specific gene expressions in the nucleus (Taki et al. 2005). It binds to the receptor CYP20-3 in chloroplasts, forming a cysteine synthase complex that adjusts the cellular redox state and regulates OPDA-responsive genes (Liu and Park 2021).

The inhibition of stromule induction by oryzalin likely affects retrograde signaling pathways, which in turn impacts the expression of genes involved in JA biosynthesis and signaling. Our results show the following:

- **JA Biosynthesis and Retrograde Signaling:** The increase in AOC expression and the decrease in OPR expression suggest that the plant attempts to modulate JA levels in response to disrupted retrograde signaling. AOC catalyzes OPDA, a precursor of JA. Then, decreased OPR expression leads to reduced conversion of OPDA to JA. Thus, the accumulation of OPDA due to this imbalance may act as a signal to the nucleus, indicating stress or damage.

This response suggests that the plant adjusts its JA biosynthesis pathway in response to altered retrograde signaling. The accumulation of OPDA, which is itself a signaling molecule, could serve as an important stress signal independent of JA.

- **JAZ1 and Retrograde Signaling:** The increase in JAZ1 expression could be a feedback mechanism to prevent excessive JA signaling, which might be detrimental under certain stress conditions. This indicates a complex interplay where retrograde signals modulate JA signaling by adjusting the levels of JAZ repressors.

This response demonstrates the plant's attempt to fine-tune its JA signaling pathway. By increasing JAZ1 expression, the plant can reduce JA responses, which might be necessary to prevent overstimulation of stress responses that could harm the plant's overall health and growth.

Stromules may serve as dynamic sensory protrusions that allow plastids to sample the cellular environment and rapidly transmit signals to the nucleus in response to stress or developmental cues. This idea is supported by the observed clustering of peroxisomes around stromules (Figure 9), which could facilitate the integration of signals from multiple organelles before transmission to the nucleus. The association of stromules with JASSY, a protein involved in jasmonate biosynthesis, provides further evidence suggesting that stromules might facilitate the transport of signaling molecules like OPDA from plastids to other cellular compartments, including the nucleus. Our results expand on these findings by demonstrating that phytohormone signaling can also modulate stromule dynamics, potentially providing an additional layer of regulation in plastid-to-nucleus communication.

In conclusion, these results collectively represent stromules as integral components of a complex retrograde signaling network capable of modulating jasmonate biosynthesis and signaling in response to environmental cues. Future studies should focus on the specific

molecular mechanisms by which stromules facilitate signaling.

5.6. Critical Evaluation of Methodological Approaches

In this section, we critically evaluate the methodological strategies employed in our study. We will specifically focus on the markers used for stromule identification, the AI-driven image analysis technique, and the statistical methods employed. This evaluation aims to highlight the strengths and limitations of our methods and demonstrate a thoughtful approach to our experimental design and data analysis.

- **Stromule Markers: Selection and Validation**

Our study utilized two distinct markers to identify and visualize stromules: Sensitive to Freezing 2 (SFR2) fused to RFP and transit peptide of ferredoxin-NADP+ reductase (tpFNR) fused with mEOS. The selection of these markers was crucial for ensuring the accurate identification of stromules and differentiating them from other organelle membranes.

SFR2-RFP is an outer envelope protein well-established in previous studies for its ability to label the chloroplast outer membrane, including stromules (Mathur et al. 2013). Its localization to the outer envelope makes it an excellent choice for visualizing the full extent of stromule projections. However, one potential limitation of using an outer membrane marker is the risk of labeling membrane protrusions that may not be true stromules. To address this concern, we also employed tpFNR-mEOS, which localizes to the stroma of plastids. The transit peptide of ferredoxin-NADP+ reductase (tpFNR) targets the protein to the plastid stroma, allowing visualization of the stroma-filled nature of true stromules (Schattat et al. 2011). Using this double-marker approach, we could confirm that the observed tubular structures were stromules containing both outer membrane and stromal components.

The agreement between these two markers in our observations confirmed that the structures we identified and measured were actual stromules, not just membrane protrusions. This labeling strategy enhances the reliability of our stromule identification and subsequent analyses. However, it is important to note that fluorescent protein fusions may alter the behavior or dynamics of the tagged proteins, a limitation inherent to many fluorescence microscopy studies (Snapp 2005).

Additionally, we should be aware of the potential limitations of this approach. Even when targeting may be accurate, the overexpression of membrane proteins can sometimes lead to changes in membrane dynamics or organelle morphology (Breuers et al. 2012). Although we did not observe any abnormalities, minor effects on stromule formation or dynamics cannot be entirely overseen. Future studies might benefit from complementary approaches, such as electron microscopy or additional markers, to further enhance the validation of stromule identification and characterization.

- **AI-Driven Image Analysis: Advancements and Considerations**

Quantifying stromule length and number is a critical challenge in the field that has typically relied on manual measurements or semi-automated image analysis techniques. Previous studies have effectively employed a variety of methods, including manual counting, automated and semi-automated analyses, and fluorescence intensity-based approaches. While these methods have yielded valuable insights, they can be time-consuming and may introduce observer bias. There is a clear need for more efficient techniques.

Our study utilized advanced artificial intelligence techniques for deep image analysis of plant cell structures. This approach, utilizing the APEER Viewer platform developed through a collaboration between ZEISS and ZEISS Arivis Cloud, represents a significant advancement in stromule quantification. The AI model, trained on a comprehensive dataset of 100 BY-2 cell images, employed pixel-based semantic segmentation to identify plastids and stromules accurately (see Section 3.9 of the Methods for further details).

This AI-driven approach offers several key benefits. Firstly, it allows for efficient high-throughput analysis, processing large datasets faster and more consistently than manual methods. Secondly, the AI's ability to recognize complex patterns and features may lead to more valid identification of stromules, reducing the chance of human error. Lastly, automation minimizes observer bias, enhancing the reproducibility of results.

It is essential to recognize the limitations of this approach. The accuracy of AI-based analysis largely depends on the quality of the training dataset. While our model was trained on many images, it may not capture the full diversity of stromule morphologies and arrangements across different experimental conditions or cell types. Additionally, the "black box" nature of deep learning algorithms can make it challenging to understand how the AI makes classifications,

leading to difficult-to-detect misclassifications. To reduce these limitations, we validated the AI results against manual measurements and apllied quality control measures. To reduce these limitations, we considerably validated the AI results against manual measurements and implemented quality control measures. Future studies can enhance this approach by using diverse training datasets, applying improved AI techniques to understand the classification process better.

- **Statistical Analysis: Addressing Non-Parametric Data with High Variance**

The nature of stromule data, which include high variance and a non-parametric distribution, presented unusual challenges for statistical analysis. Traditional parametric tests (e.g., ANOVA, t-tests) were insufficient for analysing the biological significance of our observations, particularly the differences in stromule length distributions between treatments.

After testing several statistical methods, including Duncan's test, Tukey's HSD, and Fisher's LSD, we found they did not accurately reflect the biologically relevant differences in live treated cells. This led us to embrace the Fligner-Killeen test, a non-parametric method particularly suited to our dataset. The Fligner-Killeen test offers several advantages for our analysis:

- **Reliability under Non-Normality:** Unlike parametric tests, the Fligner-Killeen test does not assume a normal data distribution, making it suitable for our highly variable stromule measurements.
- **Focus on Variance:** By assessing the equality of variances across groups, this test aligns well with our biological question, where differences in stromule length distributions are as important as differences in means.
- **Median-Based:** The use of median as a measure of central tendency makes the test less sensitive to extreme outliers, which are common in biological data.
- **Compatibility with High-Variance Data:** The test's design makes it particularly suitable for datasets where the variance is a parameter of interest, as in our stromule length distributions.

While the Fligner-Killeen test provided a more valid statistical framework for our data, it is important to note its limitation: Interpretation Complexity. Interpreting the results of variance

equality tests is often more complex than interpreting tests that compare mean differences. To reduce these limitations, we complemented our statistical analysis with comprehensive visualizations, including heatmaps and distribution plots, to provide a complete picture of stromule dynamics across different conditions.

In conclusion, despite some limitations, our combined approach of stromule identification markers, AI-driven image analysis, and non-parametric statistical testing provides a reliable framework for studying stromule dynamics. Future research could improve this by incorporating enhanced live-cell imaging techniques and more advanced AI models to better understand the complex behavior of stromules in plant cells.

6. Conclusion: Stromules as Dynamic Architects of Cellular Resilience, Implications and Future Horizons in Plant Stress Biology

Our study highlights the diverse roles of stromules in plant cellular signaling, particularly in stress responses and inter-organelle communication. These findings position stromules as integral components of a complex retrograde signaling network capable of modulating jasmonate biosynthesis and signaling in response to environmental cues. Through a combination of live-cell imaging, inhibitor treatments, and gene expression analysis, we have made several key findings that advance our understanding of stromule dynamics and their role in stress responses and hormone signaling:

I. our investigation reveals a complex interaction between phytohormones and stromule dynamics in tobacco BY-2 cells. We found that both salicylic acid (SA) and methyl jasmonate (MeJA) induce the formation and elongation of stromules. Additionally, jasmonic acid (JA) signaling plays a crucial role in SA-induced stromule formation. The complex crosstalk between SA and JA signaling pathways in stromule regulation, was elucidated through phenidone inhibition studies. Notably, we observed a hormonal priming effect, where basal JA signaling was required for SA-induced stromule formation, indicating a collaborative effort between these typically antagonistic pathways in certain aspects of cellular stress responses.

II. Our analysis of jasmonate synthesis and the expression patterns of response genes (AOC, OPR, JAZ1) under various treatments has provided important insights into the molecular mechanisms that regulate stromule activity. We observed the differential expression of JA biosynthesis and signaling genes in response to stromule inhibition by oryzalin. This suggests that stromules may play a role in transporting JA precursors between different cellular compartments. Our hypothesis is supported by the localization of JASSY and the clustering of peroxisomes around stromules, indicating that these structures act as dynamic platforms to organize multi-organelle metabolons involved in stress signaling and hormone biosynthesis. Furthermore, the spatial association of JASSY and peroxisomes with stromules provides strong evidence for the involvement of stromules in retrograde signaling from plastids to the nucleus. Importantly, the accumulation of OPDA resulting from disrupted stromule formation may function as a nuclear signal, indicating cellular stress or damage and initiates appropriate adaptive responses.

III. Our investigation elucidated the critical role of cytoskeletal architecture in stromule dynamics. We found that microtubules are essential for both the initiation and elongation of stromules beyond a specific length threshold. Time-course analyses of cells treated with methyl jasmonate (MeJA) revealed a rapid induction of stromules, along with impressive temporal stability in their lengths. Additionally, we observed an age-dependent increase in stromule formation in BY-2 cell cultures. This phenomenon was notably absent during active cell division, indicating a relationship between plastid behavior and cytoskeletal reorganization throughout the cell cycle.

These findings position stromules as dynamic sensory structures that enable plastids to effectively sample their cellular environment and rapidly transmit signals in response to stress or developmental cues. These implications hold significant potential for enhancing plant stress tolerance and resilience. However, this study has several limitations that should be addressed in future research. The experiments were mainly conducted using tobacco BY-2 cell cultures, which are a useful model system but may not fully represent the complexity of stromule behavior in real plant tissues. Additionally, our observations focused on specific stress conditions, which may have overlooked other important factors influencing stromule dynamics. Expanding our scope in future studies can give us a more comprehensive understanding of these processes.

Future research should further elucidate the molecular mechanisms linking stromule formation to cytoskeletal organization and signaling pathways. Specifically, the following areas deserve investigation:

1. **Cytoskeletal components:** Elucidation of the roles of specific cytoskeletal elements, such as motor proteins and microtubule-associated proteins (MAPs), in stromule dynamics. This could involve high-resolution imaging techniques combined with targeted protein manipulations.

2. **Metabolic pathways:** Exploration of potential roles of stromules in other metabolic pathways, such as terpenoid biosynthesis, to reveal new aspects of plastid function in plant metabolism and stress responses.

3. **Molecular triggers:** Identification of the molecular signals that initiate increased stromule formation during cellular senescence. This could involve a comprehensive

analysis of senescence-associated genes and their potential role in regulating plastid behavior.

4. **Functional significance:** Determination of the physiological advantages by increased stromulation in senescent cells. Comparative studies of stimulation that examine metabolic efficiency, stress resistance, and signaling capacity between young and senescent cells could provide valuable insights.

5. **Reversibility:** Investigation into whether the senescence-associated increase in stromulation is reversible if cellular aging is delayed or reversed. This could be explored through experiments employing senescence-delaying treatments.

6. **Stress response enhancement:** Development of strategies to modulate stromule formation and function to enhance plant responses to environmental stresses based on the insights gained from stromule biology.

These proposed research ideas expand our understanding of stromule biology in plant cellular function and stress responses. This could potentially lead to novel approaches for improving plant resilience in the face of environmental challenges.

7. Outlook

This thesis has made significant contributions to our understanding of the role of methyl jasmonate (MeJA) in the induction of stromules, particularly regarding how stromules coexist and impact biological pathways and plant defense mechanisms. The findings reveal that MeJA induces the formation of stromules, which are essencial in enhancing inter-organelle communication and thereby supporting plant biological pathways. However, as we peel back the layers of these complex cellular interactions, we find ourselves standing at the threshold of even more intriguing questions.

7.1. Beyond MeJA, How Do Stromules Sense and React to Their Ever-Changing World?

This question prompted us to explore the subcellular localization and dynamics of terpenoid precursors. Terpenoids, the largest and most diverse class of plant secondary metabolites, present a fascinating case study in metabolic complexity. These compounds are biosynthesized via two seperate routes: the mevalonate (MVA) pathway and the methylerythritol phosphate (MEP) pathway, which contribute to the diversity of terpenoid structures and functions. Terpenoids serve as a bridge between different cellular compartments. The MEP (Methylerythritol Phosphate) pathway occurs in plastids and produces GPP (Geranyl Pyrophosphate), the precursor for monoterpenes. In contrast, the MVA (Mevalonate) pathway operates in the cytosol and produces FPP (Farnesyl Pyrophosphate), the precursor for sesquiterpenes. Although GPP is primarily synthesized in plastids, small amounts can be transported to the cytosol for cytosolic terpenoid biosynthesis. Conversely, while FPP is mainly produced in the cytosol, there is evidence of some FPP synthesis occurring in plastids, allowing for potential crosstalk between the two pathways and flexibility in terpenoid production (Dudareva et al. 2013; Hsieh et al. 2008; Pulido et al. 2012).

As we explore this unknown region, we ask: Could stromules serve as metabolic highways, shuttling terpenoid precursors between organelles? Might they act as dynamic platforms for enzyme complexes involved in terpenoid biosynthesis? Alternatively, they may play a role in rapidly mobilizing these compounds in response to stress. To address these questions, we have begun mapping the subcellular landscape of terpenoid precursors. Our initial steps have yielded some results, suggesting a complex distribution of these metabolic intermediates.

7.1.1. Milestones in Our Investigation: Fundamental Questions and Research Route

We established fluorescent transgenic *Nicotiana tabacum* BY-2 cell lines as experimental models, specifically focusing on the expression of two key enzymes from Zea mays: terpene synthase TPS2 and farnesyl pyrophosphate synthase 2 (FPPS2). These cell lines served as platforms for our investigation into the subcellular dynamics of terpenoid biosynthesis. TPS2 and FPPS2 can probably utilize both geranyl pyrophosphate (GPP) and farnesyl pyrophosphate (FPP) to produce various terpenes. Additionally, to investigate the subcellular localization and dynamics of terpenoid precursors in plant cells, we utilized green-fluorescent analogs of geranyl pyrophosphate (GPP), and farnesyl pyrophosphate (FPP) fused to nitrobenzoxadiazole (NBD). These NBD-coupled precursors serve as valuable tools for visualizing the distribution and movement of terpene intermediates within living cells, offering insights into their potential interactions with cellular compartments. Here, we present our primary findings and outline the path to solving this metabolic mystery.

7.1.1.1. Subcellular Localization of Terpenoid Precursors

Endoplasmic Reticulum (ER): Our observations demonstrated that NBD-GPP forms web-like structures within the cells, closely resembling the endoplasmic reticulum (ER) network. In comparison, NBD-FPP also exhibits web-like structures, but its overlap with the ER is notably less than that of NBD-GPP. Furthermore, treatment with Brefeldin A (BFA), a fungal metabolite that disrupts vesicular trafficking between the ER and the Golgi apparatus, resulted in a marked disruption of this pattern. The application of BFA generally reduced colocalization for both precursors, indicating a potential role for the Golgi apparatus and endomembrane system in their distribution. This supports the understanding of vesicular trafficking in the movement of lipophilic compounds within plant cells.

Quantitative colocalization analysis using the Pearson Correlation Coefficient (PCC) clearly revealed that NBD-GPP had a higher degree of colocalization with the ER than NBD-FPP, suggesting a stronger association of NBD-GPP with the ER and potential differences in the compartmentalization or trafficking of these terpenoid precursors. Overall, our data indicate low colocalization between alternative precursors and the endoplasmic reticulum (ER), suggesting that many of these molecules are localized to other cellular compartments or are more spread in the cytoplasm (Supplemental Figure S5, S6).

Lipid Droplets: Our observations clearly demonstrated that both NBD-GPP and NBD-FPP formed numerous fluorescent dots that frequently colocalized with NileRed-stained lipid droplets. Quantitative analysis using the Pearson Correlation Coefficient (PCC) revealed that the colocalization of both precursors with lipid droplets reached its peak at the 1-hour mark. Importantly, NBD-GPP consistently showed higher colocalization values compared to NBD-FPP throughout the experiment. This difference suggests potential preferential storage of GPP in lipid droplets, which may be important for regulating monoterpene biosynthesis (Supplemental Figure S7, S8).

These findings indicate that lipid droplets may play a regulatory role in the storage and utilization of terpenoid precursors. GPP's stronger affinity for lipid droplets could help maintain suitable substrate levels for plastidial terpene synthases, while FPP's association may reflect a less pronounced role in cytosolic terpenoid biosynthesis. Overall, this finding highlights the significance of lipid droplets in terpenoid biosynthesis and their potential in regulating plant secondary metabolism.

Peroxisomes: Peroxisomes are vital for several metabolic processes, including the β-oxidation of fatty acids and detoxification of reactive oxygen species. Microscopic examination of cells expressing peroxisome and stromule markers showed that NBD-FPP-associated fluorescent dots did not colocalize with peroxisomes, suggesting they are distinct entities within the cell. It is important to note that, the presence of **green**-fluorescent plastids and stromules complicated the quantitative colocalization analysis, as their overlapping emission spectra with **green** NBD-FPP would restrict numerical quantification (see Supplemental Figure S9). Based on our qualitative observations, terpenoid precursors likely do not interact directly with peroxisomes during biosynthesis or trafficking.

These findings challenge initial hypotheses about the role of peroxisomes in the mevalonate (MVA) pathway and FPP production, revealing that NBD-FPP does not localize to peroxisomes. This contributes to our understanding of terpenoid precursor distribution and suggests that other organelles may be more important for FPP storage or metabolism.

7.1.1.2. Dynamics of Terpenoid Precursor Movement

To clarify the intracellular dynamics of terpenoid precursors, we used fluorescently labeled NBD-conjugated farnesyl pyrophosphate (NBD-FPP). The observed movement of NBD-FPP

suggested the involvement of cellular motor proteins. To test this, we conducted experiments using 2,3-butanedione monoxime (BDM), a well-established myosin inhibitor. Surprisingly, BDM treatment did not significantly affect NBD-FPP movement (Supplemental Figure S10), indicating that myosin motors may not be the primary drivers of NBD-FPP translocation within the cell.

We then expanded our investigation to explore alternative intracellular transport mechanisms, focusing on the actin cytoskeleton, which plays a crucial role organelle movement and metabolite trafficking. Using Latrunculin B (LatB), an inhibitor of actin polymerization, we found that treatment significantly reduced the movement of fluorescent dots associated with NBD-FPP (Supplemental Figure S11), underscoring the importance of actin filaments in transporting terpenoid precursors. It's also necessary to monitor stromule formation in the presence of cytoskeletal inhibitors. Stromules, as dynamic extensions of plastids, interact with cytoskeletal elements and may influence precursor movement. By examining stromule dynamics in conjunction with precursor movement, we aim to better understand the interplay between organelle morphology and metabolite trafficking.

Despite advances, the precise mechanisms of precursor uptake, storage, and utilization within cellular compartments are still not fully understood. To reduce these gaps, further research has focused on:

- **Enzyme Inhibition Studies:** By using inhibitors like fosmidomycin and mevinolin, we can block a biosynthetic pathway while supplying precursors from an alternative pathway, allowing us to investigate cross-talk and precursor exchange between cellular compartments. Fosmidomycin targets 1-deoxy-D-xylulose 5-phosphate reductoisomerase (DXR) in the MEP pathway, effectively halting plastidial isoprenoid production, while mevinolin inhibits 3-hydroxy-3-methylglutaryl-CoA reductase (HMGR), a crucial enzyme in the cytosolic MVA pathway. By combining the blockage of the MVA pathway with geranyl pyrophosphate (GPP) or inhibiting the MEP pathway with farnesyl pyrophosphate (FPP), we can estimate if these precursors are transported via stromules and utilized in the opposing pathway. This approach can reveal insights into compensatory mechanisms and the flexibility of isoprenoid biosynthesis in plant cells, enhancing our understanding of stromule function.
- **Metabolomic Analysis:** Conduct metabolomic studies under varying conditions to quantify precursor levels. This will enhance our understanding of metabolic fluxes and terpenoid precursor levels in plastidial metabolism.

- **Endomembrane System Exploration:** Investigate the complex roles of endomembrane components, particularly the Golgi apparatus, in the trafficking of precursors. Understanding these pathways could reveal novel insights into cellular organization and function.

7.2. From Prokaryotic Origins to Eukaryotic Adaptations: The Evolution of Chloroplast Division and Stromule Formation

As we dig deeper into the complexities of plant cell biology, future research needs to clarify the detailed molecular mechanisms responsible for stromule formation. Studying chloroplast division and stromule development in plants is an exciting area of investigation. This section highlights potential research directions and unanswered questions in three key areas: FtsZ proteins, the MIN system, and the role of the plastoskeleton in stromule formation.

The process of plastid division involves components derived from both prokaryotes and eukaryotes. Central to this process is the plastoskeleton, which includes FtsZ filaments and various structural proteins. The FtsZ proteins have developed from their cyanobacterial ancestors. In plants, two families of FtsZ proteins exist: FtsZ1 and FtsZ2. These proteins assemble into ring-like structures at the chloroplast midpoint, forming the initial scaffolding for the division machinery (Vitha et al. 2001). FtsZ1 and FtsZ2 have different but complementary functions in chloroplast division. They localize to form aligned rings at the chloroplast division site, as shown by immunofluorescence microscopy and GFP fusion studies in Arabidopsis thaliana. These FtsZ rings present in both constricted and non-constricted chloroplasts, indicating their role in the entire plastid division cycle. Proper assembly and positioning of these rings are essential for chloroplast division (TerBush et al. 2013; Vitha et al. 2001).

In bacteria, the MIN (Minicell) system regulates the positioning of the division site and is partially conserved. In plants, the MIN system consists of several key components (Nakanishi et al. 2009a; Pyke 2010): **MinD,** a stromal ATPase that plays a crucial role in positioning the division site; **MinE,** a topological specificity factor that regulates MinD activity; **ARC3**, a plant-specific protein that functions analogously to bacterial MinC, inhibiting FtsZ polymerization, and **MCD1**, a plant-specific factor that interacts with MinD and is essential for proper MinD localization.

ARC3 (Accumulation and Replication of Chloroplasts 3) is a key regulator of plant chloroplast division. Mutations in ARC3 cause enlarged chloroplasts due to defects in FtsZ ring positioning and assembly, often resulting in multiple FtsZ rings within a single chloroplast (Wilson et al. 2011). In contrast, overexpression of ARC3 in Arabidopsis thaliana inhibits FtsZ filament assembly, leading to fewer but larger chloroplasts, similar to ftsZ1 mutants (Zhang et al. 2013). Mutations in MinD, similar to ARC3, also result in multiple Z-rings and asymmetric chloroplast division, illustrating its role in FtsZ ring formation at the mid-plastid. Overexpressing MinD significantly inhibits FtsZ filament and Z-ring formation (Nakanishi et al. 2009a; Nakanishi et al. 2009b). In contrast, MinE mutants show short FtsZ filaments and enlarged chloroplasts, indicating MinE's positive influence on Z-ring assembly, while its overexpression leads to multiple Z-rings (Fujiwara et al. 2015).

The components of the chloroplast division machinery significantly influence the formation and dynamics of stromules. FtsZ proteins, especially FtsZ1, form ring-like structures within stromules, and research shows that overexpressing these proteins can induce stromule formation (Fujiwara et al. 2015). Additionally, mutations in the ARC3 gene lead to increased stromule formation, suggesting a link between defects in chloroplast division and changes in stromule dynamics. The altered morphology in ARC3 mutants may drive the extension of stromules to maintain plastid function and inter-organelle communication (Holzinger et al. 2008). Similarly, mutations in MinD and MinE impact stromule formation, with MinD mutants exhibiting a higher frequency of stromules due to disrupted spatial regulation during chloroplast division (Fujiwara et al. 2017).

ARC3, MinD, and MinE are critical regulators of chloroplast division, and their mutations or overexpression can significantly impact stromule formation. Given the complex relationship between chloroplast division machinery, and stromule dynamics, two main questions emerge as hypotheses for future investigation: Is stromule formation a direct consequence of **asymmetric chloroplast division**? How do **FtsZ, ARC3, MinD,** and **MinE** proteins contribute to regulating stromule formation?

To investigate these questions, we are conducting a series of experiments involving the generation of new BY-2 cell lines with mutations or overexpression of FtsZ, ARC3, and MinD. We have successfully created an FtsZ BY-2 line, which will serve as a valuable tool in our research.

While the behind mechanism of stromule formation is not fully understood, we argue that disruptions in the spatial regulation of division components lead to altered chloroplast morphology. This likely leads to stromule extension, which helps maintain plastid function and facilitate organelle communication. Further research is needed to clarify the relationship between chloroplast division and stromule dynamics in plant cells and how evolutionary adaptations have shaped these processes from their prokaryotic origins to their current functions in eukaryotic plant cells.

8. References

Ahmad N, Burgess SJ, Nielsen BL (2016) advances in plastid biology and its applications. vol 7. Frontiers Media SA,

Atkinson K (2017) The biology and therapeutic application of mesenchymal cells, 2 volume set. John Wiley & Sons,

Baillie AL, Falz A-L, Müller-Schüssele SJ, Sparkes I (2020) It started with a kiss: monitoring organelle interactions and identifying membrane contact site components in plants. Frontiers in Plant Science 11:533927

Bhat RA, & Thompson, R.D. (2004) The Tobacco BY-2 Cell Line as a Model System to Understand in Planta Nuclear Coactivator Interactions. . In: Nagata, T, Hasezawa, S, Inzé, D (eds) Tobacco BY-2 Cells Biotechnology in Agriculture and Forestry Springer, Berlin, Heidelberg, vol 53. doi: 10.1007/978-3-662-10572-6_21.

Breuers FK, Bräutigam A, Geimer S, Welzel UY, Stefano G, Renna L, Brandizzi F, Weber AP (2012) Dynamic remodeling of the plastid envelope membranes–a tool for chloroplast envelope in vivo localizations. Frontiers in plant science 3:17957

Browse J (2009) Jasmonate passes muster: a receptor and targets for the defense hormone. Annual Review of Plant Biology 60 (1):183-205

Bruinsma M, Van Broekhoven S, Poelman EH, Posthumus MA, Müller MJ, Van Loon JJ, Dicke M (2010) Inhibition of lipoxygenase affects induction of both direct and indirect plant defences against herbivorous insects. Oecologia 162:393-404

Brunkard JO, Runkel AM, Zambryski P (2016) Visualizing stromule frequency with fluorescence microscopy. JoVE (Journal of Visualized Experiments) (117):e54692

Brunkard JO, Runkel AM, Zambryski PC (2015) Chloroplasts extend stromules independently and in response to internal redox signals. Proceedings of the National Academy of Sciences 112 (32):10044-10049

Buschmann H, Green P, Sambade A, Doonan J, Lloyd C (2011) Cytoskeletal dynamics in interphase, mitosis and cytokinesis analysed through Agrobacterium-mediated transient transformation of tobacco BY-2 cells. New Phytologist 190 (1):258-267

Caarls L, Pieterse CM, Van Wees SC (2015) How salicylic acid takes transcriptional control over jasmonic acid signaling. Frontiers in plant science 6:170

Caplan JL, Kumar AS, Park E, Padmanabhan MS, Hoban K, Modla S, Czymmek K, Dinesh-Kumar SP (2015) Chloroplast stromules function during innate immunity. Developmental cell 34 (1):45-57

Chini A, Fonseca S, Fernandez G, Adie B, Chico J, Lorenzo O, García-Casado G, López-Vidriero I, Lozano F, Ponce M (2007) The JAZ family of repressors is the missing link in jasmonate signalling. Nature 448 (7154):666-671

Dave A, Graham IA (2012) Oxylipin signaling: a distinct role for the jasmonic acid precursor cis-(+)-12-oxo-phytodienoic acid (cis-OPDA). Frontiers in plant science 3:42

Domanov YA, Kinnunen PK (2006) Antimicrobial peptides temporins B and L induce formation of tubular lipid protrusions from supported phospholipid bilayers. Biophysical journal 91 (12):4427-4439

Dudareva N, Klempien A, Muhlemann JK, Kaplan I (2013) Biosynthesis, function and metabolic engineering of plant volatile organic compounds. New Phytologist 198 (1):16-32

Erickson JL, Adlung N, Lampe C, Bonas U, Schattat MH (2018) The Xanthomonas effector XopL uncovers the role of microtubules in stromule extension and dynamics in Nicotiana benthamiana. The Plant Journal 93 (5):856-870

Erickson JL, Ziegler J, Guevara D, Abel S, Klösgen RB, Mathur J, Rothstein SJ, Schattat MH

(2014) Agrobacterium-derived cytokinin influences plastid morphology and starch accumulation in Nicotiana benthamiana during transient assays. BMC Plant Biology 14:1-20

Fligner MA, Killeen TJ (1976) Distribution-free two-sample tests for scale. Journal of the American Statistical Association 71 (353):210-213

Footitt S, Dietrich D, Fait A, Fernie AR, Holdsworth MJ, Baker A, Theodoulou FL (2007) The COMATOSE ATP-binding cassette transporter is required for full fertility in Arabidopsis. Plant Physiology 144 (3):1467-1480

Fujiwara MT, Kojo KH, Kazama Y, Sasaki S, Abe T, Itoh RD (2015) The Arabidopsis minE mutation causes new plastid and FtsZ1 localization phenotypes in the leaf epidermis. Frontiers in Plant Science 6:823

Fujiwara MT, Yasuzawa M, Sasaki S, Nakano T, Niwa Y, Yoshida S, Abe T, Itoh RD (2017) The Arabidopsis minD mutation causes aberrant FtsZ1 ring placement and moderate heterogeneity of chloroplasts in the leaf epidermis. Plant signaling & behavior 12 (7):e1343776

Gould SB, Waller RF, McFadden GI (2008) Plastid evolution. Annu Rev Plant Biol 59 (1):491-517

Granger CL, Cyr RJ (2000) Microtubule reorganization in tobacco BY-2 cells stably expressing GFP-MBD. Planta 210:502-509

Gray J, Sullivan J, Hibberd J, Hansen M (2001) Stromules: mobile protrusions and interconnections between plastids. Plant Biology 3 (03):223-233

Gray JC, Hansen MR, Shaw DJ, Graham K, Dale R, Smallman P, Natesan SK, Newell CA (2012) Plastid stromules are induced by stress treatments acting through abscisic acid. The Plant Journal 69 (3):387-398

Gu Y, Dong X (2015) Stromules: signal conduits for plant immunity. Developmental Cell 34 (1):3-4

Guan L, Denkert N, Eisa A, Lehmann M, Sjuts I, Weiberg A, Soll J, Meinecke M, Schwenkert S (2019) JASSY, a chloroplast outer membrane protein required for jasmonate biosynthesis. Proceedings of the National Academy of Sciences 116 (21):10568-10575

Haberlandt G (1888) Die Chlorophyllkörper der Selaginellen. Flora 71:291

Hanson MR, Hines KM (2018) Stromules: probing formation and function. Plant physiology 176 (1):128-137

Hanson MR, Sattarzadeh A (2011) Stromules: recent insights into a long neglected feature of plastid morphology and function. Plant Physiology 155 (4):1486-1492

Hanson MR, Sattarzadeh A (2013) Trafficking of proteins through plastid stromules. The Plant Cell 25 (8):2774-2782

Ho J, Theg SM (2016) The formation of stromules in vitro from chloroplasts isolated from Nicotiana benthamiana. PLoS One 11 (2):e0146489

Holzinger A, Buchner O, Lütz C, Hanson M (2007) Temperature-sensitive formation of chloroplast protrusions and stromules in mesophyll cells of Arabidopsis thaliana. Protoplasma 230:23-30

Holzinger A, Kwok EY, Hanson MR (2008) Effects of arc3, arc5 and arc6 mutations on plastid morphology and stromule formation in green and nongreen tissues of Arabidopsis thaliana. Photochemistry and Photobiology 84 (6):1324-1335

Hsieh M-H, Chang C-Y, Hsu S-J, Chen J-J (2008) Chloroplast localization of methylerythritol 4-phosphate pathway enzymes and regulation of mitochondrial genes in ispD and ispE albino mutants in Arabidopsis. Plant molecular biology 66:663-673

Ishida H, Yoshimoto K, Izumi M, Reisen D, Yano Y, Makino A, Ohsumi Y, Hanson MR, Mae T (2008) Mobilization of rubisco and stroma-localized fluorescent proteins of chloroplasts to the vacuole by an ATG gene-dependent autophagic process. Plant physiology 148

(1):142-155
Ismail A, Riemann M, Nick P (2012) The jasmonate pathway mediates salt tolerance in grapevines. Journal of Experimental Botany 63 (5):2127-2139
Kessler A, Baldwin IT (2002) Plant responses to insect herbivory: the emerging molecular analysis. Annual review of plant biology 53 (1):299-328
Kohler RH, Cao J, Zipfel WR, Webb WW, Hanson MR (1997) Exchange of protein molecules through connections between higher plant plastids. science 276 (5321):2039-2042
Köhler RH, Hanson MR (2000) Plastid tubules of higher plants are tissue-specific and developmentally regulated. Journal of cell science 113 (1):81-89
Kumar AS, Park E, Nedo A, Alqarni A, Ren L, Hoban K, Modla S, McDonald JH, Kambhamettu C, Dinesh-Kumar SP (2018) Stromule extension along microtubules coordinated with actin-mediated anchoring guides perinuclear chloroplast movement during innate immunity. Elife 7:e23625
Kwok E, Hanson M (2004) Stromules and the dynamic nature of plastid morphology. Journal of Microscopy 214 (2):124-137
Kwok EY, Hanson MR (2003) Microfilaments and microtubules control the morphology and movement of non-green plastids and stromules in Nicotiana tabacum. The Plant Journal 35 (1):16-26
Leon-Reyes A, Van der Does D, De Lange ES, Delker C, Wasternack C, Van Wees SC, Ritsema T, Pieterse CM (2010) Salicylate-mediated suppression of jasmonate-responsive gene expression in Arabidopsis is targeted downstream of the jasmonate biosynthesis pathway. Planta 232:1423-1432
Leontovyčová H, Kalachova T, Trdá L, Pospíchalová R, Lamparová L, Dobrev PI, Malínská K, Burketová L, Valentová O, Janda M (2019) Actin depolymerization is able to increase plant resistance against pathogens via activation of salicylic acid signalling pathway. Scientific reports 9 (1):10397
Livak KJ, Schmittgen TD (2001) Analysis of relative gene expression data using real-time quantitative PCR and the 2− ΔΔCT method. methods 25 (4):402-408
Machettira AB, Groß LE, Tillmann B, Weis BL, Englich G, Sommer MS, Königer M, Schleiff E (2012) Protein-induced modulation of chloroplast membrane morphology. Frontiers in plant science 2:118
Maisch J, Nick P (2007) Actin is involved in auxin-dependent patterning. Plant Physiology 143 (4):1695-1704
Mathur J (2021) Organelle extensions in plant cells. Plant Physiology 185 (3):593-607
Mathur J, Barton KA, Schattat MH (2013) Fluorescent protein flow within stromules. The Plant Cell 25 (8):2771-2772
Matoušková J, Janda M, Fišer R, Šašek V, Kocourková D, Burketová L, Dušková J, Martinec J, Valentová O (2014) Changes in actin dynamics are involved in salicylic acid signaling pathway. Plant Science 223:36-44
Mercx S, Smargiasso N, Chaumont F, De Pauw E, Boutry M, Navarre C (2017) Inactivation of the β (1, 2)-xylosyltransferase and the α (1, 3)-fucosyltransferase genes in *Nicotiana tabacum* BY-2 cells by a multiplex CRISPR/Cas9 strategy results in glycoproteins without plant-specific glycans. Frontiers in plant science 8:403
Mur LA, Kenton P, Atzorn R, Miersch O, Wasternack C (2006) The outcomes of concentration-specific interactions between salicylate and jasmonate signaling include synergy, antagonism, and oxidative stress leading to cell death. Plant physiology 140 (1):249-262
Nagata T, Kumagai F (1999) Plant cell biology through the window of the highly synchronized tobacco BY-2 cell line. Methods in Cell Science 21:123-127
Nagata T, Matsuoka K, Inzé D (2006) Tobacco BY-2 cells: from cellular dynamics to omics, vol 58. Springer Science & Business Media,

Nagata T, Nemoto Y, Hasezawa S (1992) Tobacco BY-2 cell line as the "HeLa" cell in the cell biology of higher plants. In: International review of cytology, vol 132. Elsevier, pp 1-30

Nakanishi H, Suzuki K, Kabeya Y, Miyagishima S-y (2009a) Plant-specific protein MCD1 determines the site of chloroplast division in concert with bacteria-derived MinD. Current Biology 19 (2):151-156

Nakanishi H, Suzuki K, Kabeya Y, Okazaki K, Miyagishima S-y (2009b) Conservation and differences of the Min system in the chloroplast and bacterial division site placement. Communicative & Integrative Biology 2 (5):400-402

Natesan SKA, Sullivan JA, Gray JC (2005) Stromules: a characteristic cell-specific feature of plastid morphology. Journal of Experimental Botany 56 (413):787-797

Natesan SKA, Sullivan JA, Gray JC (2009) Myosin XI is required for actin-associated movement of plastid stromules. Molecular Plant 2 (6):1262-1272

Newell CA, Natesan SK, Sullivan JA, Jouhet J, Kavanagh TA, Gray JC (2012) Exclusion of plastid nucleoids and ribosomes from stromules in tobacco and Arabidopsis. The Plant Journal 69 (3):399-410

Oikawa K, Hayashi M, Hayashi Y, Nishimura M (2019) Re-evaluation of physical interaction between plant peroxisomes and other organelles using live-cell imaging techniques. Journal of integrative plant biology 61 (7):836-852

Park S-W, Kaimoyo E, Kumar D, Mosher S, Klessig DF (2007) Methyl salicylate is a critical mobile signal for plant systemic acquired resistance. Science 318 (5847):113-116

Pucadyil TJ, Schmid SL (2008) Real-time visualization of dynamin-catalyzed membrane fission and vesicle release. Cell 135 (7):1263-1275

Pulido P, Perello C, Rodriguez-Concepcion M (2012) New insights into plant isoprenoid metabolism. Molecular plant 5 (5):964-967

Pyke KA (2010) Plastid division. AoB plants 2010:plq016

Roy S, Hsiung F, Kornberg TB (2011) Specificity of Drosophila cytonemes for distinct signaling pathways. Science 332 (6027):354-358

Ruan J, Zhou Y, Zhou M, Yan J, Khurshid M, Weng W, Cheng J, Zhang K (2019) Jasmonic acid signaling pathway in plants. International journal of molecular sciences 20 (10):2479

Sattarzadeh A, Krahmer J, Germain AD, Hanson MR (2009) A myosin XI tail domain homologous to the yeast myosin vacuole-binding domain interacts with plastids and stromules in Nicotiana benthamiana. Molecular plant 2 (6):1351-1358

Schaller F, Schaller A, Stintzi A (2004) Biosynthesis and metabolism of jasmonates. Journal of Plant Growth Regulation 23:179-199

Schattat M, Barton K, Baudisch B, Klösgen RB, Mathur J (2011) Plastid stromule branching coincides with contiguous endoplasmic reticulum dynamics. Plant physiology 155 (4):1667-1677

Schattat MH, Barton KA, Mathur J (2015) The myth of interconnected plastids and related phenomena. Protoplasma 252:359-371

Schattat MH, Klösgen RB (2011) Induction of stromule formation by extracellular sucrose and glucose in epidermal leaf tissue of Arabidopsis thaliana. BMC Plant Biology 11:1-10

Schattat MH, Klösgen RB, Mathur J (2012) New insights on stromules: stroma filled tubules extended by independent plastids. Plant signaling & behavior 7 (9):1132-1137

Senn G (1908) Die Gestalts-und Lageveränderung der Pflanzen-Chromatophoren: mit einer Beilage: Die Lichtbrechung der lebenden Pflanzenzelle. W. Engelmann,

Snapp E (2005) Design and use of fluorescent fusion proteins in cell biology. Current protocols in cell biology 27 (1):21.24. 21-21.24. 13

Srba M, Černíková A, Opatrný Z, Fischer L (2016) Practical guidelines for the characterization of tobacco BY-2 cell lines. Biologia plantarum 60 (1):13-24

Stachowiak JC, Hayden CC, Sasaki DY (2010) Steric confinement of proteins on lipid membranes

can drive curvature and tubulation. Proceedings of the National Academy of Sciences 107 (17):7781-7786

Su T, Li X, Yang M, Shao Q, Zhao Y, Ma C, Wang P (2020) Autophagy: an intracellular degradation pathway regulating plant survival and stress response. Frontiers in plant science 11:164

TerBush AD, Yoshida Y, Osteryoung KW (2013) FtsZ in chloroplast division: structure, function and evolution. Current opinion in cell biology 25 (4):461-470

Thines B, Katsir L, Melotto M, Niu Y, Mandaokar A, Liu G, Nomura K, He SY, Howe GA, Browse J (2007) JAZ repressor proteins are targets of the SCFCOI1 complex during jasmonate signalling. Nature 448 (7154):661-665

Tripathy BC, Oelmüller R (2012) Reactive oxygen species generation and signaling in plants. Plant signaling & behavior 7 (12):1621-1633

Vitha S, McAndrew RS, Osteryoung KW (2001) FtsZ ring formation at the chloroplast division site in plants. The Journal of cell biology 153 (1):111-120

Wasternack C, Hause B (2013) Jasmonates: biosynthesis, perception, signal transduction and action in plant stress response, growth and development. An update to the 2007 review in Annals of Botany. Annals of botany 111 (6):1021-1058

Waters MT, Fray RG, Pyke KA (2004) Stromule formation is dependent upon plastid size, plastid differentiation status and the density of plastids within the cell. The Plant Journal 39 (4):655-667

Weigel D, Glazebrook J (2006) Vectors and Agrobacterium hosts for Arabidopsis transformation. Cold Spring Harbor Protocols 2006 (7):pdb. ip29

Wilson ME, Jensen GS, Haswell ES (2011) Two mechanosensitive channel homologs influence division ring placement in Arabidopsis chloroplasts. The Plant Cell 23 (8):2939-2949

Yanagisawa M, Chuong SD (2023) Chloroplast Envelopes Play a Role in the Formation of Autophagy-Related Structures in Plants. Plants 12 (3):443

Yang J, Duan G, Li C, Liu L, Han G, Zhang Y, Wang C (2019) The crosstalks between jasmonic acid and other plant hormone signaling highlight the involvement of jasmonic acid as a core component in plant response to biotic and abiotic stresses. Frontiers in plant science 10:1349

Zhang M, Schmitz AJ, Kadirjan-Kalbach DK, TerBush AD, Osteryoung KW (2013) Chloroplast division protein ARC3 regulates chloroplast FtsZ-ring assembly and positioning in Arabidopsis through interaction with FtsZ2. The Plant Cell 25 (5):1787-1802

Zhao Y, Zhao S, Mao T, Qu X, Cao W, Zhang L, Zhang W, He L, Li S, Ren S (2011) The plant-specific actin binding protein SCAB1 stabilizes actin filaments and regulates stomatal movement in Arabidopsis. The Plant Cell 23 (6):2314-2330

9. Appendix

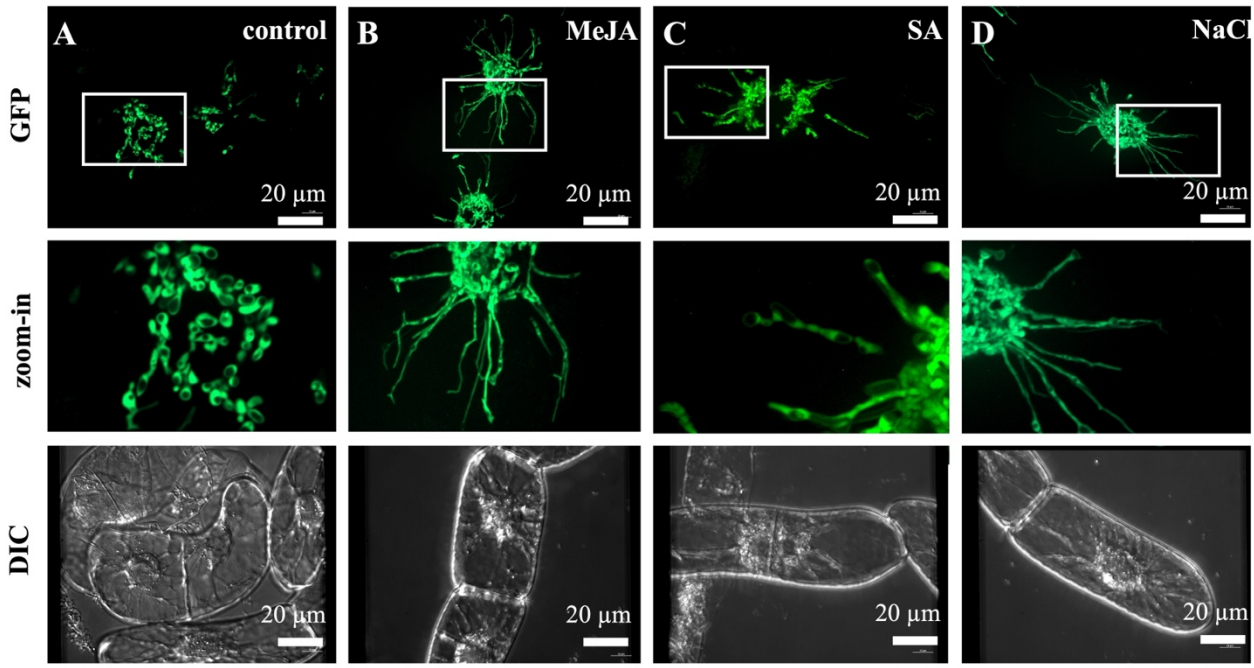

Supplemental Figure S1. Induction of stromulation by stress-related phytohormones and salinity in tobacco BY-2 cells. Geometric projections of confocal z-stacks for representative cells expressing the N-terminal fragment of ferredoxin NADPH oxidoreductase (tpFNR-mEOS) localised in the stroma in fusion with eGFP. **A** Untreated control cell. **B** Cell after treatment with 100 µM of Methyl Jasmonate (MeJA) for 1 h. **C** Cell after treatment with 100 µM of Salicylic Acid (SA) for 1 h. D Cell after treatment with 100 mM NaCl for 1 h. The zoom-in refers to the white square in the GFP image. Differential Interference Contrast image of the same cell is shown to connect the topology of the stromule signal.

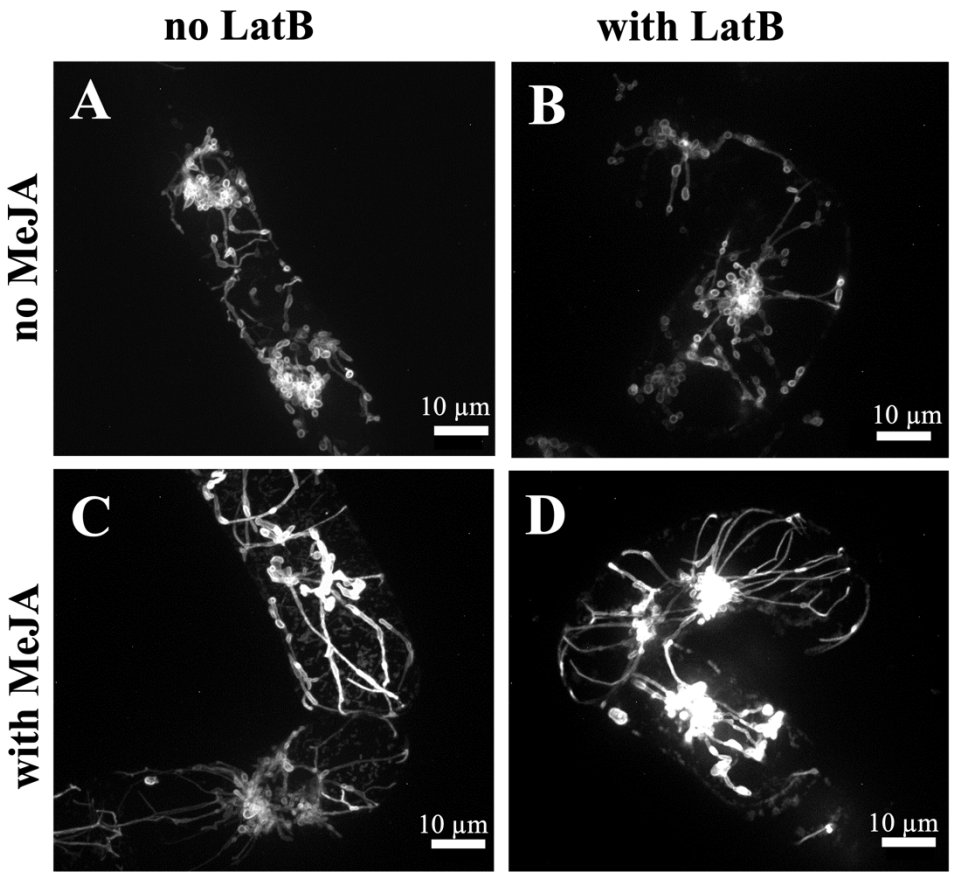

Supplemental Figure S2. MeJA-induced stromulation cannot be blocked by Latrunculin B, a compound eliminating actin filaments. Representative tobacco BY-2 cells expressing Sensitive to Freezing 2 (SFR2) localised in the outer plastid membrane in fusion with mRFP are shown. Images are geometric projections of confocal z-stacks. **A** Untreated control. **B** Treatment with 2 µM of Latrunculin B for 120 min. **C** Treatment with 100 µM of MeJA for 60 min. **D** Treatment with 100 µM of MeJA following a pre-treatment with 2 µM of Latrunculin B for 60 min.

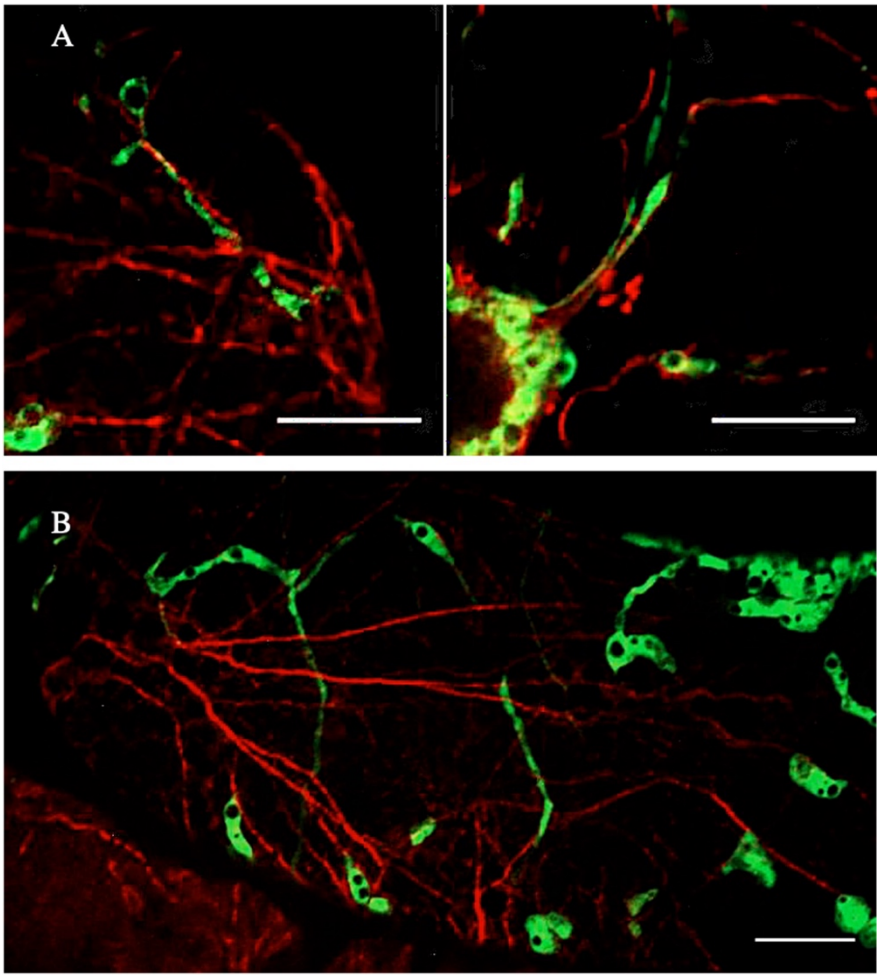

Supplemental Figure S3. Visualization of Plastid Bodies, Stromules, and Actin Filaments Following Exogenous MeJa (100 µM) Activation. Actin filaments are stained in red using TexasRed-Phalloidin, while stromules and plastid bodies are visualized in green through the expression of tpFNR-mEos. **A** Stromules align with actin filaments, demonstrating a coordinated interaction in response to MeJa treatment. **B** Stromules and actin filaments exhibit occasional different orientations, indicating variability in their interactions. This variability may reflect dynamic changes in the cellular architecture or differential responses to MeJa.

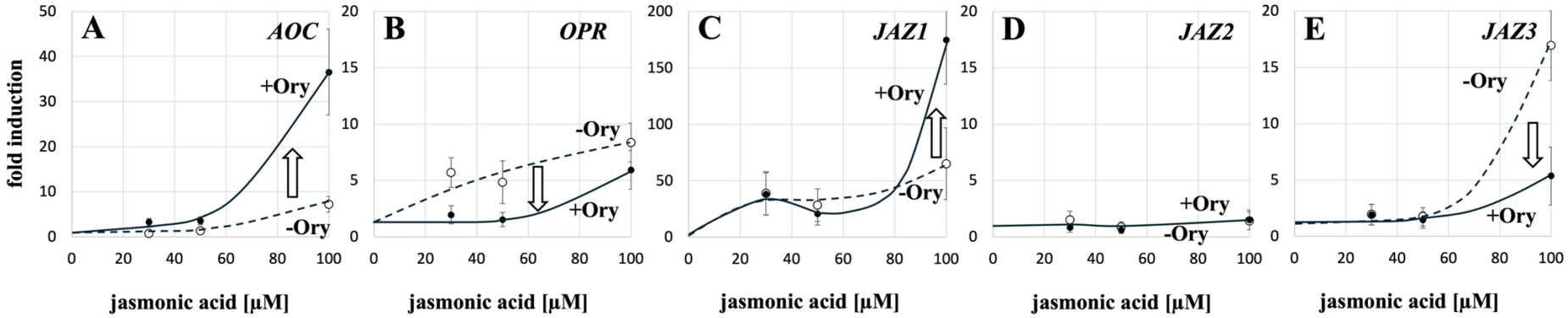

Supplemental Figure S4. Dose-response of jasmonate synthesis and jasmonate response genes over exogenous jasmonic acid either without (-Ory) or with (+Ory) pretreatment with 10 µM of Oryzalin prior to addition of jasmonic acid and incubation for additional 60 min. Induction of steady-state transcript levels for Allene Oxide Cyclase (AOC, **A**), OPDA Reductase (OPR, **B**), and jasmonate response genes JAZ1 (**C**), JAZ2 (**D**), or JAZ3 (**E**) over untreated control cells are shown. Data represent means of three independent experimental series, each in technical triplicates. The arrows demonstrate the effect of the Oryzalin treatment. Note the tenfold compression of the y-axis in **C**.

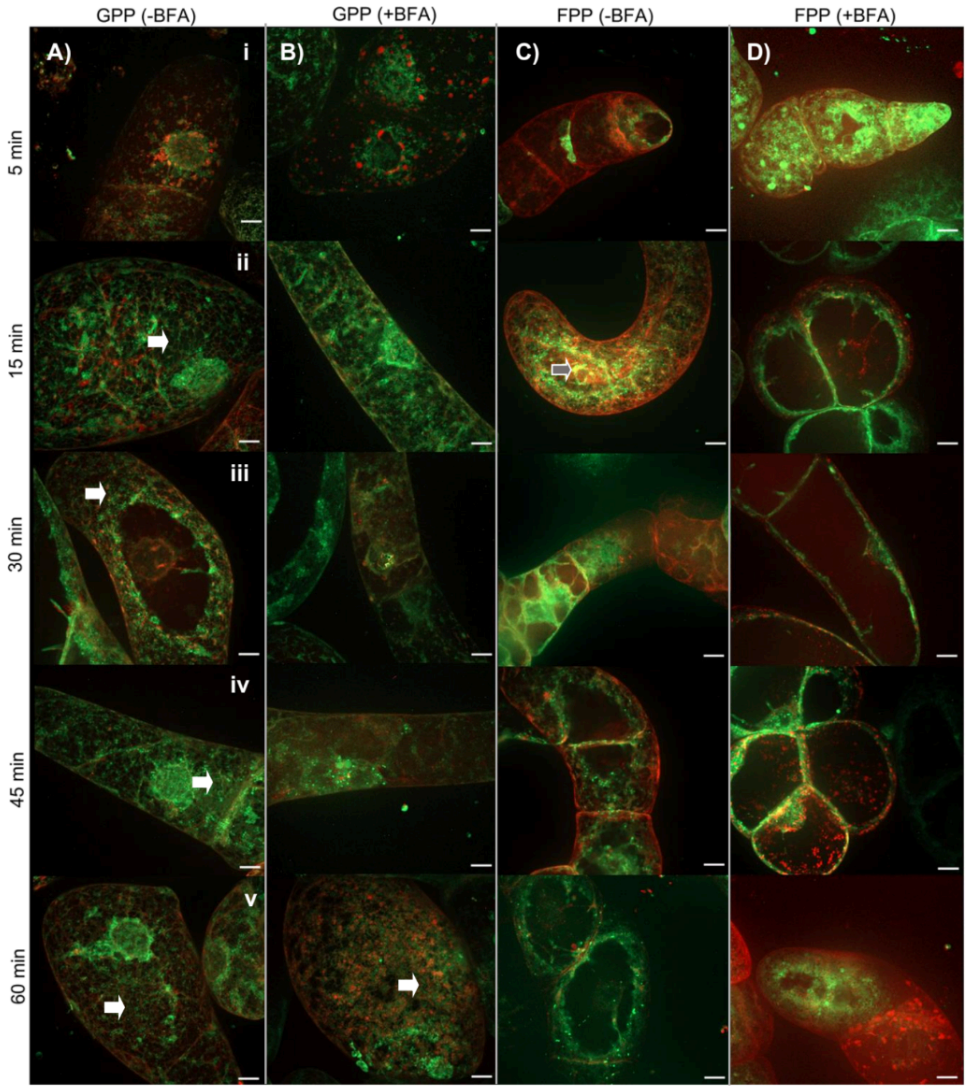

Supplemental Figure S5. Colocalization analysis of endoplasmic reticulum with NBD-GPP and NBD-FPP in the presence and absence of Brefeldin A (BFA). HDEL-RFP-expressing cells were examined for colocalization with NBD-GPP **(Ai-Bv)** or NBD-FPP **(Ci-Dv)**. Time-course experiments were conducted for NBD-GPP without BFA **(Ai-v)** and with BFA **(Bi-v)**, and for NBD-FPP without BFA **(Ci-v)** and with BFA **(Di-v).** Images were captured at 5, 15-, 30-, 45-, and 60-minutes post-exposure to the fluorescent isoprenoid precursors. White arrowheads indicate NBD-GPP mesh structures. Grey-filled arrows highlight partial overlap of NBD-FPP with red-fluorescent structures. Orthogonal projections of merged eGFP and mRFP channel images are shown. Scale bar: 10 µm. Results demonstrate differential localization patterns between NBD-GPP and NBD-FPP, with NBD-GPP showing higher colocalization with the endoplasmic reticulum, particularly in BFA-treated cells.

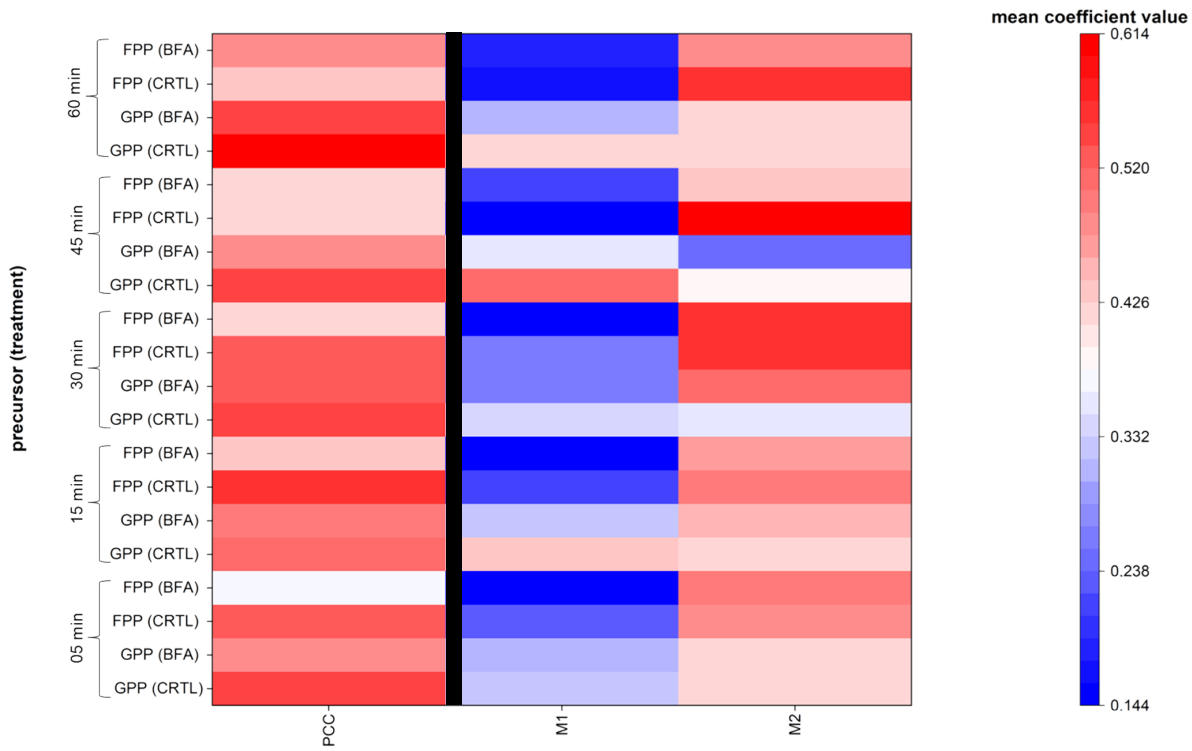

Supplemental Figure S6. Heatmap illustrating average colocalization coefficient values calculated using JaCoP for NBD-GPP and NBD-FPP under various conditions. Pearson's Correlation Coefficient (PCC), Manders' Overlap Coefficients M1 and M2 were assessed. Conditions include no treatment (Control) and Brefeldin A treatment (BFA) for 15 minutes prior to exposure. The ordinate represents exposure time to synthetic prenyl diphosphates, while the abscissa indicates the colocalization coefficient used. Values are color-coded from red (lowest, 0.20) to blue (highest, 0.52). Two biological replicates were conducted for each treatment and compound, with n = 8 images per time point. Statistical analysis using Kruskal-Wallis test followed by Dunn's post-hoc test revealed no significant differences in PCC, M1, or M2 coefficients. Results suggest consistent colocalization patterns over time, with NBD-GPP and NBD-FPP showing increased colocalization in treated conditions.

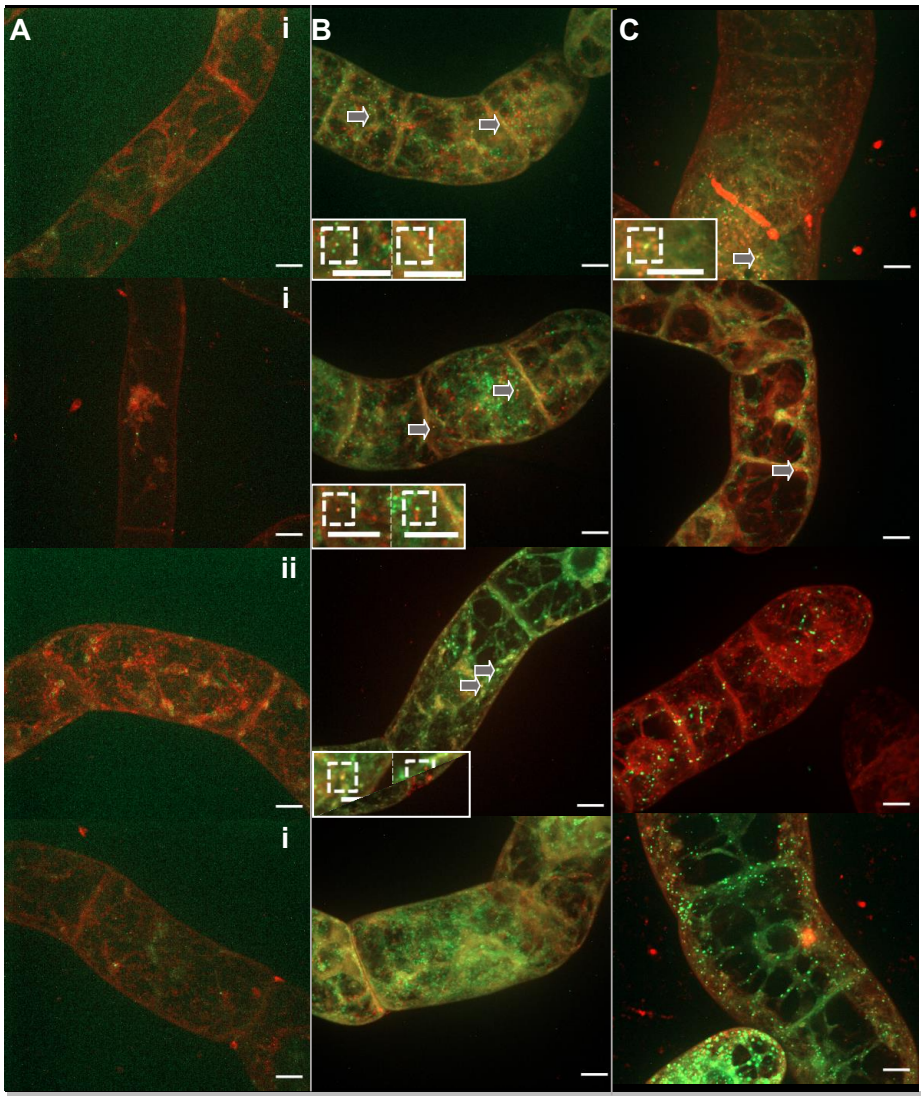

Supplemental Figure S7. Qualitative colocalization analysis of lipid droplets with NBD-coupled GPP and FPP. Representative images of cells after stained with NileRed (red fluorescence). **Ai-iv)** Negative control (NC) without synthetic precursors showing autofluorescence. **Bi-iv)** NBD-GPP (GPP) and **Ci-iv)** NBD-FPP (FPP) exposed cells visible with green fluorescence. Cells were imaged in a time course experiment 05 min, 1 h, 2 h and 3 h after exposing to terpenoid compounds. Images show frontal orthogonal projections in XY of Z-stacks for merged picture using the eGFP and mRFP channels. Grey-filled arrow point to overlapping signals with a close-up shown in a box. Orthogonal projections with a scale bar that represents 10 µm.

A)

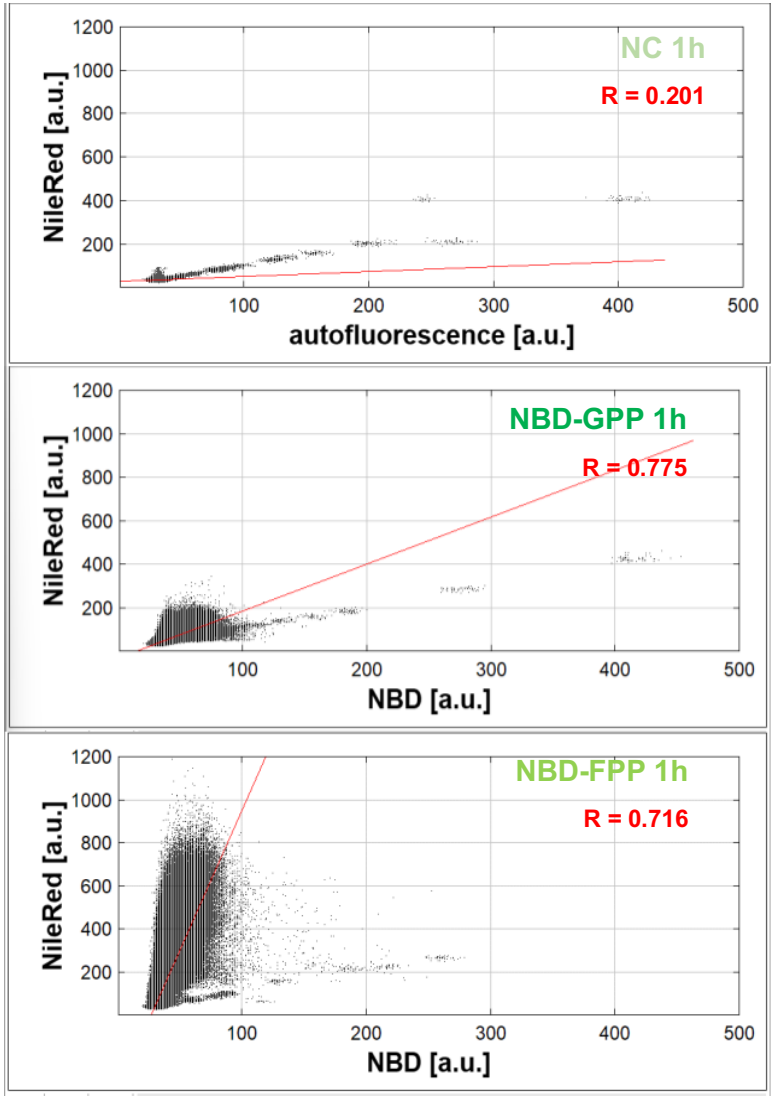
NC 1h
R = 0.201
NileRed [a.u.]
autofluorescence [a.u.]
NBD-GPP 1h
R = 0.775
NileRed [a.u.]
NBD [a.u.]
NBD-FPP 1h
R = 0.716
NileRed [a.u.]
NBD [a.u.]

B)

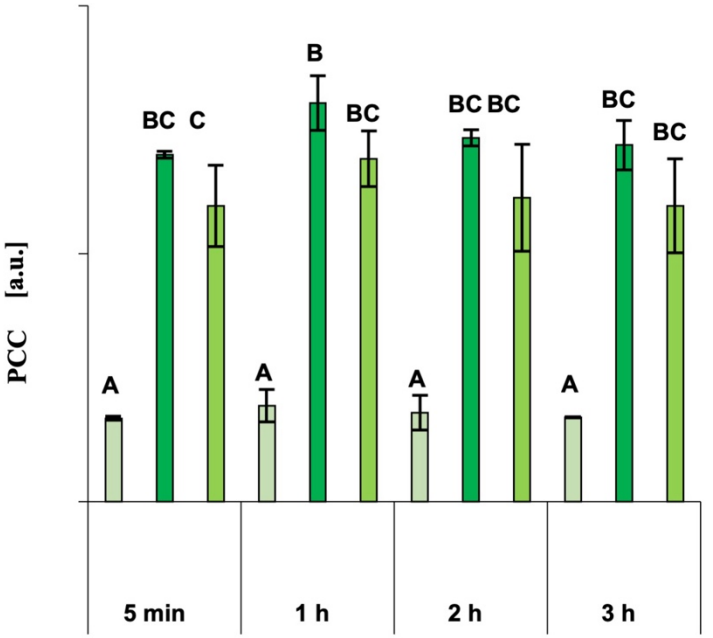
PCC [a.u.]
A
BC
C
A
B
BC
A
BC
BC
A
BC
BC
5 min
1 h
2 h
3 h

C)

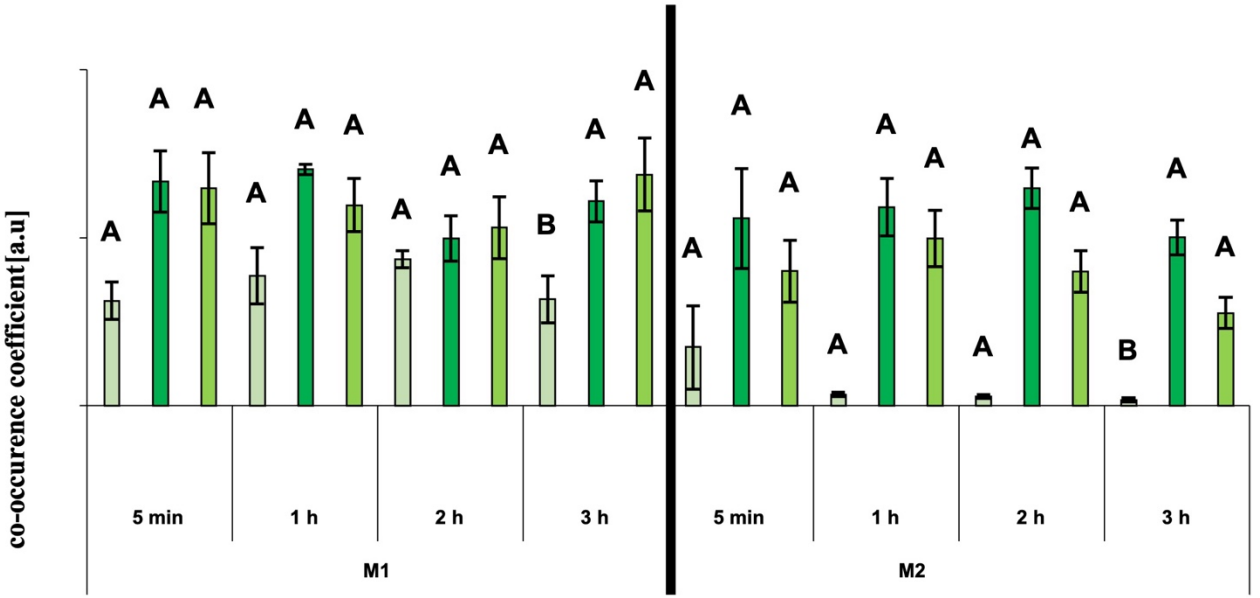

Supplemental Figure S8. Quantitative Colocalization Analysis of Lipid Droplets with NBD-GPP and NBD-FPP. A) Cytofluorogram: This section presents representative graphs showing the distribution of pixel intensities for the fluorescent emission of Nile Red, autofluorescence (negative control), and NBD. The upper graph displays the distribution for NBD-GPP-treated cells after 1 hour of exposure, with a correlation coefficient (R) of 0.775. The lower graph shows NBD-FPP-exposed cells after 1 hour, with R = 0.716. **B)** Average PCC: The average Pearson's Correlation Coefficient (PCC) is shown for negative control, NBD-GPP, and NBD-FPP at time points 5 minutes, 1 hour, 2 hours, and 3 hours post-exposure. **C)** Co-occurrence Analysis (M1 and M2): This analysis was conducted for the negative control, NBD-GPP, and NBD-FPP using JaCoP. Bar charts with standard error bars represent the average of three biological replicates, with each treatment having n = 12 images per time point. A One-Way ANOVA test followed by Tukey's post-hoc test was performed, with significant differences indicated by letters. NBD-GPP and NBD-FPP show higher colocalization values over time compared to Control and BFA, indicating enhanced interaction with lipid droplets.

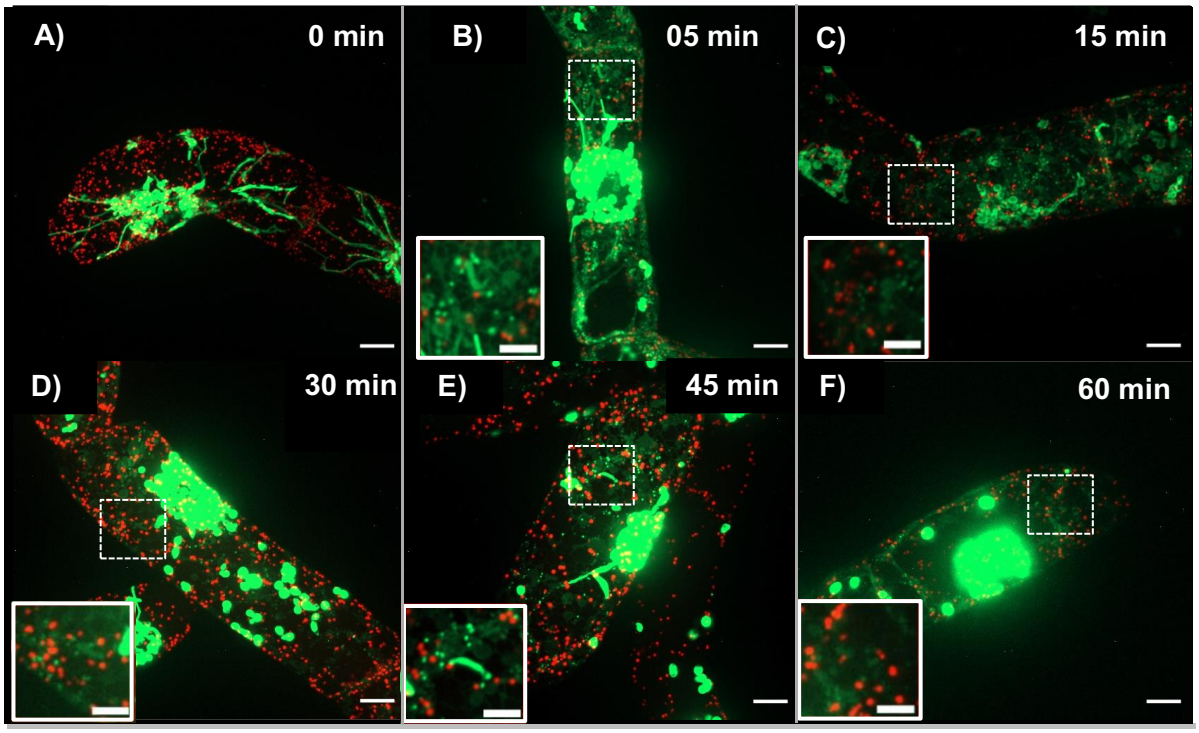

Supplemental Figure S9. Qualitative Colocalization Analysis of Peroxisomes with NBD-Coupled FPP. A) Control: Images of cell lines expressing stromule and peroxisome markers without treatment. B-F) Time Course Experiment: Cells treated with NBD-FPP were imaged at 5 min **(B)**, 15 min **(C)**, 30 min **(D)**, 45 min **(E)**, and 60 min **(F)** after exposure to the synthetic sesquiterpene precursor. White boxes highlight specific regions where peroxisomes and NBD-FPP colocalization are visible, as indicated by dashed boxes. Orthogonal projections of merged images from eGFP and mRFP channels are shown, with scale bars representing 5 µm in close-ups and 10 µm for the entire image. The analysis reveals that there is no significant colocalization observed between NBD-FPP and peroxisomes, indicating minimal interaction under these conditions.

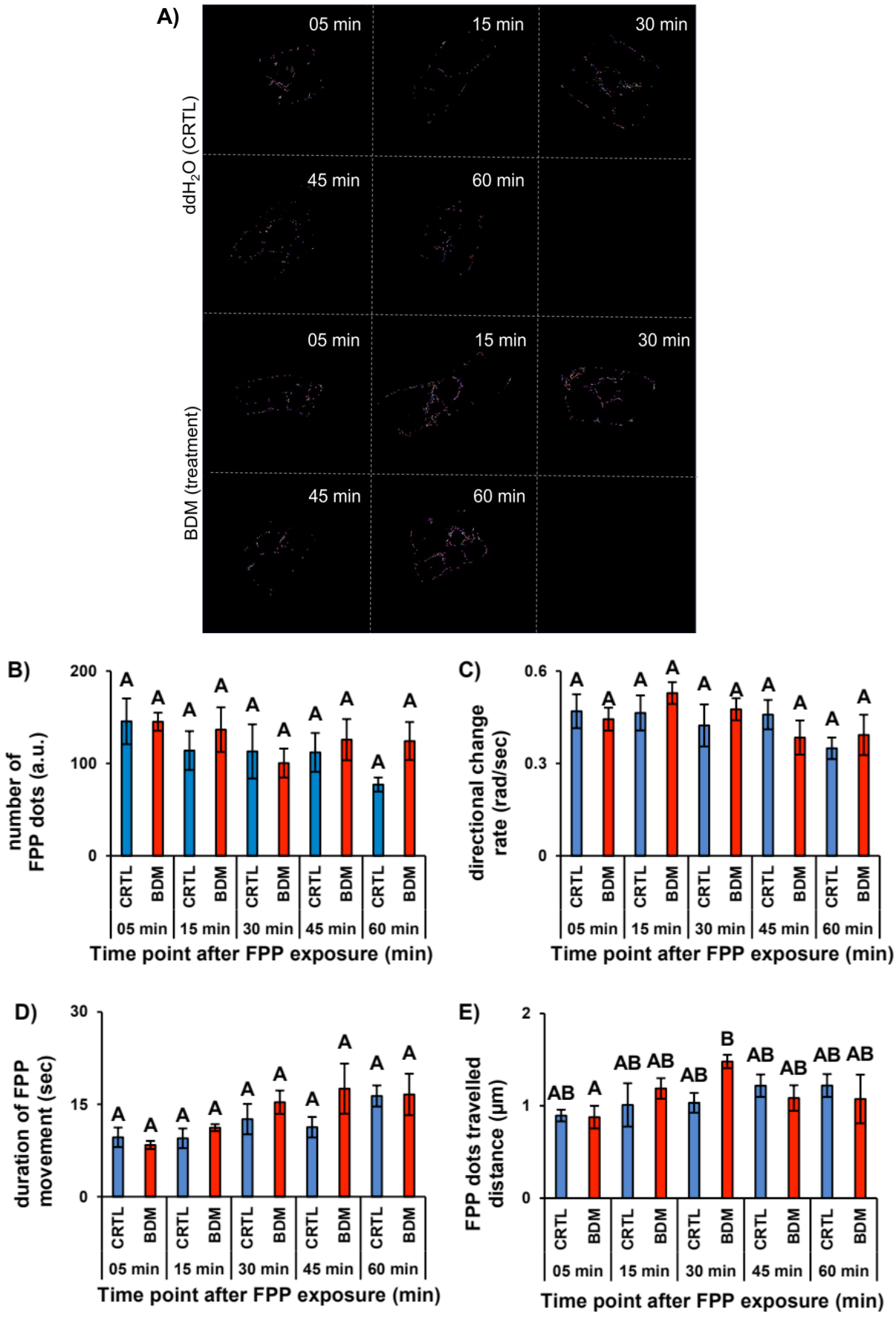
A)
05 min
15 min
30 min
45 min
60 min
ddH2O (CRTL)
BDM (treatment)
B)
number of FPP dots (a.u.)
C)
directional change rate (rad/sec)
D)
duration of FPP movement (sec)
E)
FPP dots travelled distance (µm)
CRTL
BDM
Time point after FPP exposure (min)

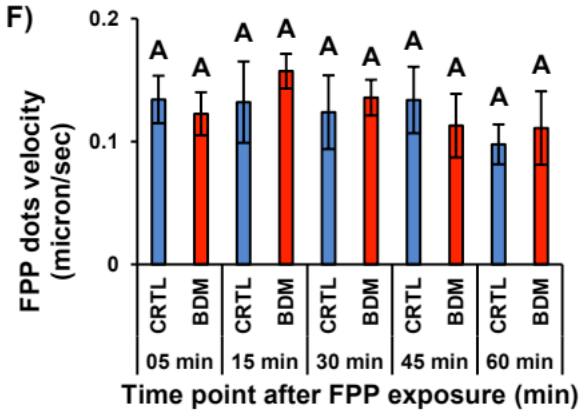

Supplemental Figure S10. Quantitative Analysis of NBD-FPP Translocation During Myosin Inhibition. A) Representative Panel: Detected NBD-FPP dots visualized using TrackMate. Purple circles indicate NBD-FPP dots, with lines showing the distance traveled at each time point (5, 15, 30, 45, and 60 minutes) for control (ddH2O) and inhibitor (BDM) treatments. B-F) Quantitative Measurements: Average values for NBD-FPP dots are shown. Blue represents ddH2O, and red represents BDM at each time point post-exposure.

B) Number of Dots: Detected NBD-FPP dots.

C) Directional Change Rate: Measured in radians per second.

D) Duration of Movement: Recorded for each dot.

E) Traveled Distance: Inside the cell.

F) Mean Velocity: Of the dots.

Bar charts with ± standard error bars represent the average of three biological replicates, with each treatment having n = 12 images. A One-Way ANOVA test followed by Tukey's post-hoc test was performed, with significant differences indicated by letters.

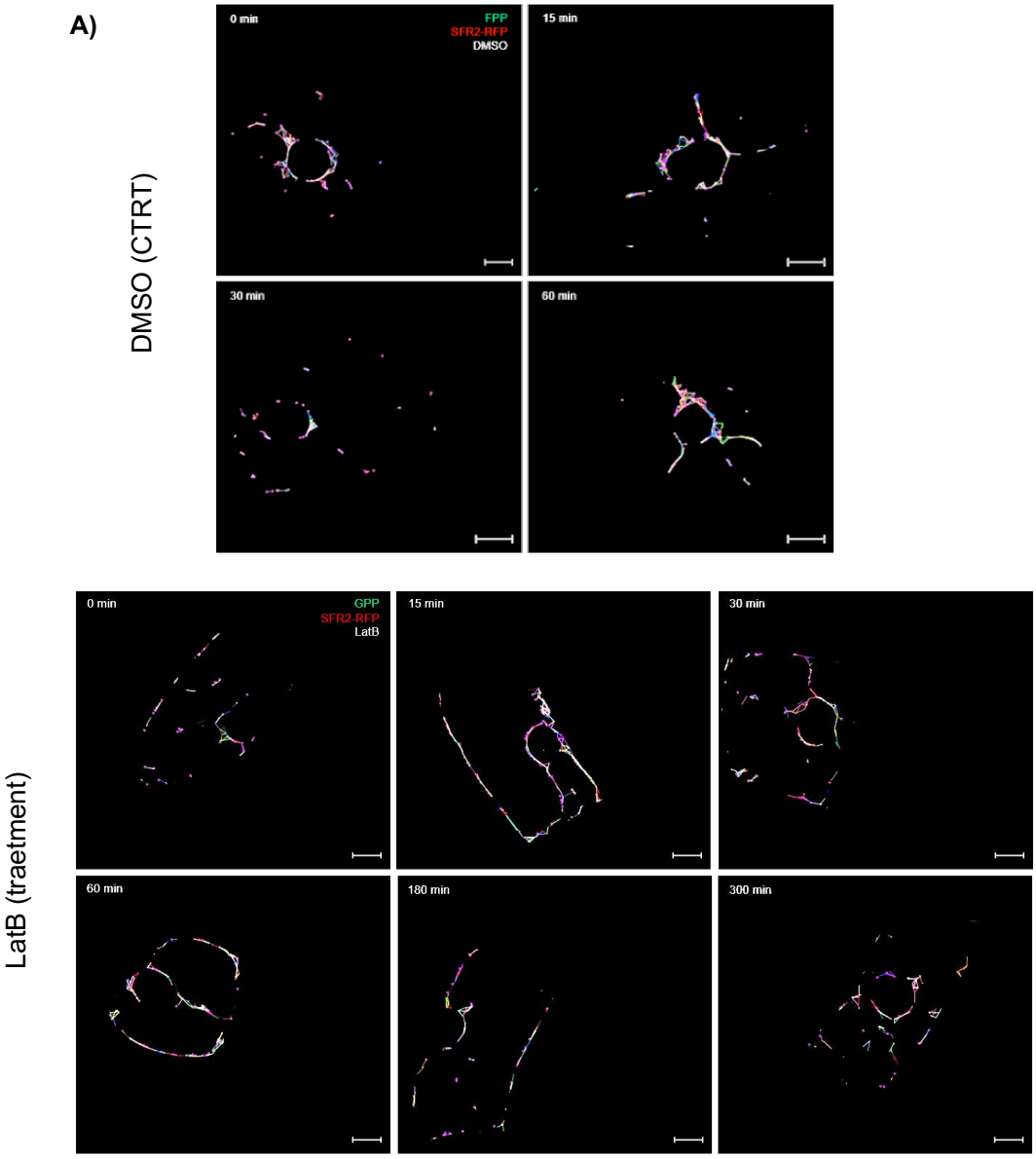
A)
DMSO (CTRT)
0 min
FPP
SFR2-RFP
DMSO
15 min
30 min
60 min
LatB (traetment)
0 min
GPP
SFR2-RFP
LatB
15 min
30 min
60 min
180 min
300 min

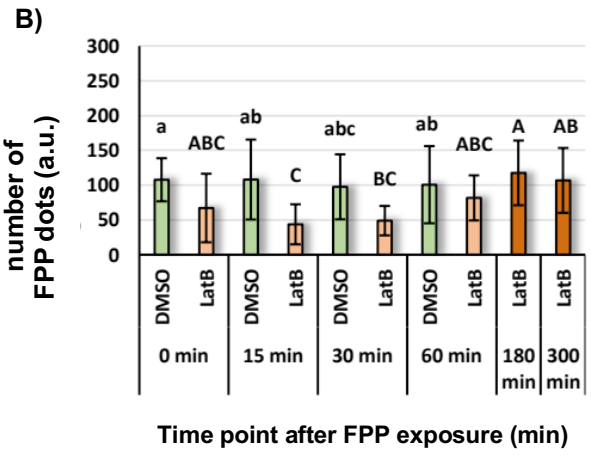
B)
number of FPP dots (a.u.)
300
250
200
150
100
50
0
a
ABC
ab
C
abc
BC
ab
ABC
A
AB
DMSO
LatB
0 min
15 min
30 min
60 min
180 min
300 min
Time point after FPP exposure (min)

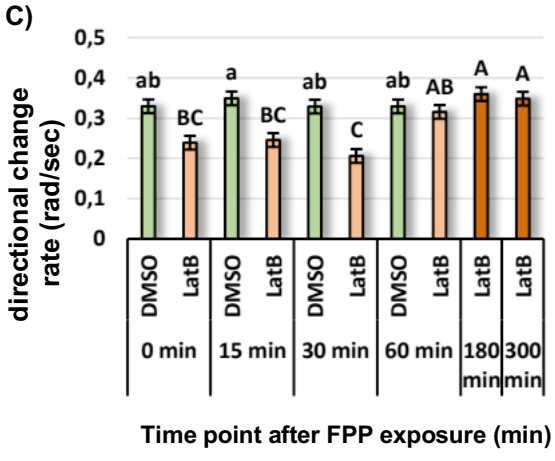
C)
directional change rate (rad/sec)
0,5
0,4
0,3
0,2
0,1
0
ab
BC
a
BC
ab
C
ab
AB
A
A
DMSO
LatB
0 min
15 min
30 min
60 min
180 min
300 min
Time point after FPP exposure (min)

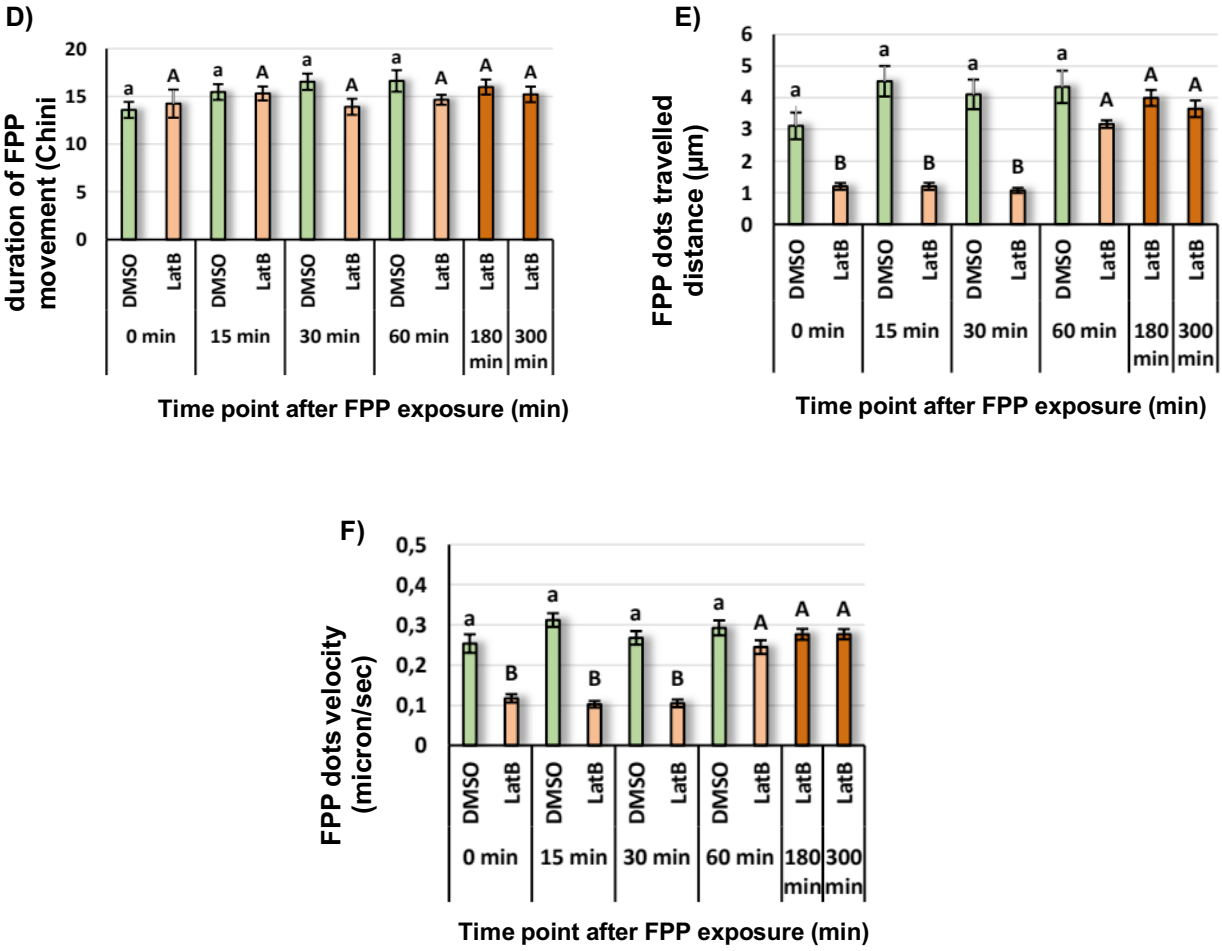

Supplemental Figure S11. Dynamics of NBD-FPP Translocation Under Actin Inhibition. A) Visualization Panel: TrackMate was used to detect NBD-FPP dots, shown as purple circles, with lines indicating distances traveled at each time point for control (DMSO) and LatB-treated samples.

B-F) Quantitative Metrics: The average values for NBD-FPP dots are illustrated. Green represents DMSO, while pink denotes LatB across time points.

B) Dot Count: Total number of detected NBD-FPP dots.

C) Directional Change Rate: Measured in radians per second.

D) Movement Duration: Time recorded for each dot's movement.

E) Travel Distance: Distance covered within the cell.

F) Mean Velocity: Average speed of the dots.

Bar charts with ± standard error bars show the average of three biological replicates, each treatment consisting of n = 12 images. A One-Way ANOVA followed by Tukey's post-hoc test was performed, with significant differences indicated by letters.